DYNAMIC SIMULATION OF SHAKING TABLE TESTS FOR A SHEAR-WALL BUILDING HAVING TORSION

THESIS SUBMITTED TO
THE GRADUATE SCHOOL OF NATURAL AND APPLIED SCIENCES
OF
MIDDLE EAST TECHNICAL UNIVERSITY

BY

SAEIDEH NAZIRZADEH

IN PARTIAL FULFILLMENT OF THE REQUIREMENTS
FOR
THE DEGREE OF THE MASTER OF SCIENCE
IN
EARTHQUAKE STUDIES

FEBRUARY 2012

Approval of the thesis:

DYNAMIC SIMULATION OF SHAKING TABLE TESTS FOR A SHEAR-WALL BUILDING HAVING TORSION

submitted by **SAEIDEH NAZIRZADEH** in partial fulfillment of the requirements for the degree of **Master of Science in Civil Engineering Department, Middle East Technical University** by,

Prof. Dr. Canan Özgen ____________________
Dean, **Graduate School of Natural and Applied Sciences**

Prof. Dr. Ali Koçyiğit ____________________
Head of Department, **Earthquake Studies**

Prof. Dr. Ahmet Yakut ____________________
Supervisor, **Civil Engineering Dept., METU**

Prof. Dr. Murat Dicleli ____________________
Co- advisor, **Engineering Sciences Dept., METU**

Examining Committee Members:

Doç. Dr. Ayşegül Askan Gündoğan ____________________
Earthquake Studies Dept., METU

Prof. Dr. Ahmet Yakut ____________________
Civil Engineering Dept., METU

Prof. Dr. Murat Dicleli ____________________
Engineering Sciences Dept., METU

Doç. Dr. Afşin Sarıtaş ____________________
Civil Engineering Dept., METU

Volkan Aydoğan ____________________
PROMER Consultancy Engineering Ltd. Co.

Date: 10.02.2012

I hereby declare that all information in this document has been obtained and presented in accordance with academic rules and ethical conduct. I also declare that, as required by these rules and conduct, I have fully cited and referenced all material and results that are not original to this work.

Name, Last name : Saeideh NAZIRZADEH

Signature :

ABSTRACT

DYNAMIC SIMULATION OF SHAKING TABLE TESTS FOR A SHEAR-WALL BUILDING HAVING TORSION

NAZIRZADEH, Saeideh

M.Sc., Department of Earthquake Studies
Supervisor: Prof. Dr. Ahmet YAKUT

February 2012, 104 pages

Simulating the non-linear response of reinforced concrete (RC) buildings subjected to a sequence of input earthquake records, is an extremely complex concern in the field of the Earthquake Engineering. Buildings with no symmetry in plan have much more complicated behavior under earthquake effects than symmetric buildings. Torsional irregularity in plan is the main topic of many current researches. In previous decades, considerable amount of numerical and experimental studies have been conducted, but more researches are needed in order to confirm a better understanding of the concept of seismic behavior of these structures.

In this study modeling and analyses efforts to simulate the experimental response of a scaled three dimensional reinforced concrete shear wall structure tested on a shaking table, are presented.

The model structure is a ¼ scale of a three story reinforced concrete building that has torsion due to plan irregularity and layout of structural walls. In order to simulate response quantities measured for the specimen tested on a shaking table, a series of non-linear time history analyses were performed. This structure subjected to AZALEE shaking table tests in Saclay, France under the

project of “SMART 2008” which was led by CEA (Atomic energy agency). The model building was tested under a set of bi-directional synthetic and real ground motions that have varying intensities, peak ground accelerations ranging from 0.1g to 1g. Ground motions were applied sequentially to the specimen, starting with the one having the smallest intensity. Displacements and accelerations measured at different locations on the plan at third story were compared with the numerically computed values in order to check the validity of the Finite Element Model that has been obtained in ANSYS ver.12.1.

Keywords: Shear Wall Structure, Azalee Shaking Table, Finite Element Method

ÖZ

BURULMA DÜZENSİZLİĞİ OLAN PERDE DUVARLI BİR BİNA İÇİN SARSMA TABLASI DENEYLERİNİN DİNAMİK ANALİZİ

NAZIRZADEH, Saeideh

Yüksek Lisans, Deprem Çalışmaları Bölümü

Tez Yöneticisi: Prof. Dr. Ahmet YAKUT

Şubat 2012, 104 sayfa

Bir dizi deprem kaydı altında betonarme perde duvarlı bir binanın lineer olmayan davranışını incelemek ve bu deprem yükleri altındaki tepkisini tahmin etmek deprem mühendisliği açısından oldukça karmaşıktır. Simetrik olmayan binaların deprem yükleri altındaki davranışını tahmin etmek ise simetrik binalara göre daha karmaşıktır. Burulma düzensizliği, günümüzde yapılan birçok çalışmanın konusunu teşkil etmektedir. Bu yapıların davranışını inceleyen analitik ve deneysel birçok çalışma olmasına rağmen, sismik davranışının daha iyi anlaşılabilmesi için daha fazla çalışmaya ihtiyaç vardır.

Bu çalışmada, burulma davranışı bulunan perde duvarlı bir yapının sarsma tablası deney sonuçları analitik modelleme ile tahmin edilmeye çalışılmıştır.

Model, burulma düzensizliği ve plan düzensizliği bulunan ¼ ölçekli üç katlı betonarme perde duvarlı bir binadan oluşmaktadır. Bu yapı Fransa, Saclay de bulunan AZALEE sarsma tablası deneylerine; CEA tarafindan düzenlenen ve yönetilen "SMART 2008" projesi altında tabi tutulmuştur. Yapının tepkisini farklı parametreler ile inceleyebilmek için bir takım zaman alanında tanımlı lineer olmayan deprem analizleri yapılmıştır. Model bina, iki doğrultu da etki etmek

üzere büyüklükleri 0.1g ile 1.0g arasında değişen bir takım gerçek ve sentetik yer hareketlerine maruz bırakılmıştır. Sarsma tablası deneyleri küçük değerlikli yer ivmesinden başlayıp 1,0 g' ye kadar ard arda gerçekleştirilmiştir. Plan üzerinde belirlenen belli noktalardan alınan deplasman ve ivme değerleri ile deneyden elde edilen sonuçları ANSYS v. 12.1'den elde edilen sonlu elemanlar modeli ile karşılaştırılmıştır.

Anahtar Kelimeler: Perde Duvarlı Bina, Azalee Sarsma Tablası, Sonlu Elemanlar Metodu, Zaman Alanında Tanımlı Deprem Analizi

To My Family for Their Heartily Support

ACKNOWLEDGMENTS

First I offer my sincerest gratitude to my supervisor, Prof. Dr. Ahmet Yakut, whose invaluable encouragement and support from the initial to the final level of the research enabled me to develop an understanding of the subject and I consider it an honor to work with him.

I would like to convey thanks to my co-advisor Prof. Dr.Murat Dicleli for his guidance and suggestions.

Scientific and Technological Research Council of Turkey (TÜBİTAK – 109M707), which is financially supporter of this study, is gratefully acknowledged.

I am particularly indebted to my dear friend, Vesile Hatun Akansel,whose positive, informed, and encouraging nature has been an inspiration throughout.

I am also grateful to all of my friends, especially; Begüm Yılmaz, Aida Azari, Sahar Nasouti and Elnaz Alizadeh for their support and kind friendship and special thanks to Dr. İlker Kazaz for his guidance and suggestions throughout this study.

I express my deepest gratitude to my family especialy my brother, Mohammad Javad Nazirzadeh, for their love and encouragement.

Lastly, I offer my regards and blessings to all of those who supported me in any respect during the completion of the project.

TABLE OF CONTENTS

LIST OF TABLES

TABLES

LIST OF FIGURES

FIGURES

CHAPTER 1

INTRODUCTION

1.1. Background

Simulating the non-linear response of reinforced concrete (RC) buildings subjected to a sequence of input earthquake records, is an extremely complex concern in the field of the Earthquake Engineering. Buildings with no symmetry in plan have much more complicated behavior under earthquake effects than symmetric buildings. Torsional irregularity in plan is the main topic of many current researches. In previous decades, considerable amount of numerical and experimental studies have been conducted, but more researches are needed in order to confirm a better understanding of the concept of seismic behavior of these structures.

There is interaction between lateral translation and rotational displacement. The irregular distribution of the main load carrying components, such as columns and shear walls causes difficulty in understanding the nonlinear effects under cyclic loadings during earthquakes.

Dynamic analysis of structures assists the validation of computational methods for evaluating behavior of structures under earthquake loads. Among several different experimental techniques to generate test data and verify the seismic behavior of reinforced concrete walls and also having a benchmark for numerical modeling, large scale shake table testing is a reliable method (Lu and Wu, 2000; Kazaz et al, 2006).

A shake table is a platform for testing the resistance of structural models or building components to seismic shaking, with a wide range of simulated ground motions, including reproductions of recorded earthquakes time-histories.

Model tests are essential when the prototype behavior is complex and it is hard to test the structures in full scale because of the technological challenge and expense that it represents. The model buildings are mostly scaled mock-ups, although facilities such as the E-Defense in Kobe, Japan, permit full-size structures to be tested realistically. In model testing, usually the boundary conditions of a prototype problem are reproduced in a small-scale model (S.K.Prasad et al., 2004; Nakashima et al., 2008; Chung et al., 2010).

This study is the complementary to the benchmark contest Phase 1b of the SMART[1] - 2008 project. This structure was a highly idealized ¼ scaled mock – up of a French shear wall nuclear power plant structure component. It was subjected to the AZALEE shaking table tests in which different seismic excitation simulations were carried out in Saclay, Paris, in France under the leadership of Commissariat Energie Atomique (CEA). Experimental behavior of the mock-up has been simulated through numerical modeling and analyses. The details of the project will be provided in the following chapters.

1.2.Literature Survey

In order to provide a background for this research an overview of previous studies on related topics are presented in this chapter. Previous research on shaking table tests and numerical modeling are presented separately. Since the SMART project deals with buildings with RC walls, emphasis is given on these types of members and structures.

Concrete shear-wall buildings have exhibited outstanding seismic performance in earthquakes. Shear walls are the walls that resist wind or

[1] SMART = Seismic design and best – estimate Methods Assessment for Reinforced concrete buildings subjected to Torsion and non – linear effects

earthquake loads acting parallel to the plane of the wall in addition to the gravity loads from floors and roof adjacent to the wall. These walls provide lateral support for the rest of the structure (MacGregor and Wight, 2005).

Review of analytical methods for static and dynamic calculations for the design of shear wall buildings returns to the 1960s. Due to low speed and capacity of computers, researchers were forced to use simplified methods and hand calculations in design offices (Khan and Sbarounis, 1964; Rosman, 1968).

With progression of technology of computers, after the 1960's, a large amount of substantial analytical and experimental research, executed all through the world, using commercial software based on finite element methods. Those researches, collected many practical information on the earthquake response of shear wall structural systems. Also, starting from 1950's a considerable body of information was assembled on performance of buildings in actual earthquakes.

"The design seismic forces acting on a structure as a result of ground shaking are usually determined by one of the following methods:

- Static analysis, using equivalent seismic forces obtained from response spectra for horizontal earthquake motions.
- Dynamic analysis, either modal response spectrum analysis or time history analysis with numerical integration using earthquake records." (Kazaz et al. 2005)

"The dynamic time history analysis can be classified as either elastic or inelastic. The inelastic analysis of structures requires a non-linear dynamic time-history procedure past the elastic response and up to collapse." (Chopra, 1995)

Gülkan and Sözen (1974) performed the dynamic tests on one– story, one-bay reinforced concrete frames subjected to strong ground motion, for the purpose of verifying the effects of changes in stiffness and energy dissipation capacity on dynamic response. They inferred that the maximum inelastic earthquake response of reinforced concrete structures, can be approximated by linear response analysis using a reduced stiffness and a deputy damping ratio.

Wallace and Moehle (1992) evaluated the displacement capacity and demands in walls according to past earthquakes such as the Chile Earthquake, 1986. They formulated use of ideas presented by Sözen (1989) to be able to get the fundamental period of a building and then used the single degree of freedom (SDOF) oscillator method developed by Newmark and Hall (1982) and Shimazaki and Sözen, (1984) to determine the maximum elastic and inelastic response. Kabeyasawa et al (1983) tested a full – scale seven storey reinforced concrete structure for its pseudo – dynamic earthquake response. Subsequently, analytical models were developed for estimating the response under earthquakes by comparing with the experimental results and past earthquakes.

Clough et al. (1965), initiated the numerical modeling of RC elements. Since then several advancements were done in the area of modeling of RC elements including shear walls.

There are two principal approaches to model RC component behavior: microscopic finite element (FE) analysis and macroscopic models.

"The advancing application of the finite element modeling (FEM) to RC structures in the last 20 years, has proven it to be a very powerful tool in engineering analysis. The wide distribution of computers and the development of the finite element method have provided means for analysis of much more complex systems in a much more realistic way." (Abdollahi, 1996; Clough, 1980)

Micro modeling is suitable for capturing the local behavior in the structure. Micro modeling represents the behavior of different materials that compose the RC element and the interaction between them. The member is discretized into small elements and principles of equilibrium are applied.

The most general method that is used for simulating the behavior of RC elements using micro-modeling, is finite element method. The FEM is powerful tool for the analysis of RC structures, including three-dimensional and nonlinear analysis. The FEM of analysis is capable of tracking the member's global behavior (e.g. member forces and displacements) in addition to its local behavior (e.g. crack pattern, material stresses and strains). Many researchers have used micro modeling approach to simulate the experimental measurements (Kwak and Kim, 2004; Palermo and Vecchio, 2007).

Macro-modeling represents the overall behavior of the RC element. The global behavior of the RC element using a macro-model should be calibrated using an experimental verification to adjust the parameters needed for the model (Ile and Reynouard 2003, 2005; Kazaz et al, 2006; Ile et al., 2008; Fischinger and Isakovic, 2000; K.Galal and H. EL-Sokkary, 2008)

ANSYS (Desalvo and Swanson 1983), ABAQUS (Hibbitt 1984), VecTor 2 and 3 (Vecchio 1989), ADINA (1992) and DIANA are some of the finite element softwares.

Many shaking table tests have been performed to evaluate the inelastic seismic response of lightly reinforced concrete wall, and a modeling strategy and numerical modeling for RC walls was proposed.

Jingjiang et al. (2007) performed earthquake simulator tests of a RC frame-wall model and compared the analytical and experimental results, and presented conclusions related to seismic design and damage evaluation of RC structures.

Moehle (1984) investigated the seismic behavior of simplified models of multi-story building frames, consisted of combinations of frames and frame-wall.

The effects of setbacks on the earthquake response of six-story buildings were evaluated by performing shake table tests by Shahrooz et al. (1990). They proposed the design method for setback buildings.

Hosoya et al. (1995) excited two 1:7 scale models to understand the performance of high-rise frame structures with wall columns (piers) and validated an analytical model with test results.

In order to investigate the structural effect of weak/soft story at the first story and confirmation of the relevant design code provision, Lu et al. (1999) conducted the shaking table tests of two six-story reinforced concrete frames: one with a tall first story, and the other having a discontinuous interior column.

Kim et al. (2002) performed the shaking table test of a six-story building with a weak/soft story having torsional irregularity at the first story.

Yong Lu (2002) conducted experimental investigation and associated analytical evaluation to verify the seismic performance of a wall-frame structure with comparison to a ductile bare frame.

Palermo and Vecchio (2002) studied the behavior of three-dimensional reinforced concrete shear walls under static cyclic displacements.

"Shaking table tests for full-scale seven-story RC wall structures and six-story RC wall frame buildings were performed by using large shaking tables in USA and Japan, respectively. Generally, the height of the structures was medium-rise or less than twelve stories for all previously mentioned tests. While most of the shaking table tests were performed for a medium-rise frame building, few shaking table tests were examined for irregular high-rise wall buildings. Several previous studies by the authors were conducted to investigate the seismic response of the three individual building models having different layouts of the vertical earthquake-resistant elements in the lower soft stories." (Lee HS et al. 2002, Ko DW et al. 2006).

The effect of torsion and the seismic behavior of a lightly reinforced wall specimen under bi-directional loading was reviewed by Ile and Reynoaurd (2003).

The dynamic performance of two reinforced concrete buildings tested on a shaking table during the CAMUS 2000 experimental research program was simulated using two different simplified modeling strategies (a fibre and a beam model) and two resolution schemes (implicit and explicit, respectively) by J.Mazars et al. (2004).

Ile et al. (2004) compared numerical and experimental results of the U-shaped walls subjected to lateral cyclic loadings applying the shell refined model .

Two structures, considering the “multifuse” and “monofuse” concept, using Bernoulli multi-layered beam elements and advanced constitutive laws based on damage mechanics and plasticity, were simulated, CAMUS I and CAMUS III, in order to test the ability of the proposed numerical tools, (Spatial and time discretization, modeling and damping mechanism and materials constitutive relations) to simulate the non-linear behavior of the structures following different design philosophies (Kotronis et al. 2005). They also conducted dynamic shaking table tests on AZALEE shaking table.

Kazaz et al. (2006) using ANSYS simulated the seismic response of a 5-story RC shear wall specimen on shaking table subjected to progressive damage under sequence of ground motions.

Han-Seon Lee et al. (2007) studied the seismic performance of high-rise reinforced concrete wall buildings with different irregularities in lower stories. They studied the comparative investigation of the seismic performance of all three high-rise RC bearing-wall building models with respect to variation in the irregularity in the lower soft stories consisting of a space frame with or without an infilled shear wall.

The effect of viscous wall dampers on seismic performance of RC frames, using shaking table tests and numerical analysis, was examined by Lu et al. (2008).

Ile et al. (2007) and Lu et al. (2008) performed shaking table tests to evaluate the inelastic seismic response of lightly RC walls subjected to seismic excitations, in the framework of ECOLEADER and CAMUS research projects.

An asymmetric frame building was tested on the shaking table, by Gallo et al. (2011) in order to study the seismic vulnerability of non-ductile RC frame buildings and investigate the retrofit solutions.

Dynamic interaction between the shaking table and the structure has been studied by Le Maoult et al. (2011). They demonstrate that most of the interaction for AZALEE shaking table is due to the platform deformation during the tests.

1.3.Object and Scope

The primary objective of this study is the simulation of shaking table tests in order to assess the seismic 3D effects such as torsion and non-linear response of RC structures, in a reduced scaled model of a nuclear shear wall structure which was tested in France on AZALEE shaking table.

For this reason, two models were generated. In the first model, the effect of shaking table was ignored and the base of the specimen was considered as fixed. In the second model, the shaking table was also included in the model. In order to check adequacy of the model, first experimentally obtained modal properties that is modal frequencies were compared with numerical ones. Then, displacement time histories and response spectra computed at different points on the third floor were compared.

Contents of each chapter are as follows:

Chapter 2 is devoted to information about the modeling specifications and experimental results of the SMART 2008 specimen.

In Chapter 3, the results of analysis of both fixed-base and shaking table models, are presented and calculated frequencies, displacements and accelerations are compared with the experimental results.

In Chapter 4, results are interpreted. Experimental measurements are investigated and influence of the shaking table is discussed.

In Chapter 5, the summary of the results is discussed and the conclusions obtained from this study are presented. Finally, the recommendations are listed to make this study much more relevant to practice.

CHAPTER 2

DESCRIPTION OF BUILDING MODEL AND EXPERIMENTAL RESULTS

2.1. SMART 2008 Experimental Program

In order to identify the behavior of shear walls under seismic excitations and to assess the seismic three dimensional effects (such as torsion) and non-linear response of reinforced concrete buildings, a program entitled ***S**eismic estimate **M**ethods **A**ssessment for **R**einforced concrete buildings subjected to **T**orsion and non-linear effects* has been initiated by the Commissariat à l'Energie Atomique et aux Energies Alternatives (CEA) and Electricité de France (EDF) in 2008.

The main objective of this project is to evaluate and compare different proposed modeling techniques and strategies, in order to clarify and assess the structural behavior of a model representative of the reinforced concrete buildings designed according to the French nuclear practices. A reduced scaled model (scale of 1/4th) of a nuclear reinforced concrete building was tested on the AZALEE shaking table at Commissariat à l'Energie Atomique (CEA Saclay, France). The loadings applied to the model ranged from very low seismic motions to five times the design level.

The SMART-2008 project consisted of two phases. A brief description of the phases includes:

The first phase of the project, also consisted of two parts, Phase 1A and Phase 1B (RAPPORT DM2S, 2007 and RAPPORT DM2S, 2009). Phase 1A presented a contest related to blind prediction of the structure behavior under different seismic loads, opened to teams from the practicing structural engineering as well as the academic and research community, worldwide.

Phase 1B was related to the benchmark study. The main aim was to allow the participants to improve their best estimate predictions by updating their model with information available for some of the seismic runs, as to perform new analyses at higher loading levels.

The second phase of the project was dedicated to the variability, sensitivity and vulnerability analysis, by using numerical models of the SMART specimen carried out in the previous stages. The objectives of the phase 2 of the SMART benchmark are to quantify variability in the seismic response of the structure and identify contribution coming from uncertainties in input parameters and to investigate and compare different methods for fragility curves elaboration.

In the present study, Phase 1B of the SMART-2008 project has been studied. The objectives of the Phase 1B are to investigate the efficiency of the model in the non-linear range through the comparison with the experimental results and to adjust the model in order to match the experimental response of the specimen under different seismic loadings.

The primary objective of this thesis is to obtain a valid and adequate model that can simulate the experimental response of the specimen. For this reason, two models were generated. In the first model, the effect of shaking table was ignored and the base of the specimen was considered as fixed. In the second model, the shaking table was also included in the model.

In order to check adequacy of the model, first experimentally obtained modal properties that is modal frequencies were compared with numerical ones. Then, displacement time histories and response spectra computed at different points on the third floor were compared.

2.2. Description of the Specimen

2.2.1. Geometrical Properties

The model building is a 1/4 scale trapezoidal, three-story reinforced concrete structure tested on the shaking table Azal′ee (France). It is composed of three reinforced concrete (RC) shear walls forming a U shape, connected through rigid diaphragms with a column and a beam dividing the slab in two parts.

The height of the floor levels are, accordingly, 1.25 m, 2.45m, and 3.65 m from the basement. The thickness of the slab is 10 cm. The geometrical details of column and walls are shown in Figure 2.1 - 2.3 and given in Table 2.1.

Table 2-1 Dimension of Structural Elements

	Length (m)	Thickness (m)	Height (m)
Wall (#V01+#V02)	3.1	0.1	3.65
Wall #V03	2.55	0.1	3.65
Wall #V04	1.05	0.1	3.65
Beam	1.45	0.15	0.325
Column	3.8	0.2	0.2

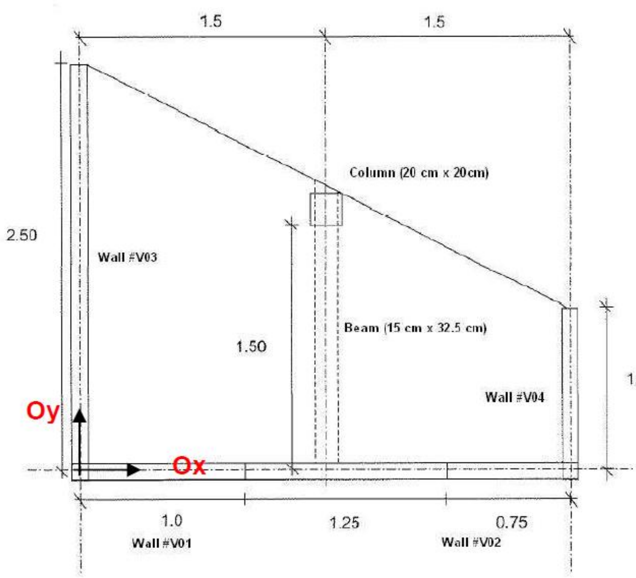

Figure 2-1 Plan view of the SMART-2008 Specimen

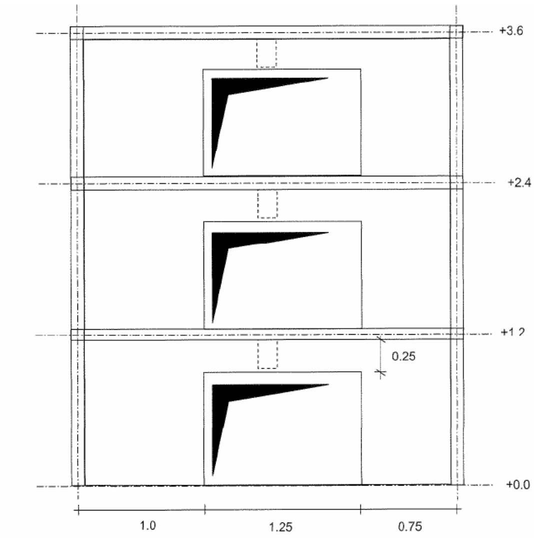

Figure 2-2 Elevation of wall #V01 & #V02

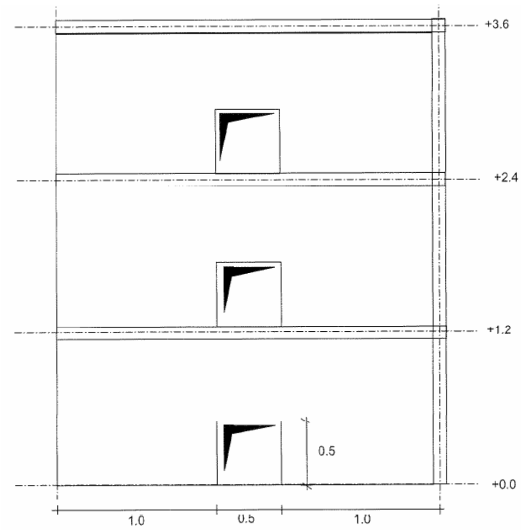

Figure 2-3 Elevation of wall #V03

2.2.2. Foundations

The wall's foundations were made of a continuous reinforced concrete footing. The footing was 38 cm wide, 15 cm high and lay on a 62*2 cm high steel plate. The reinforced concrete column was directly anchored on a 62 by 62 cm steel plate (Figure 2.4). The steel plates were bolted on AZALEE shaking table with M36 screws.

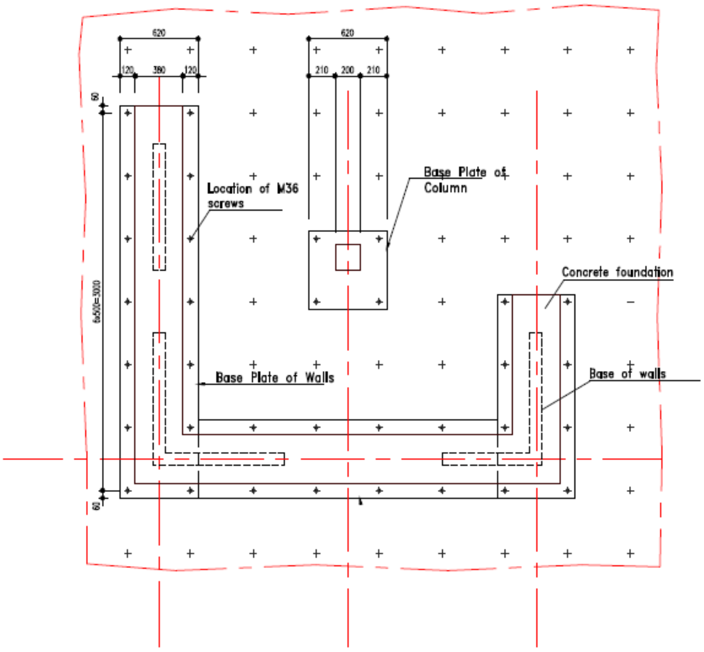

Figure 2-4 Top view of foundations

2.2.3. Material Properties

The following information was provided for the blind predictive benchmark. The main characteristics (Compressive strength, Tensile strength, Concrete Young modulus, Poisson's ratio) are given in Table 2.2.

Table 2-2 Material characteristics

f_{cj} (MPa)	f_{tj} (MPa)	E_c (MPa)	ν_c	ν_s
30	2.4	32000	0.2	0.3

The steel reinforcement was defined according to the European design codes (EC2). Steel reinforcement FeE500-3 is used in details and its yielding stress (Fe) is 500 MPa.

2.2.4. Additional Loadings

Additional loads were applied on the slab at each level in order to recreate the structural and additional masses of the real structure. The total mass of the specimen was estimated at about 434.485 kN (44.29 T) in the SMART 2008-Phase 2 Contest Report (RAPPORT DM2S, 2009). Additional loadings on the floor levels are given below:

Additional loading on the 1st slab ~ 11.60 T
Additional loading on the 2nd slab ~ 12.00 T
Additional loading on the 3rd slab ~ 10.25 T

The concrete density, according to the test cylinders is estimated to be about 2372 kg/m^3, and that of the steel reinforcement at about 88 kg/m^3.

The average density of the reinforced concrete of the structure was taken 2460 kg/ m^3 as given in the SMART 2008 Phase 2 report (RAPPORT DM2S, 2009).

2.2.5. Shaking Table

The Azalée shaking table, with 6x6 m dimensions, was put in service in 1990. This table is the biggest European shaking table and is utilized to test large-dimension specimen with an important mass (up to 100 tons).

This shaking table is fixed to eight hydraulic actuators (4 in the horizontal direction and 4 in the vertical direction). The AZALEE shaking table can be considered as a rigid block with a total mass of 25 tons (Figure 2.5).

Dynamic behavior of the shaking table during each seismic experimental test was recorded. Two accelerometers for the two horizontal reference measurements were fixed in the centre of the table on the upper face of the table: AXTAB, AYTAB, in order to apprehend the accelerations at the table’s level (z = -0.17m).

Also the displacements at the table's level, the accelerations at the foundation level (z = 0) and the frequencies of the specimen before specified runs, are available.

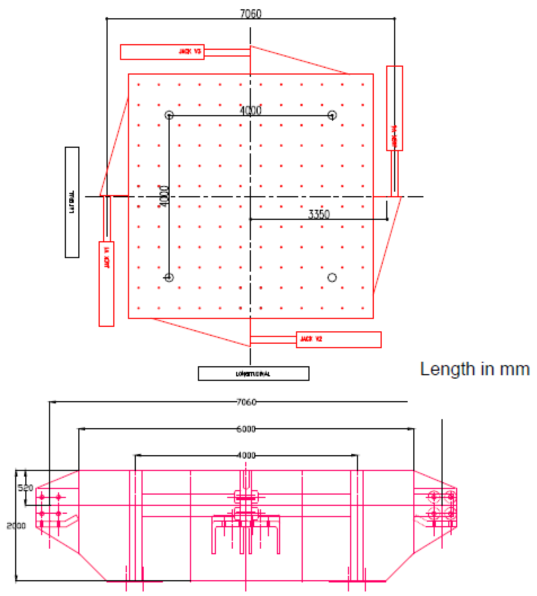

Figure 2-5: AZALEE shaking table- top view and elevation

(RAPPORT DM2S- SEMT/EMSI/RT/08-022/A Presentation of the benchmark contest Phase 1b Project SMART 2008)

The origin of the vertical axis (z = 0) for the specimen is the top of the foundation. The thickness of the foundation (including the steel plate) is 17 cm.

Data concerning the global behavior of the shaking table, for each degree of freedom in translation (Ox, Oy and Oz direction) and rotation (Roll, Pitch and Yaw) are available in the following figure:

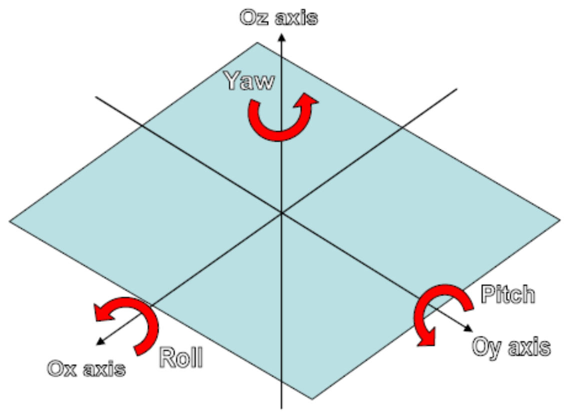

Figure 2-6 DOF of AZALEE shaking table

The distance between two vertical jacks is 4 meters while two horizontal jacks are placed at distance of 7.06 meters from each other. The jacks controlling the horizontal motion of the table are located at 1.02 m below the upper face of the shaking table (Figure 2.7).

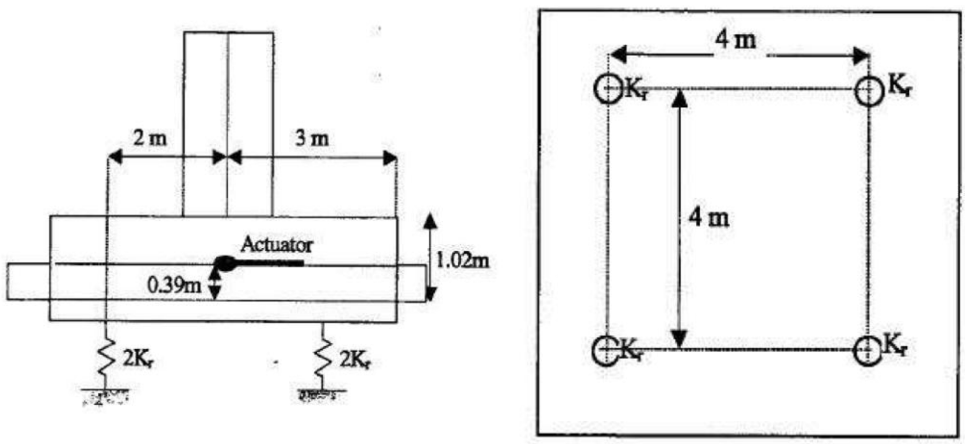

Figure 2-7 Simplified model of the shaking table AZALEE (plan and elevation)

All the jacks are controlled during the experiment (active systems). In order to simulate the foundation- shaking table connection, the spring constant value of 215 MN/m could be used for each vertical jack (Specification DM2S-

SEMT/EMSI/PT/07-003/C- Presentation of the blind prediction contest Project SMART 2008).

The orientation of the specimen and the position of the origin point and reference axis can be observed from Figure 2.8.

The AZALEE plate level is at z=-0.17m. The specimen was placed on the table so that its centre of mass corresponds to the centre of the shaking table (Table 2.3 and Figures 2.9 and 2.10).

Table 2-3 Centre of gravity for the system coordinates presented in Figure 2.9.

	x_g (m)	y_g (m)
Table	1.50	0.94
Specimen	1.28	0.92

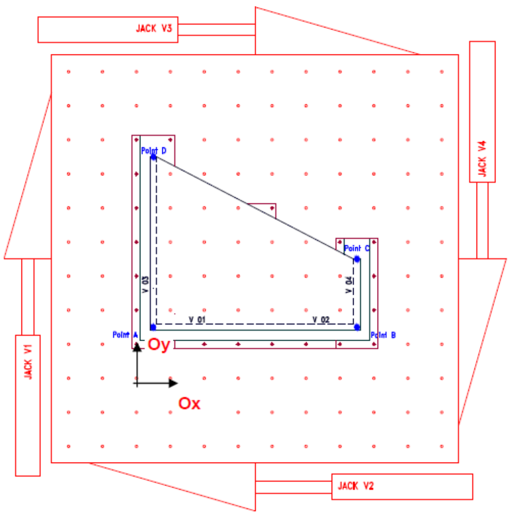

Figure 2-8 Reference axis

Each corner of the model is identified with a letter (A to D). Three additional specific points were defined on each slab. The results have to be computed at these locations. It is fixed at crossing of horizontal axis of wall #V03 and #V 01.

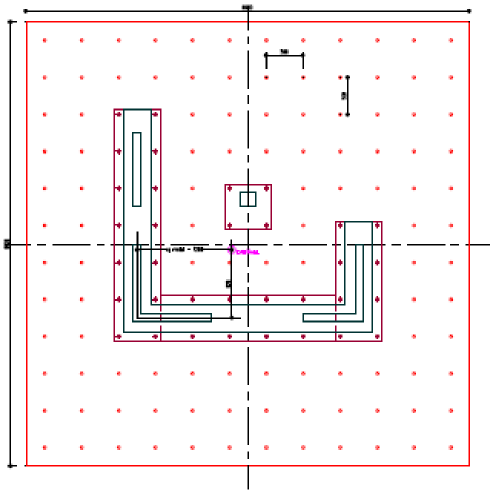

Figure 2-9 Position of the specimen on the shaking table and centre of gravity

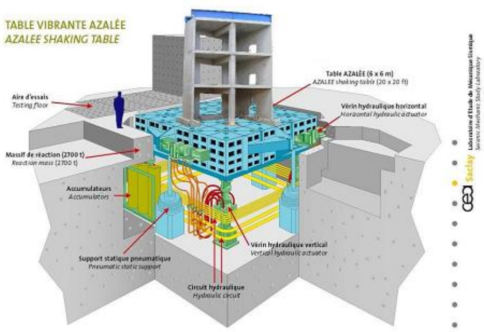

Geometry and performances of table Azalée	
Dimensions of table	6x6 m
Mass of table	25 tons
Maximum mass of specimen	100 tons
Maximum height of the specimen	12 m
Excitement axis	Tri-axial
	X-Y-Z
	6 degrees of freedom
Strength of actuators	X: 2 x 1000 kN
	Y: 2 x 1000 kN
	Z: 4 x 1000 kN
Maximum displacement	X ± 125 mm
	Y ± 125 mm
	Z ± 100 mm
Maximum speed	Seism: 1 m/s
	Sinus: 0.7 m/s
Maximum acceleration (specimen: 100 tons)	1 g
Excitement frequencies	0 to 100 Hz

Figure 2-10 Position of the specimen on the shaking table (3D) and detailed information about the shaking table

2.3. Experimental program and summary of results

Two types of input motion were used in the experimental program. Three real (naturally recorded seismogram) and ten synthetic (an artificial record) accelerograms set were applied to the SMART specimen. Each set is composed of 1 accelerogram for each horizontal direction applied simultaneously. Real accelerograms were defined for 2 orthogonal horizontal directions. The details are presented in Table 2.4 and Figure 2-11.

Table 2-4 Real accelerogram sets

No	Real earthquakes	M	Distance (km)	Pga (g)
1	Eq. UMBRO-MARCH(AS)	5.2	23	0.05
2	Eq. MANJIL(AS)	4.4	14	0.05
3	UMBRO-MARCHIGIANO	5.9	81.4	0.05

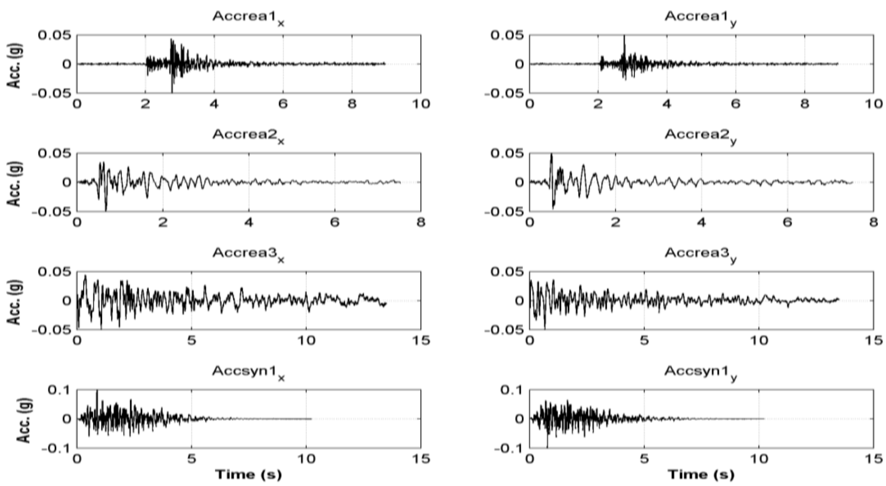

Figure 2-11 Real Ground Motion data used in the experiments

Synthetic accelerograms were defined for 2 orthogonal horizontal directions based on the response spectra-pga ranging from 0.1g to 1.0g.

These ground motions were applied sequentially to the specimen and caused cumulative increase of the damage.

The mock-up resembles a typical nuclear building, scaled by a factor of ¼. In consideration of keeping the same acceleration (gravity load can not be changed) as well as the same material properties, the scaling of ¼ of the structure's dimension implies to scale the mass by 1/16 and the time by ½.

The scaling values applied to the different parameters are given in Table 2.5.

Table 2-5 Scaling factors of parameters and their units:

	Scaling factor
Length (m)	$4=(\lambda)$
Mass (kg)	$16=(\lambda^2)$
Time (sec)	$2=(\lambda^{1/2})$
Acceleration (g*)	1
Stress (MPa)	1
Frequency (Hz)	0.5
Force (N)	16
Steel reinforcement area (m^2)	16
$*1\ g= 9.81\ m/s^2$	

The summary of experimental studies which was part of SMART 2008, Phase 1 project, at specific points as given in Figure 2-12 are used in this study.

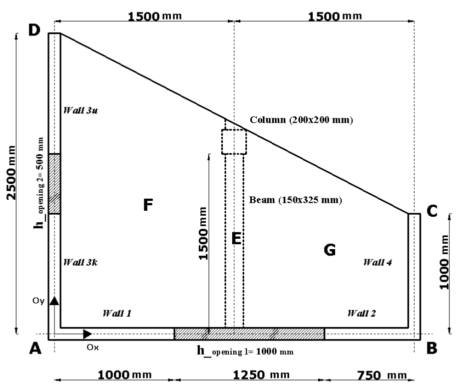

Point	X (m)	Y (m)
A	0	0
B	3	0
C	3	1
D	0	2.5
E	1.5	0.75
F	0.75	1.03
G	2.25	0.65

Figure 2-12 Identification of the locations where results have to be computed and result locations in the system coordinates

Figure 2-13 SMART Specimen, unloaded and fully loaded (Lermitte et al., 2008)

Using transducers and gages, local behavior of the mock-up at specific locations was monitored and the experimental results were obtained. 42 steel gages were placed on bars at the foundations, walls and lintels and 42 concrete gages were placed at the base of walls and on lintels of the first level, 55 displacement transducers were placed on walls and lintels and 6 crack opening transducers were placed at the base of wall 3 and wall 4. Concrete gages were glued on walls at each selected location (Horizontal, Diagonal and Vertical Strain, Figure 2-14).

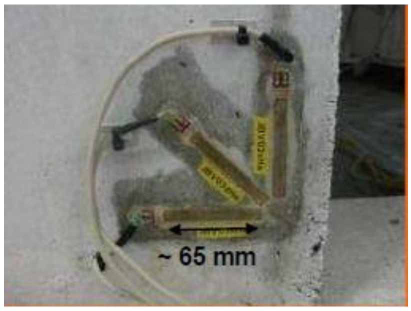

Steel gages on lintel concrete gages on walls

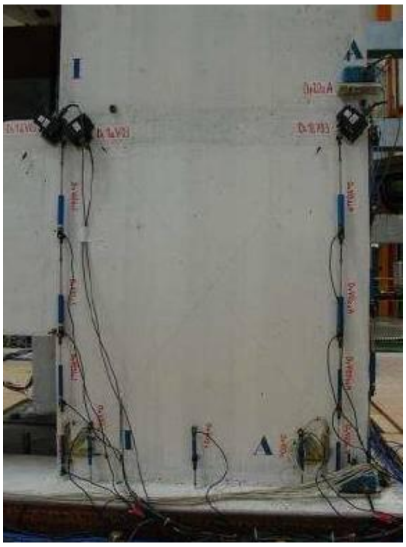

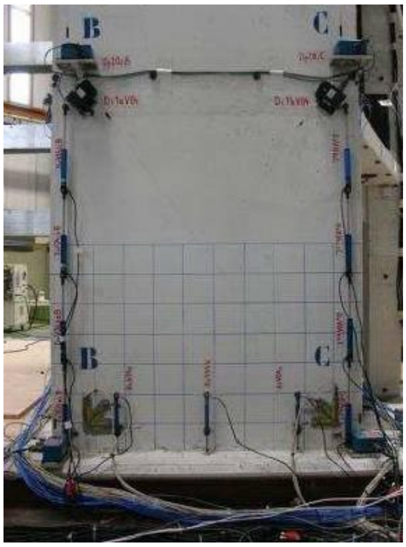

Figure 2-14 Displacement transducers on wall 3 and 4

Each seismic test was recorded with two categories of cameras: 3 DV cameras for general views of the specimen and 2 high speed cameras for image analyses (~100 images/s). Figure 2.15 shows the time histories of the measured displacement responses of 3rd floor level for Run 10 and 13 at points A,B,C and D. The measured maximum displacement is 20 mm at point D, and 36 mm in point D at runs 10 and 13, respectively.

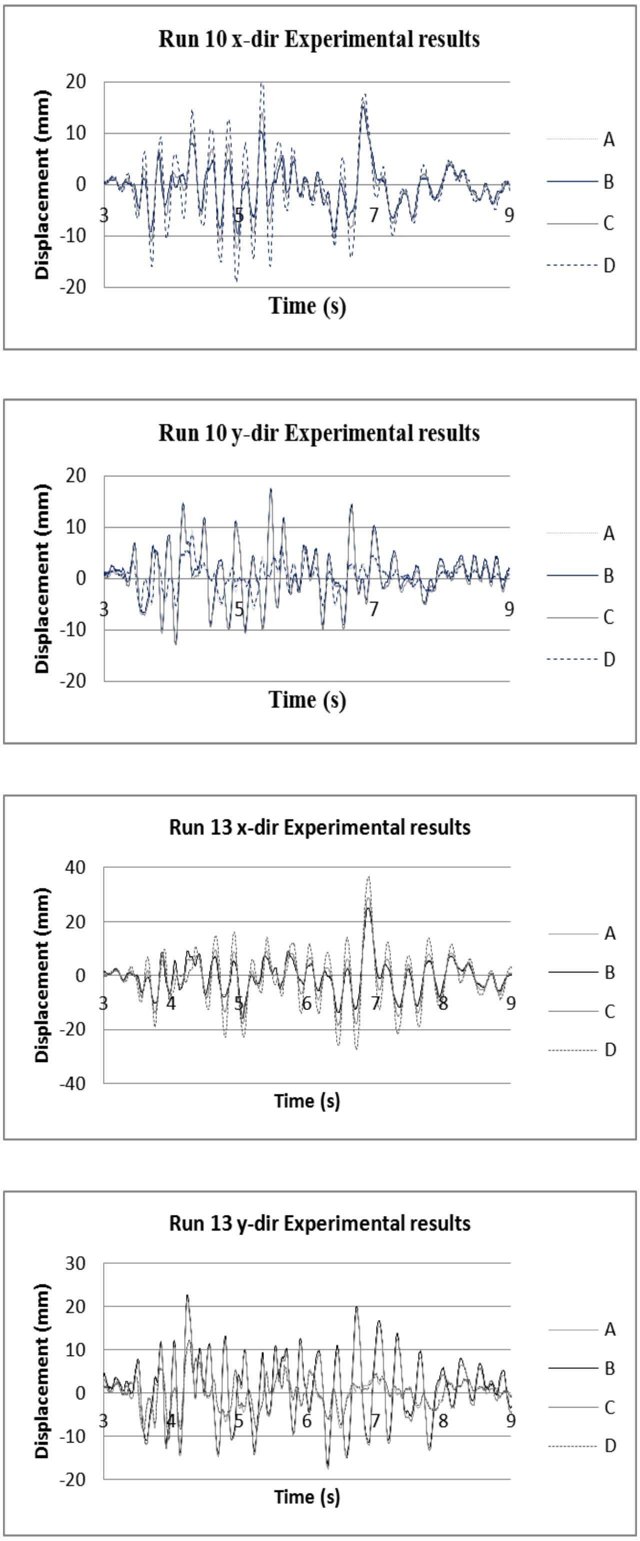

Figure 2-15 The time histories of the measured displacement responses at point D of 3rd floor level for Run 10 and 13

In Figures 2.16 to 2.18 the maximum measured values from experimental study are presented. It is obvious that the measured maximum acceleration and displacement values increase along with the increasing the run-levels. Building response is dominant in the X direction.

The measured floor acceleration values are closely similar at specified points in X direction for low seismicity. Increase in acceleration level of the applied seismic excitation results in separation on the responses of the points at the same floor level.

The displacement response also increases similar to acceleration response and varies in different points on the same floor level (Figure 2.16-2.18).

In run 5 the highest displacement response is measured at point D at the first floor level for the X direction.

Comparing the results to the other points in the same floor level reveals that the difference is so much. In run 13, transducers measured the highest displacement response at point D for Y direction at first floor level.

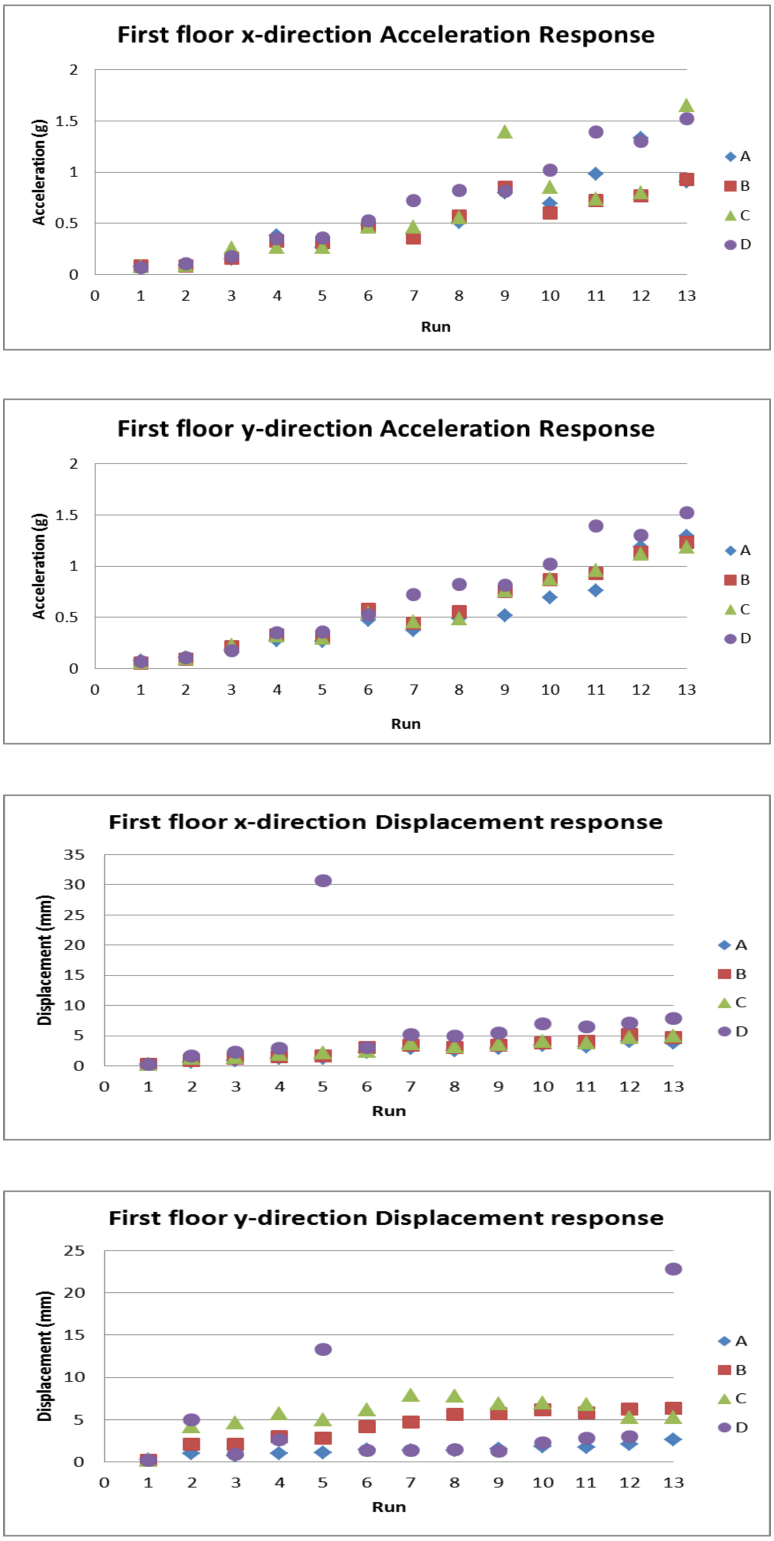

Figure 2-16 Maximum measured relative acceleration and displacement responses at first floor

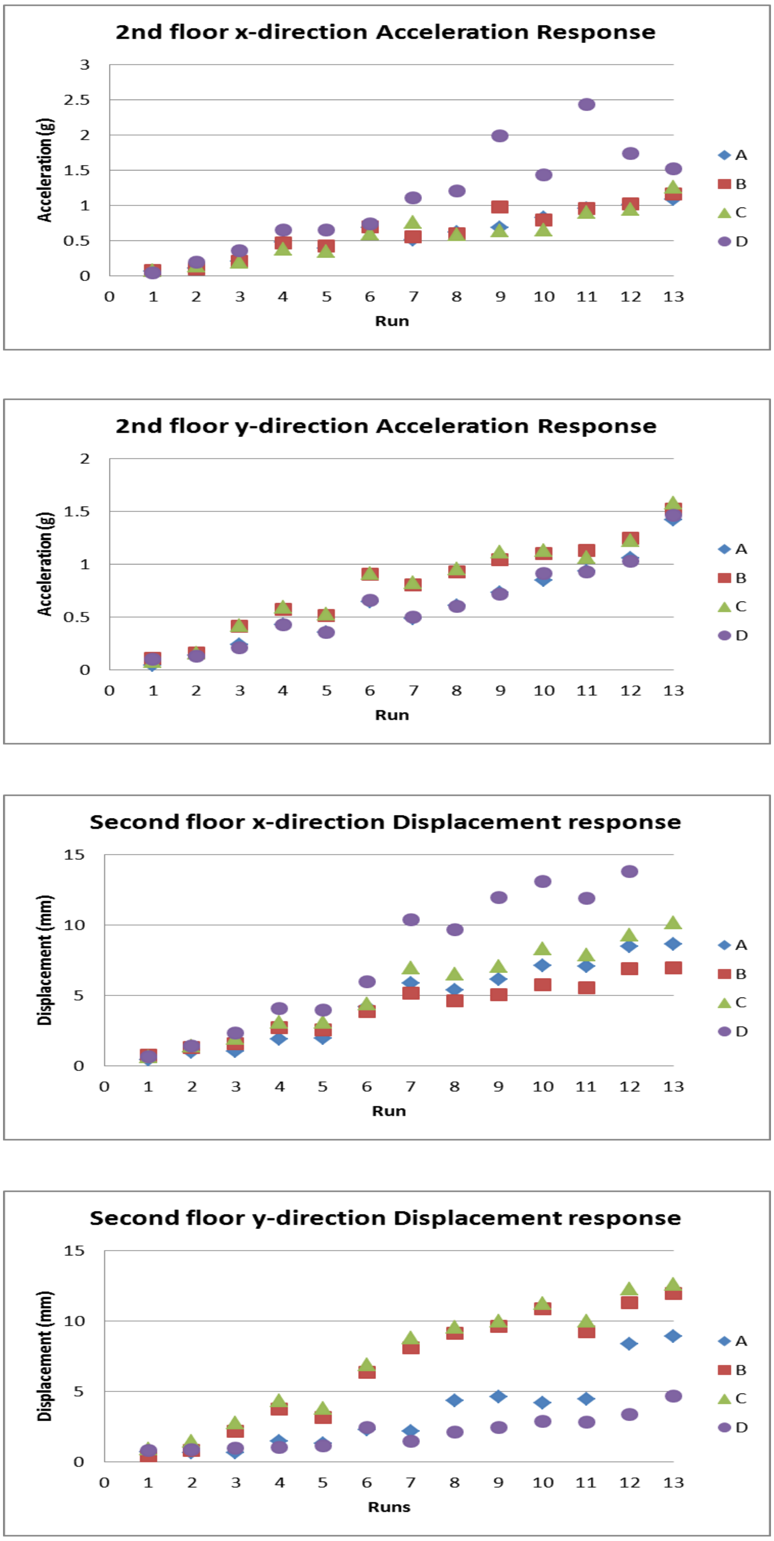

Figure 2-17 Maximum measured relative acceleration and displacement responses at second floor

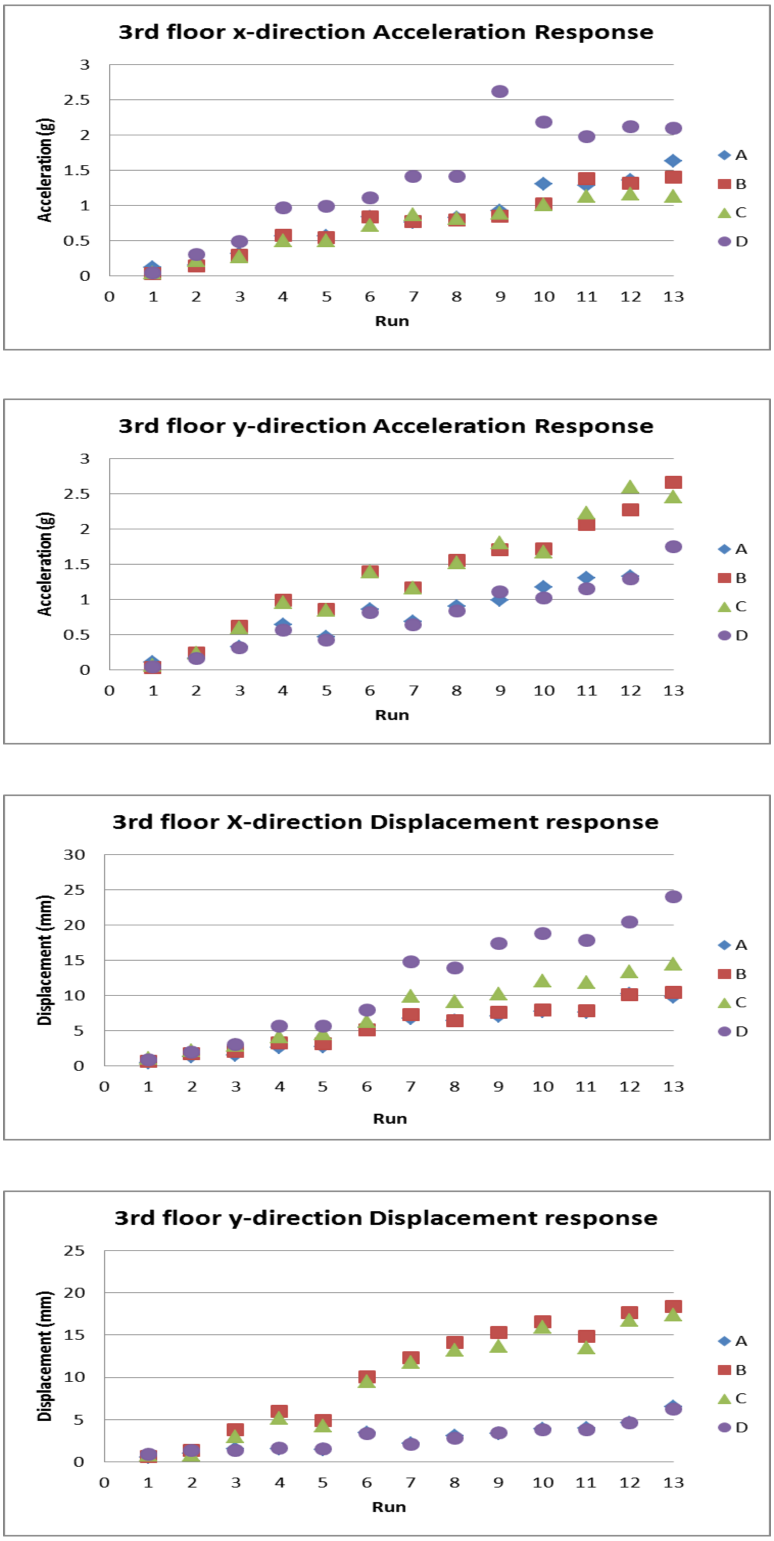

Figure 2-18 Maximum measured relative acceleration and displacement responses at 3rd floor

The relative horizontal displacements of each corner of the structure at 3rd floor under 0.1 g seismic test are presented in Figure 2.19. Displacements have been scaled to exhibit the structure behavior. Mass center and shear center are located on the figure (Lermitte et al., 2008). Blue data clouds show the top floor horizontal displacement time history data under 0.1 g (Run4) seismic test. These results show clear torsional behavior around shear center.

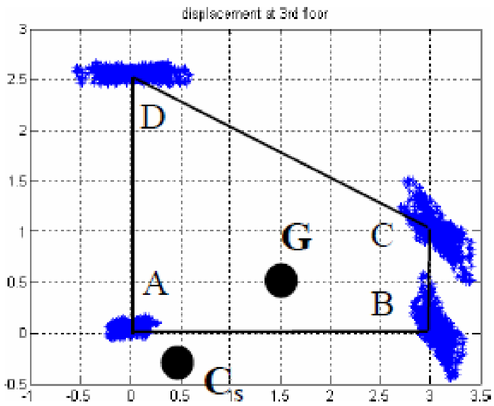

Figure 2-19 Top floor horizontal displacement - 0.1g (Run 4) seismic test, (G=Center of mass, C_s=Shear center),(Lermitte et al.,2008)

Results of the modal analysis for first seismic test in which PGA=0.05g are presented in Table 2.6.

Table 2-6 Initial natural frequencies (Lermitte et al., 2008)

Modes	f (Hz)	Type
Mode 1	6.24	Bending (Ox)
Mode 2	7.86	Bending (Oy)
Mode 3	15	Torsion

From the first 5 seismic tests, the structure did not suffer damage and no crack opennings were observed.

In Figure 2.20, crack patterns during the seismic excitation are observable. From Figure 2.20 it can be noted that the relatively wide cracks in the structure were obtained after 0.5 g seismic excitation level.

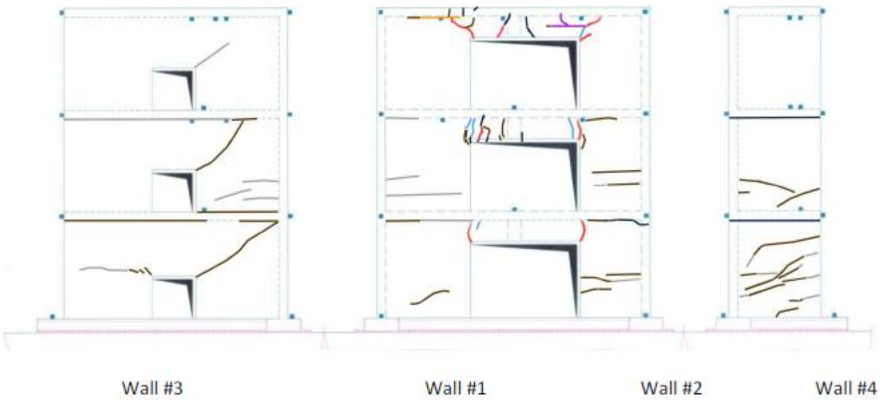

Legend	Red	Green	Blue	Black	Pink	Orange	Brown	Grey
Cracks	before	during	during	during	during	during	during	during
Acc (g)	0.3	0.35	0.55	0.56	0.67	0.77	1.06	1.13

Figure 2-20 Cracks after the seismic tests

2.4. The Modeling of Specimen

On account of developing a numerical model, which accurately reflects the properties of the system, the mock-up should be tested with the available analytical tools.

In this study, ANSYS R 12.1 was used as the analytical tool. ANSYS is a widely used finite element analysis (FEA) software which has many capabilities, ranging from a simple linear static analysis to a complex nonlinear transient dynamic analysis.

2.4.1. Element Types Used in the Analysis

In this study, shaking table and structural walls were modeled with SOLID 65 element. The reinforcing bars were modeled in a smeared manner by using the special rebar feature of the SOLID 65. COMBIN 14 (a spring element) was used for modeling the vertical rods supporting the shaking table. Also, MASS 21 element was used in order to assign mass to the system.

A description of finite elements and material models used in this study are presented below.

2.4.1.1. 3-D Reinforced Concrete Element (SOLID 65)

SOLID 65 element can be used for the three-dimensional modeling of reinforced concrete solids with or without reinforcing bars. The solid is capable of cracking in tension and crushing in compression. This element has eight nodes and each node has three translational degrees of freedom. Up to three different rebar specifications may be defined. Reinforcement in concrete can be added to the model by the "Smeared" approach for SOLID 65 or using the LINK 8, three dimensional truss elements. In this study, the smeared reinforcement method was used. The concrete material was assumed to be initially isotropic (Figure 2.21).

"The most important feature of this element is the behavior of nonlinear material properties. The concrete is capable of cracking (in three orthogonal directions), crushing, plastic deformation, and creep. The rebar is capable of carrying tension and compression, but not shear. They are also capable of plastic deformation and creep." (ANSYS R 12.1)

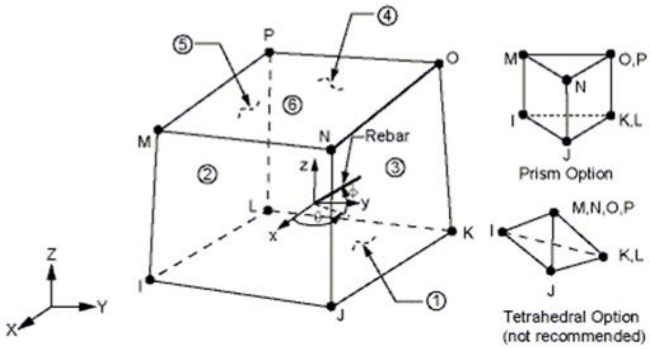

Figure 2-21 SOLID 65 (3-D Reinforced Concrete Element) (ANSYS R12.1)

2.4.1.1.1. Mathematical Description of SOLID 65 Element

SOLID 65 is an eight-noded isoparametric brick element and utilizes linear interpolation functions for the geometry and the displacements with the eight integration points (2x2x2). The interpolation function is given as follows:

$$N_i = \tfrac{1}{8}\,(1 \pm \xi)\,(1 \pm \eta)\,(1 \pm \xi), \qquad \text{where } i \in 1, \ldots , 8 \qquad (2.1)$$

According to this interpolation function, the nodal displacements (u_i, v_i, w_i,) calculated at the nodes are interpolated at any point (ξ, η, ζ) within the element as

$$u = u_1 N_1 + u_2 N_2 + \ldots + u_8 N_8$$

$$v = v_1 N_1 + v_2 N_2 + \ldots + v_8 N_8$$

$$w = w_1 N_1 + w_2 N_2 + \ldots + w_8 N_8 \qquad (2.2)$$

Variable integration scheme (Gauss integration) of 2x2x2 is employed for calculation of the displacement field in the element.

2.4.1.1.2. Assumptions and Restrictions for SOLID 65 Element

Zero volume elements are not allowed and all elements must have eight nodes. Cracking is permitted in three orthogonal directions at each integration point. The orientation of the reinforcement and local coordinates are defined in Figure 2.22. If cracking occurs at an integration point, the cracking is modeled through an adjustment of material properties which effectively treats the cracking as a "smeared band" of cracks, rather than as discrete cracks. The sum of the volume ratios for all rebar must not be greater than 1.0.

"When both cracking and crushing are used together, care must be taken to apply the load slowly to prevent possible fictitious crushing of the concrete before proper load transfer can occur through a closed crack. This usually happens when excessive cracking strains are coupled to the orthogonal uncracked directions through Poisson's effect.

Also, at those integration points where crushing has occurred, the output plastic and creep strains are from the previous converged substep. Furthermore, when cracking has occurred, the elastic strain output includes the cracking strain. The lost shear resistance of cracked and/or crushed elements cannot be transferred to the rebar, which have no shear stiffness. In addition to cracking and crushing, the concrete may also deform plastically, with the Drucker-Prager failure surface being most commonly used. In this case, the plasticity check is done before the cracking and crushing checks. The element is nonlinear and requires an iterative solution." (ANSYS.12.1)

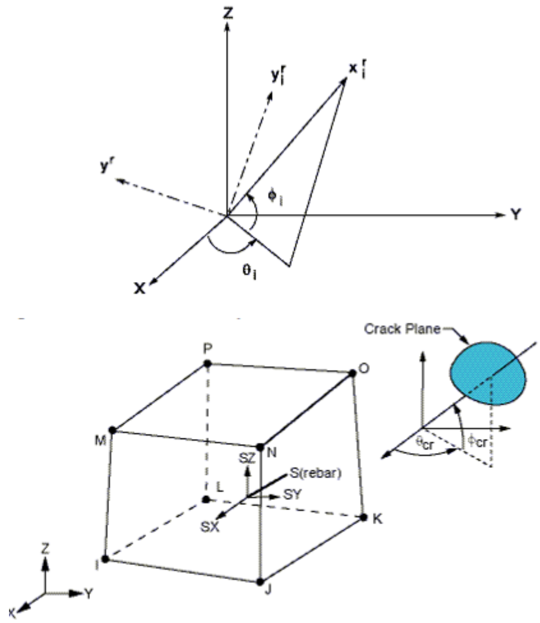

Figure 2-22 Reinforcement Orientation in SOLID 65

2.4.1.2. MASS21 (Structural Mass)

MASS21 is a point element that has up to six degrees of freedom (DOF). These DOFs are translations in the nodal x, y, and z directions and rotations about the nodal x, y, and z axes (Figure 2.23). A different mass and rotary inertia may be assigned to each nodal coordinate direction.

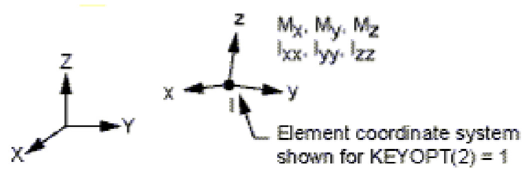

Figure 2-23 MASS21 Geometry

2.4.1.3. COMBIN 14

"In the numerical model vertical rods supporting the shaking table were included and assigned a stiffness to capture the measured vertical frequencies. For these rods, a spring element, COMBIN 14 was used. This element has longitudinal or torsional capability in 1-D, 2-D or three-dimensional applications. The geometry, node locations, and the coordinate system for this element are shown in Figure 2.24. The longitudinal spring-damper option is a uniaxial tension compression element with up to three degrees of freedom at each node:

Translations in the nodal x,y and z directions. No bending or torsion is considered.

The torsional spring-damper option is a purely rotational element with three degrees of freedom at each node:

Rotations about the nodal x,y and z axes. No bending or axial loads are considered." (ANSYS.12.1)

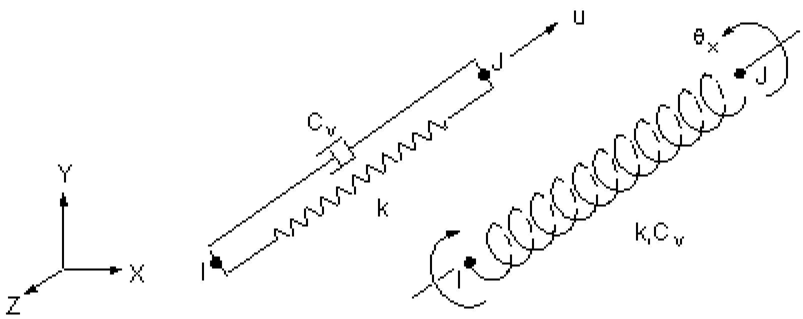

Figure 2-24 COMBIN 14 (ANSYS R12.1)

The spring-damper element has no mass. Masses can be added by using the appropriate mass element (MASS 21). The element is defined by two nodes, a spring constant (k), and damping coefficients $(c_v)_1$ and $(c_v)_2$. The elastic constant of each spring element was taken as K=215 MN/m (in accordance with the experimentally measured response) in the numerical computations.

2.4.2. Material Properties

Density of the concrete is considered as 2460 kg/ m^3 and Young Modulus of concrete is 32000 MPa according to the SMART 2008 Phase 2 report given by CEA as described in 2.2.1.1 (RAPPORT DM2S, 2009).

MKIN and CONCRETE are used for the concrete in the model. MKIN (Multi linear kinematic hardening), rate-depended plasticity is used (Figure 2.26).

CONCRETE is a defined material model in ANSYS for Willam – Warnke material model. For this material type open shear transfer coefficient, 0.2 and closed shear transfer coefficient, 0.8, are used. Uniaxial cracking stress is 2.4 MPa.

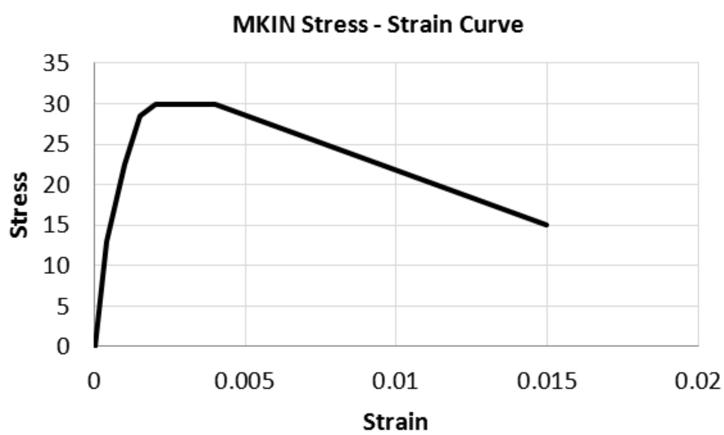

Figure 2-25 MKIN stress- strain curve

2.4.3. Meshing

Meshing type is one of the significant aspects of the finite element modeling. The model building walls are meshed by mapping with hexahedral shapes. The important point in mapping in this study is that to keep the element dimension ratio smaller than 1.5. The slabs and the connections between the column-slab and column- beam were meshed with the sweep option in ANSYS (ANSYS R 12.1). The model representation is given in Figures 2.27 and 2.28. The thickness of the walls and the slabs depth divided into two pieces to be able to capture the behavior under seismic activity.

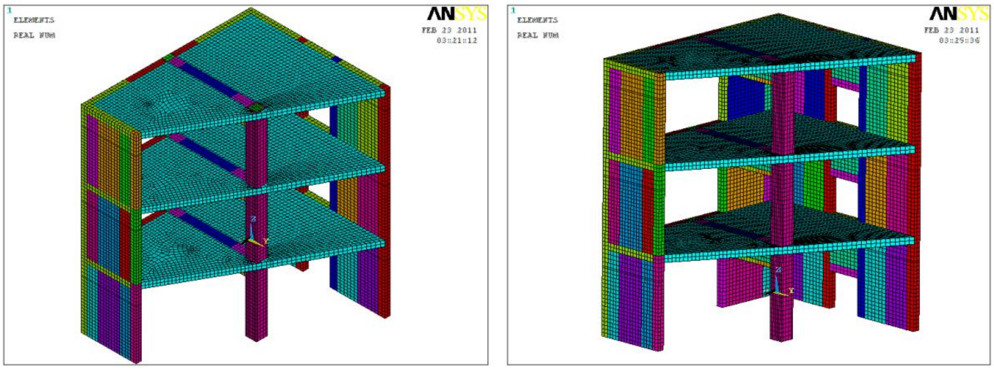

Figure 2-26 Representations of the fixed-base model building

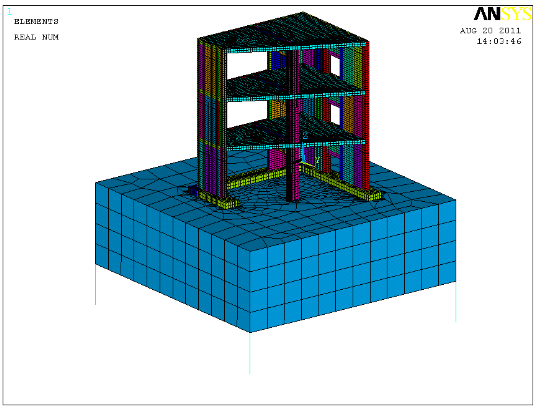

Figure 2-27 Representations of the shaking table model building

2.4.4. General Information for the simulation

The fixed-base model developed for this study consists of 28740 SOLID65 (3-D Reinforced concrete elements) and 5282 MASS21 (Structural mass) element types. Also, the model has 43179 nodes for calculations. Seismic excitations were applied at basement level in the analytical model.

The given figures of the model (Figures 2.27-2.28) were chosen for their real constant change. In other words, different colors in the model represent the change in the reinforcement ratios in concrete elements. 74 real constants were defined in the model for the reasonably accurate simulation of the real structure with smeared modeling approach of the reinforcement.

Shaking table model consists of 36074 SOLID 65 and 5282 MASS 21 and 4 COMBIN 14 element types. Number of nodes for calculations is 52008. 78 real constants were defined in shaking table model. Total mass of the structure is equal to 68,212 kg (specimen + shaking table).

The structural damping value was considered 2 % in time history analyses. Damping parameters (Alpha and Betha) were calculated according to the Reyleigh method (Chopra, 2000). For model with the shaking table:

α (Mass matrix multiplier for damping) = 1.085

β (Stiffness matrix multiplier for damping) = 3.7 e^{-4}

CHAPTER 3

ANALYSIS OF MODELS

3.1. General

The primary objective of the analyses was to obtain a valid and adequate model that can simulate the experimental response of the specimen. For this reason, two models were generated. In the first model, the effect of shaking table was ignored and the base of the specimen was considered as fixed.

In the second model, the shaking table was also included in the model. In order to check adequacy of the model, first experimentally obtained modal properties that is modal frequencies were compared with ones obtained from numerical analysis. Then, displacement time histories and response spectra computed at different points on the third floor were compared.

The analyses for Runs 1-10 were carried out sequentially in order to represent the actual loading history. In time history analyses, a constant damping ratio of 2% was assumed for each mode.

3.1.1. Fixed-base model

The mock-up was modeled in ANSYS software according to the specifications described in the SMART 2008 Phase 1 report (ANSYS R 12.1). The seismic excitations used in experimental runs were applied consecutively in the time history analysis. This means that following response in the elastic range, plastic deformations increased cumulatively. The results were compared to the experimental results. In first model, the shaking table was not included and the base of the specimen was considered as fixed (Figure 2.27).

3.1.1.1. Comparison of frequencies

Modal analyses were performed to obtain the frequencies from the two models developed. The first three mode shapes are given in Figure 3.1 for the case of fixed base. Modal frequencies of the specimen were measured and reported during the experimental phase (Table 2-6). The frequencies obtained from analyses are compared with the experimental ones in Table 3.1. These results indicate that the numerical model is stiffer than the mock-up as it yields larger frequencies in all modes.

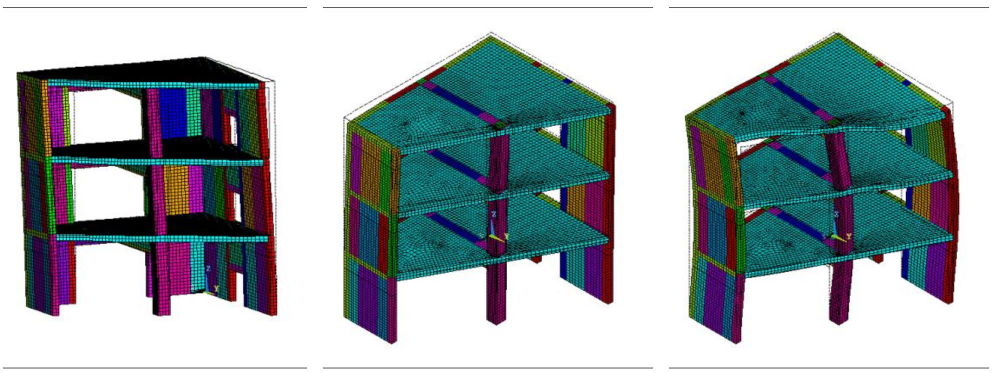

a) b) c)

Figure 3.1 First three modes of the specimen calculated for the fixed base model a) Mode 1: F=9.23 (Hz), b) Mode 2: F=15.93 (Hz), c) Mode 3: F=32.76 (Hz)

Table 3-1 Comparisons of Frequencies obtained from Fixed-base Model with Experimental results

Modes	Frequency (Hz)	
	Experimental	Model with fixed base
Mode 1	6.24	9.23
Mode 2	7.86	15.93
Mode 3	15.00	32.76

3.1.1.2. Comparison of displacements

In following figures the displacements of fixed-base model obtained from FEA at each point on the third floor are compared with measured results. It is observable that the finite element model cannot replicate the behavior under the low seismic excitation.

This difference may come from many reasons such as the connection problem of the mock-up to the shaking table, element inadequacy of finite model or assumptions made for the basement nodes.

Low excitations are influenced more from noise as well. Additionally, there are many other unknown variables that may affect this behavior under the stronger seismic excitations.

At larger excitation levels, the match between the measured and calculated response improves such that a better representation on the experimental behavior is achieved. The time step in the acceleration data was 0.025 second and time duration for each run was approximately 6 seconds.

Experimental and analytical results are in phase yielding better agreement especially at point A that has relatively less torsional response. The match is not as good at other points where analytical results generally yielding smaller displacements.

The difference between trend of displacements at points A,B,C and D is due to torsional behavior of the structure.

Also it is to be noted that, the maximum values of displacement in numerical and experimental results are in the same frequency.

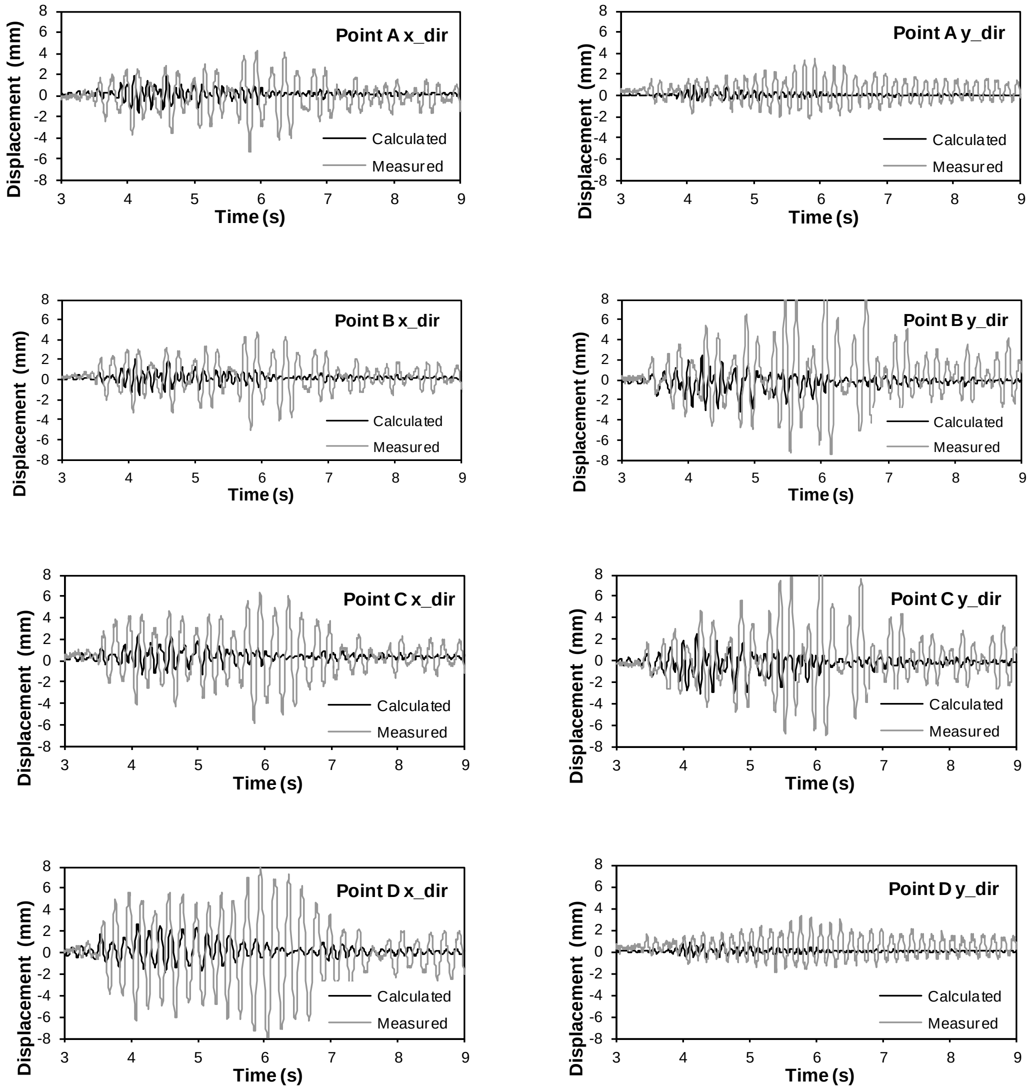

Figure 3.2 Displacement comparison of the experimental results and analytical results at the 3rd floor for Run 3 (Accsyn-0.3g) fixed-base model

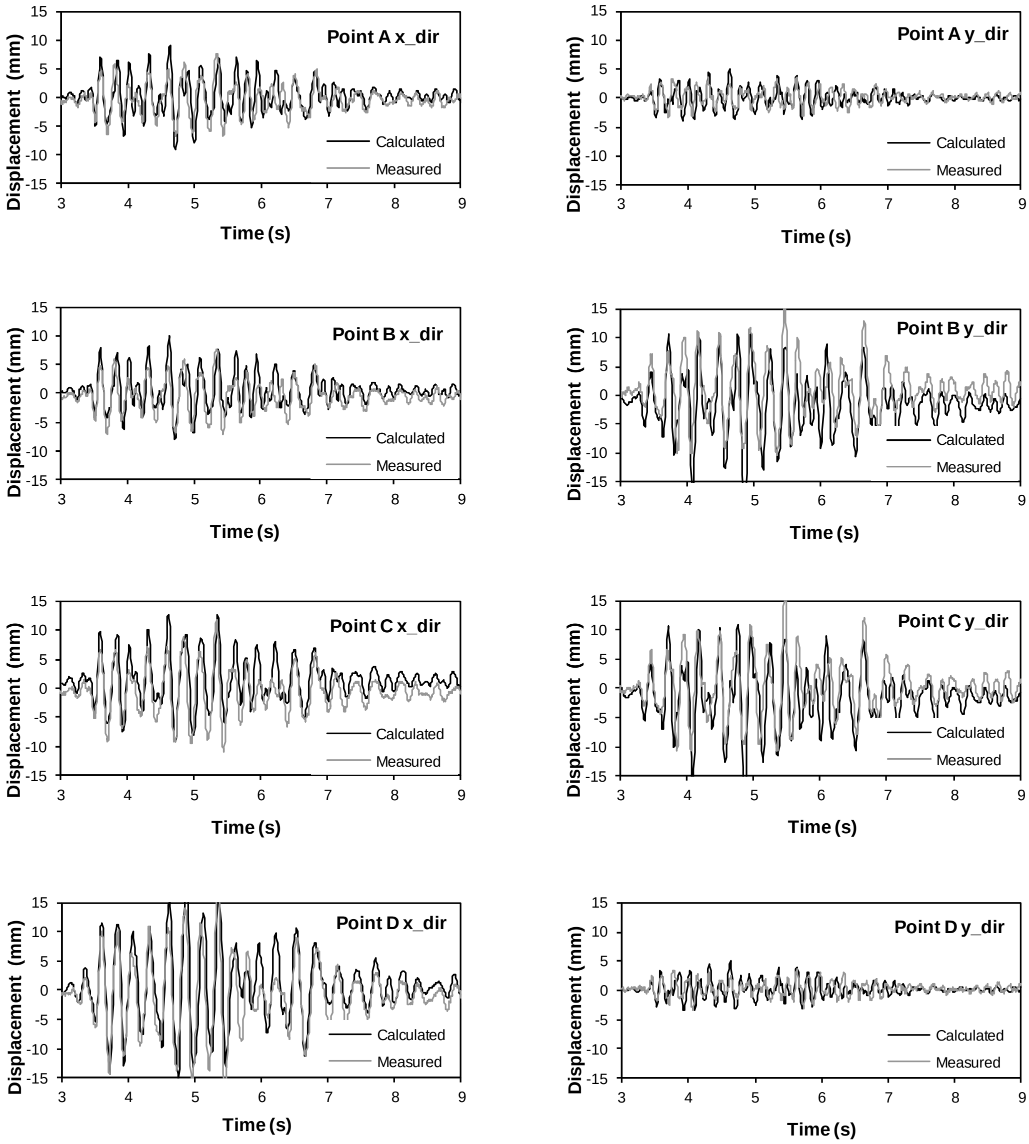

Figure 3.3 Displacement comparison of the experimental results and analytical results at the 3rd floor for Run 7 (Accsyn-0.7g) fixed-base model

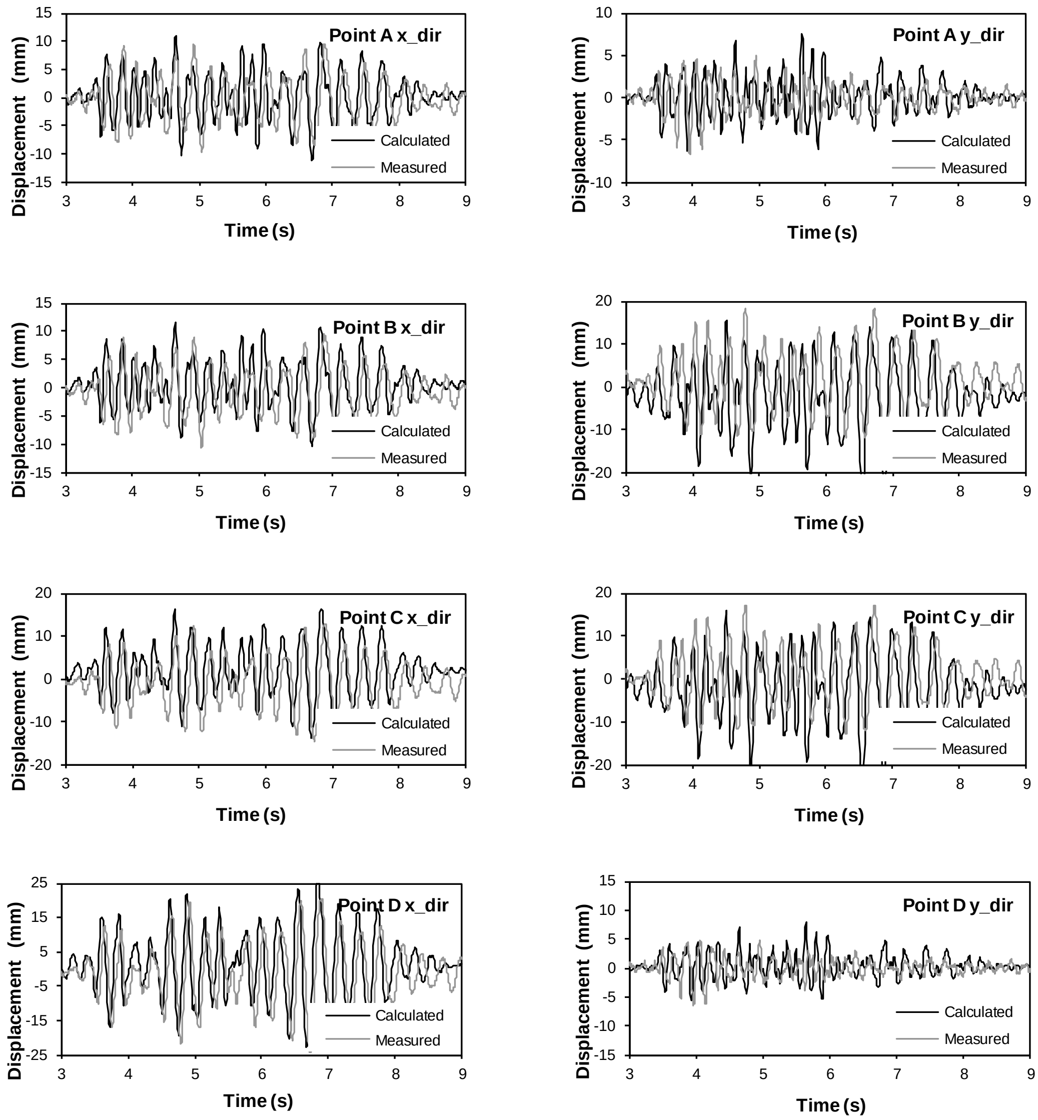

Figure 3.4 Displacement comparison of the experimental results and analytical results at the 3rd floor for Run 10 (Accsyn-1.0 g) fixed-base model

3.1.1.3. Comparison of accelerations

For analyzing the performance of the structure in earthquakes and assessing the peak response of building to earthquake, the response spectrum plot considering the damping ratio as 5% for each point at the 3rd floor were generated.

The results were compared with the experimental results. In the following figures the response spectra for accsyn 0.3, 0.7 and 1.0 g are given (Figures 3.5-3.7).

These comparisons reveal unsatisfactory results obtained from numerical analyses. Due to stiffer nature of the numerical model experimental spectra are underestimated. Additionally, frequency content and spectral values are not adequately predicted.

It is observable that, except point D, the maximum value of accelerations of numerical model occurs in y-direction. The maximum spectral acceleration is 5.99 g corresponding to frequency of 10.12 Hz at point B, y-direction for Run3.

For Run 7 we can observe that similar to Run 3, this maximum value is 12.49 g corresponding the frequency of 6.69 Hz at point B, y-direction.

At Run 10 the value of maximum spectral acceleration is 16.5 g at frequency of 14.17 Hz and occurs at point D, x-direction.

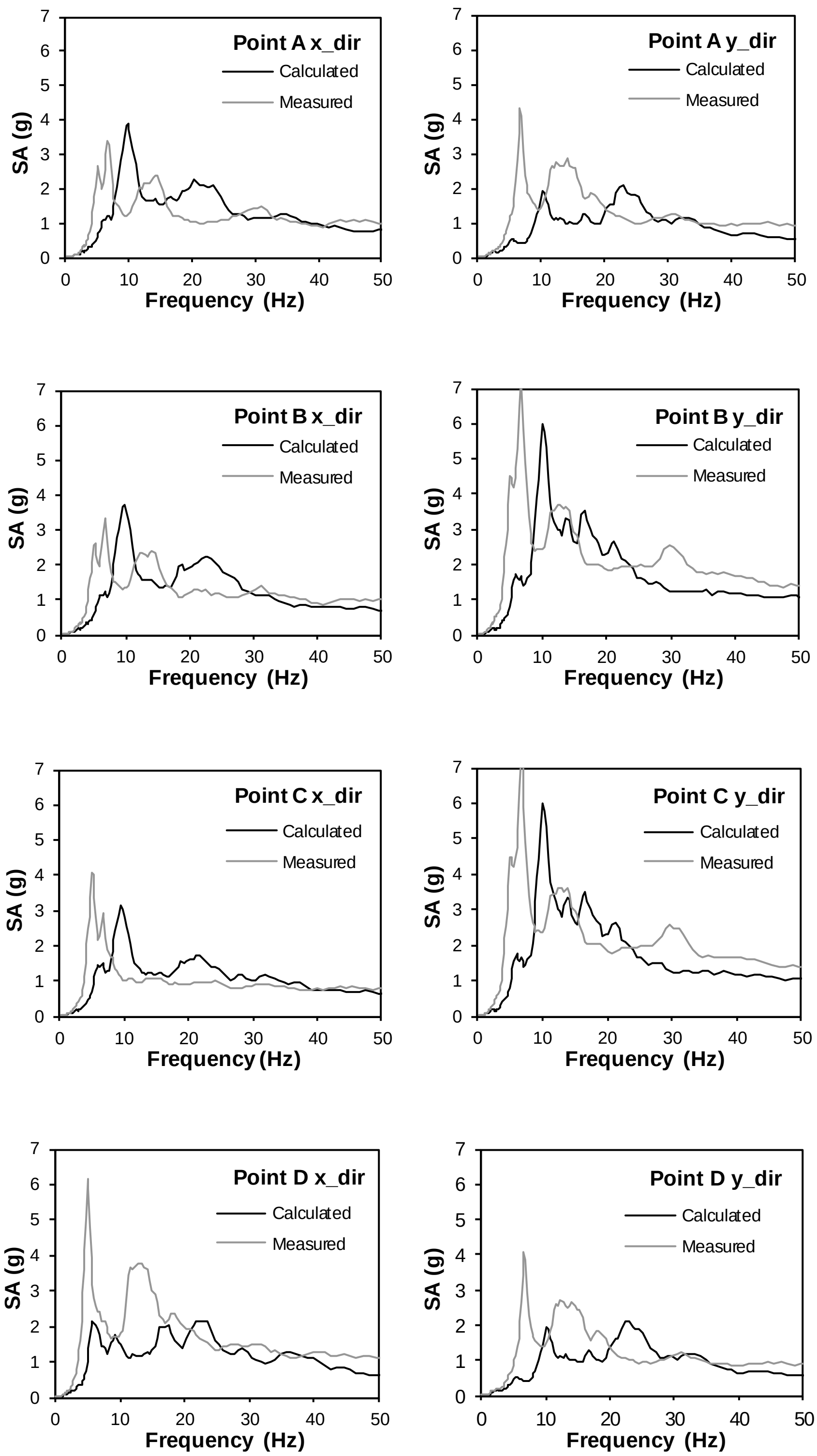

Figure 3.5 Acceleration Response Spectrum comparison of the experimental and analytical results at the 3rd floor for Run 3 (Accsyn-0.3 g) fixed-base model, Damping ratio=5 percent

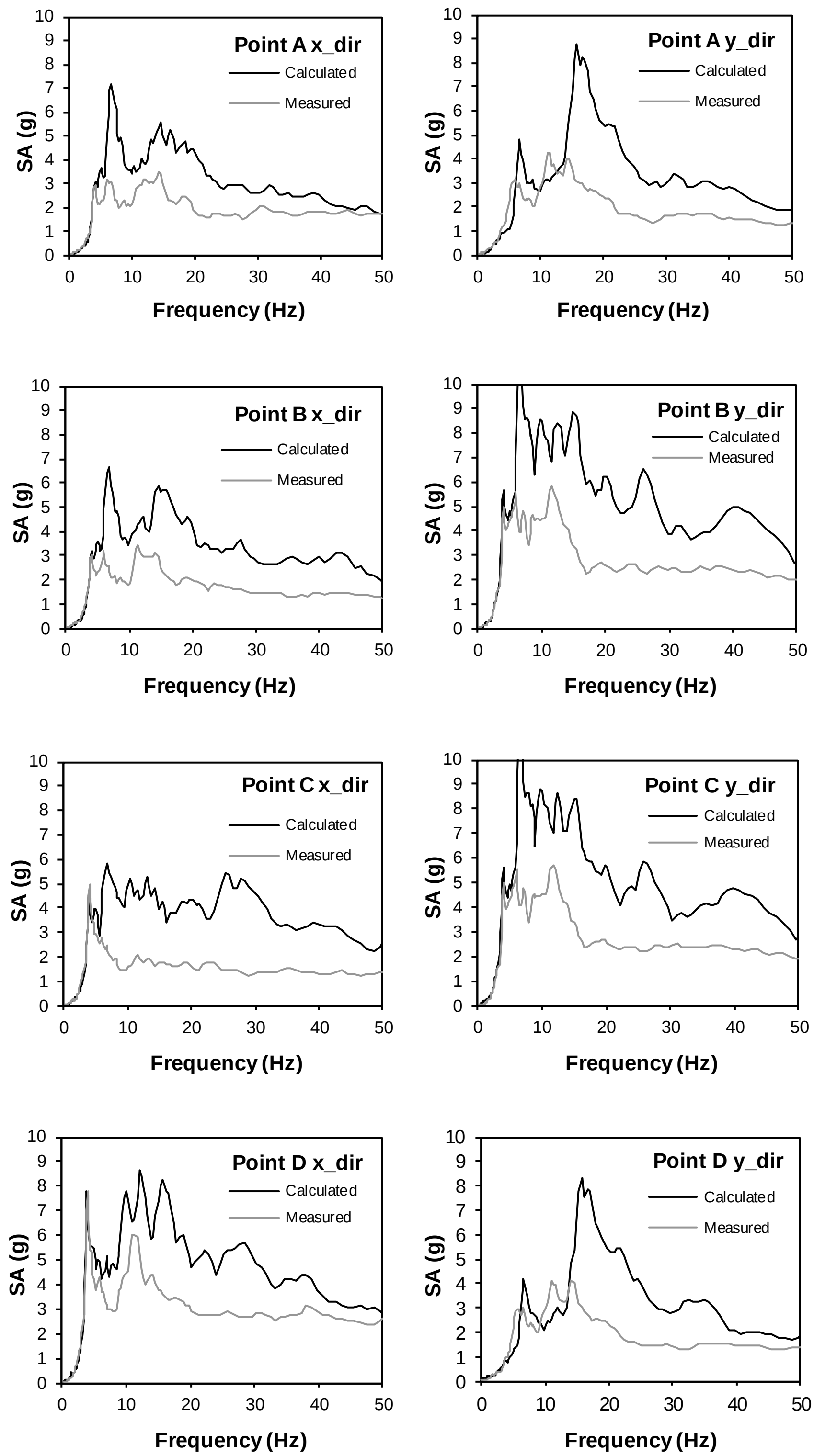

Figure 3.6 Acceleration Response Spectrum comparison of the experimental and analytical results at the 3rd floor for Run 7 (Accsyn-0.7 g) fixed-base model, Damping ratio=5 percent

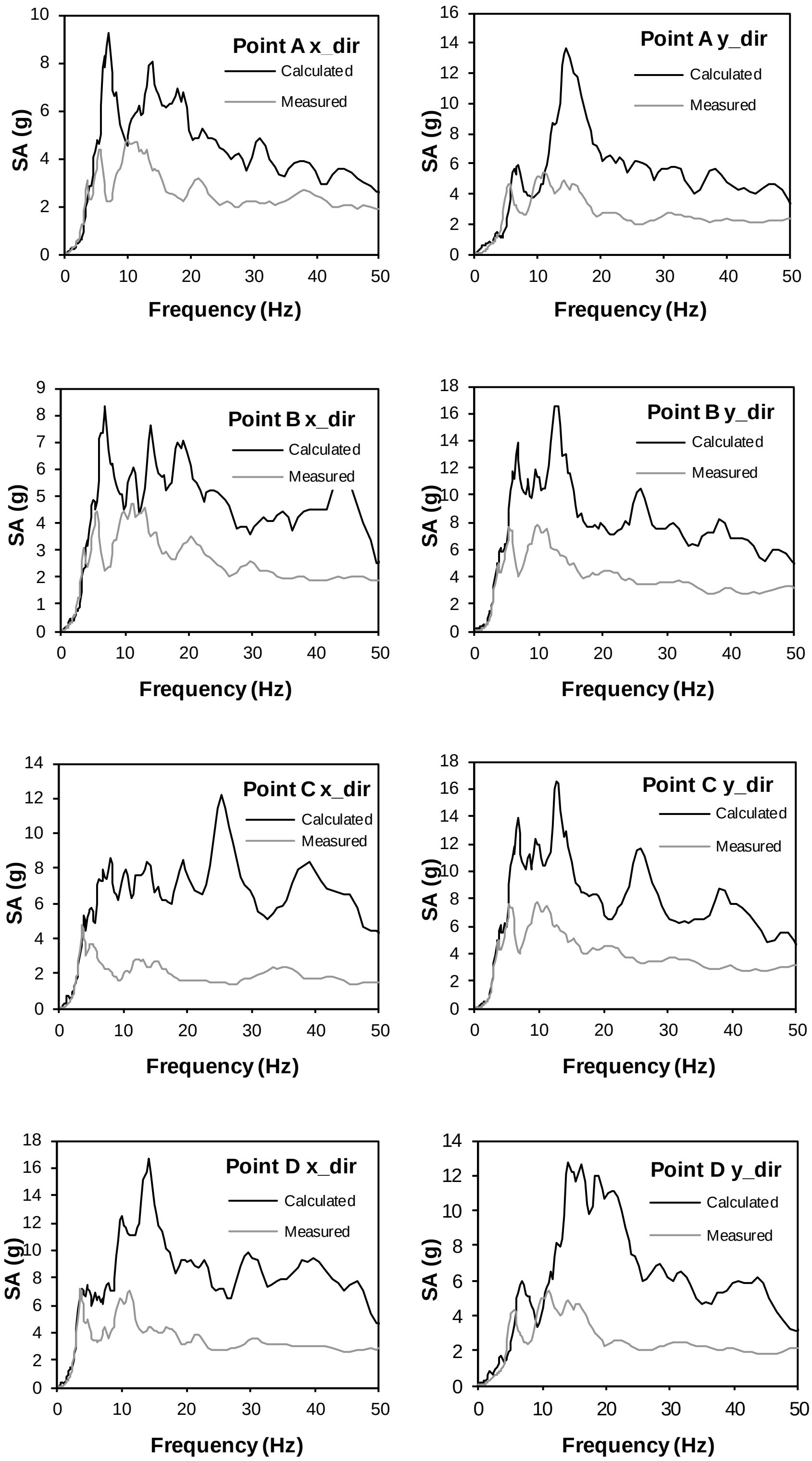

Figure 3.7 Acceleration Response Spectrum comparison of the experimental and analytical results at the 3rd floor for Run 10 (Accsyn-1.0 g) fixed-base model, Damping ratio=5 percent

3.1.2. Shaking-table Model

The shaking table model reshown in Figure 3.8 incorporates the flexibility that has been reported to be as an issue of the shaking table that may influence the results. Ground motions measured on the table were found to be different from the ones applied through actuators pointing to the table's flexibility. This flexibility was introduced through four springs defined at the bottom of the table which is also included in the model.

Considering the high stiffness of the shaking table, the finite element representing the shaking table were assumed to remain elastic and almost infinitely rigid. The total mass of the shaking table was uniformly distributed to these finite elements.

After modeling the foundations and shaking table the modal and time history analyses that were carried out for the fixed-base model were repeated.

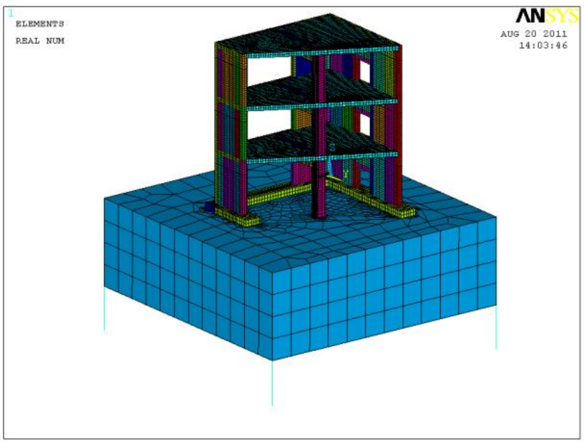

Figure 3.8 Model with simulation of shaking table

In the following sections comparison of frequencies, displacements and accelerations are investigated.

3.1.2.1. Comparison of frequencies

Mode shapes obtained from the model with shaking table are shown in Figure 3.9. Table 3.2 presents the first 8 frequencies for this model. The first three frequencies are compared with experimental ones in Table 3.3. It appears that the modal properties obtained from the model with shaking table are much closer to measured ones. The oscillation of the specimen causes vertical displacements on the shaking table and results in significant reductions of the corresponding natural frequencies of the system (shaking table + specimen).

Table 3-2 Results of Modal analysis for shaking-table model

Mode	Frequency (Hz)
1	7.8705
2	10.619
3	16.605
4	22.173
5	34.157
6	37.337
7	38.767
8	40.521

Table 3-3 Comparisons of Frequencies and Periods obtained from Shaking table Model with Experimental results

a) Comparison of frequencies:

	Experimental –f (Hz)	Model with shaking table-f(Hz)
Mode 1	6.24	7.87
Mode 2	7.86	10.62
Mode 3	15	16.61

b) Comparison of periods:

	Experimental –T(s)	Model with shaking table-T (s)
Mode 1	0.16	0.13
Mode 2	0.13	0.09
Mode 3	0.07	0.06

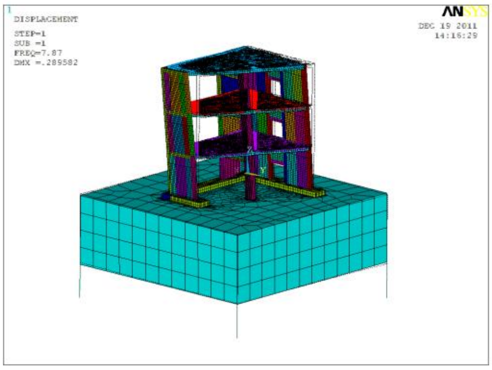

a)

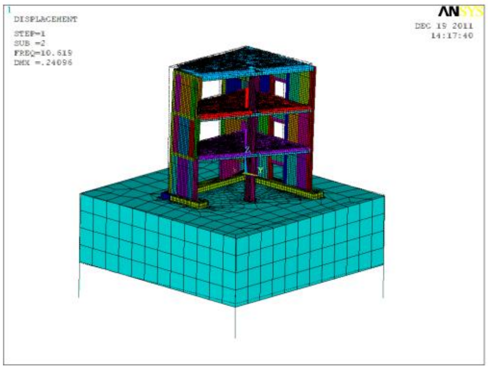

b)

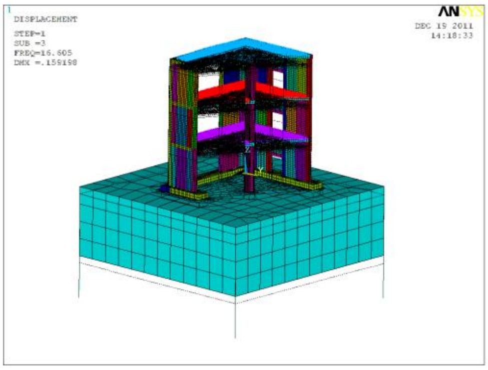

c)

Figure 3.9 First three modes of the specimen calculated for the fixed base model a) First mode shape-Model with shaking table f=7.8705 Hz b) Second mode shape Model with shaking table f=10.619 Hz c) 3rd mode shape-Model with shaking table f=16.605 Hz

3.1.2.2. Comparison of displacements

The displacement traces calculated from the model at the specified points are compared with the experimental results in Figures 3.10-3.12. Displacement trends obtained are similar to the ones observed in the fixed base model: at larger excitations better match is obtained. Flexibility of the model is well reflected in the comparisons as calculated response appears to be generally overestimating the experimental ones.

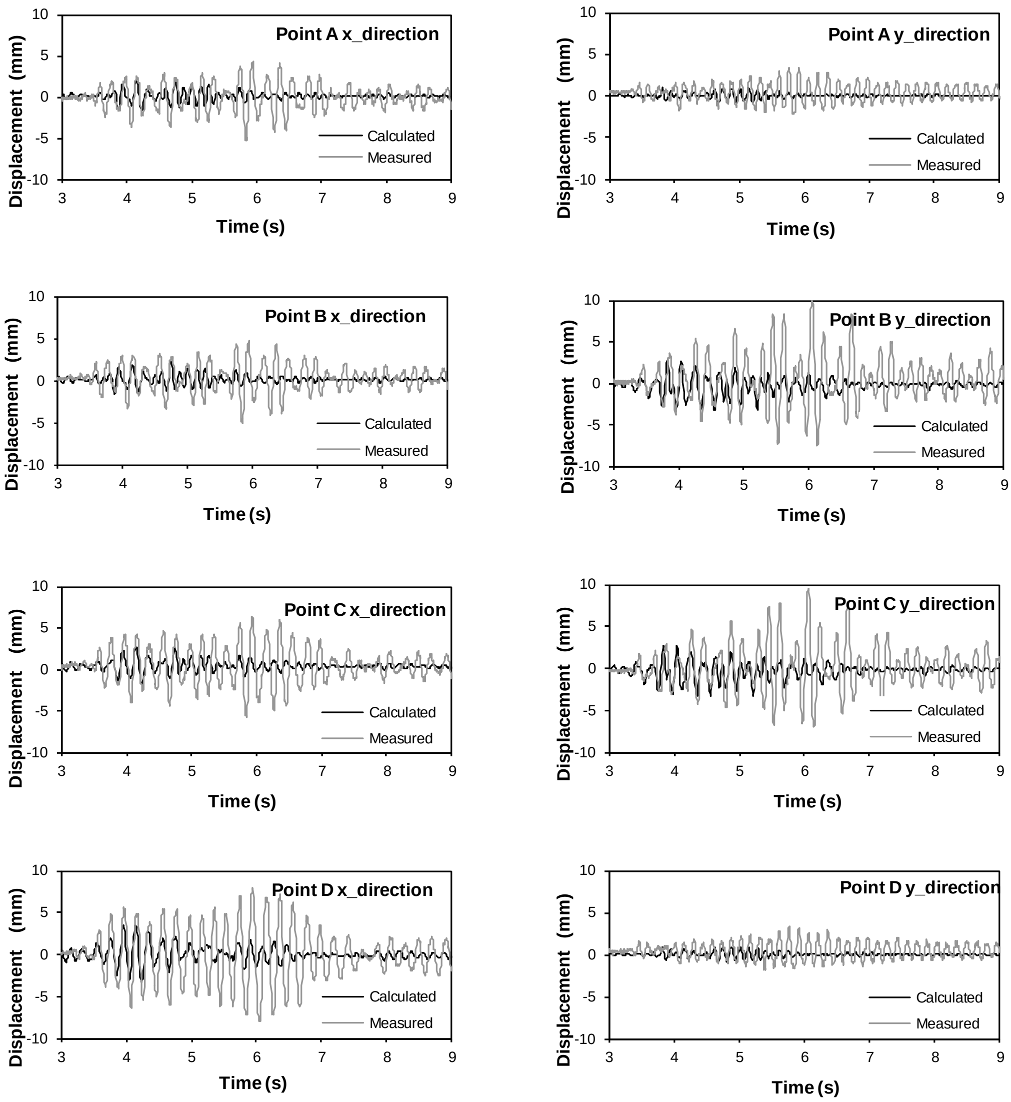

Figure 3.10 Displacement comparison of the experimental results and analytical results at the 3rd floor for Run 3 (Accsyn-0.3g) shaking table model

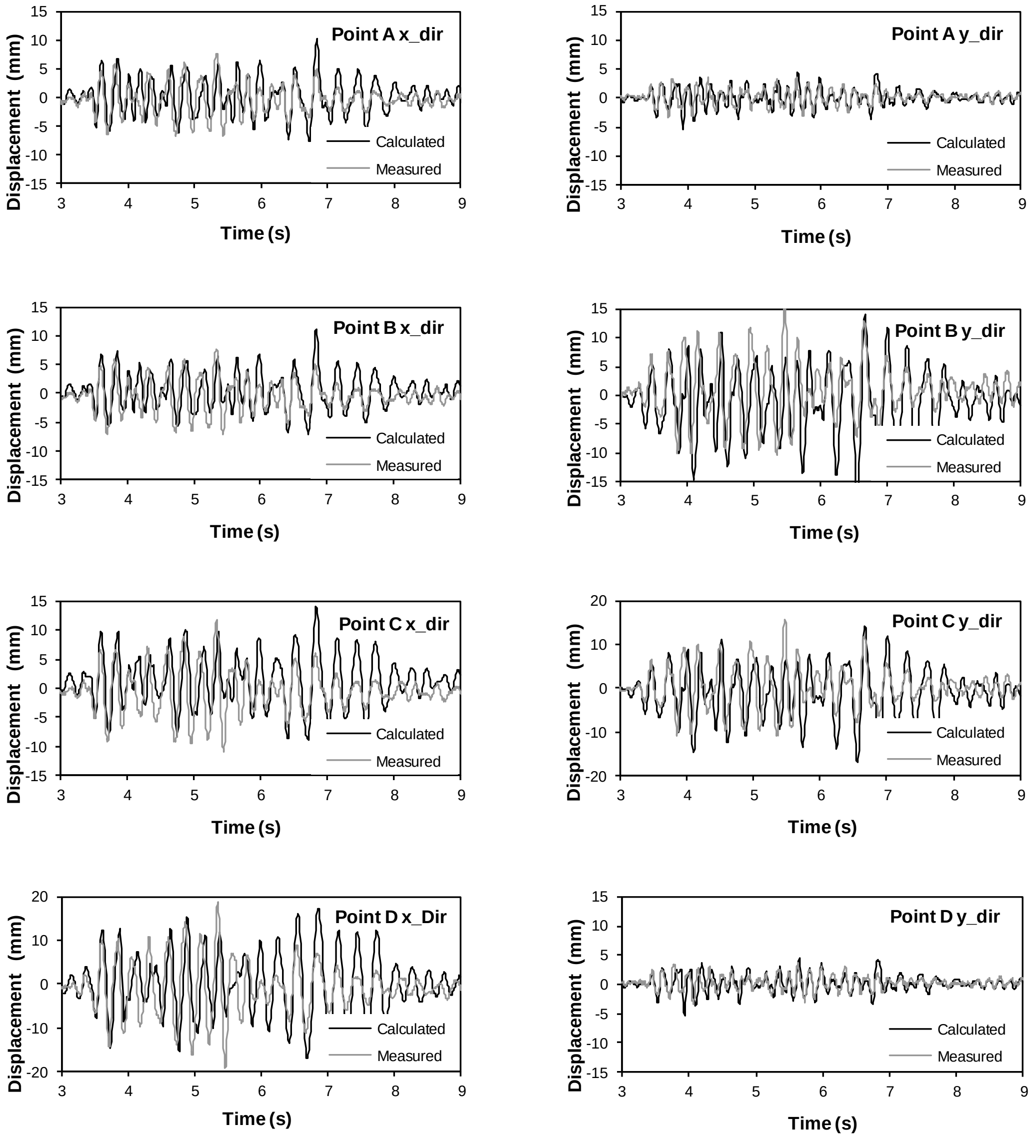

Figure 3.11 Displacement comparison of the experimental results and analytical results at the 3rd floor for Run 7 (Accsyn-0.7g) shaking table model

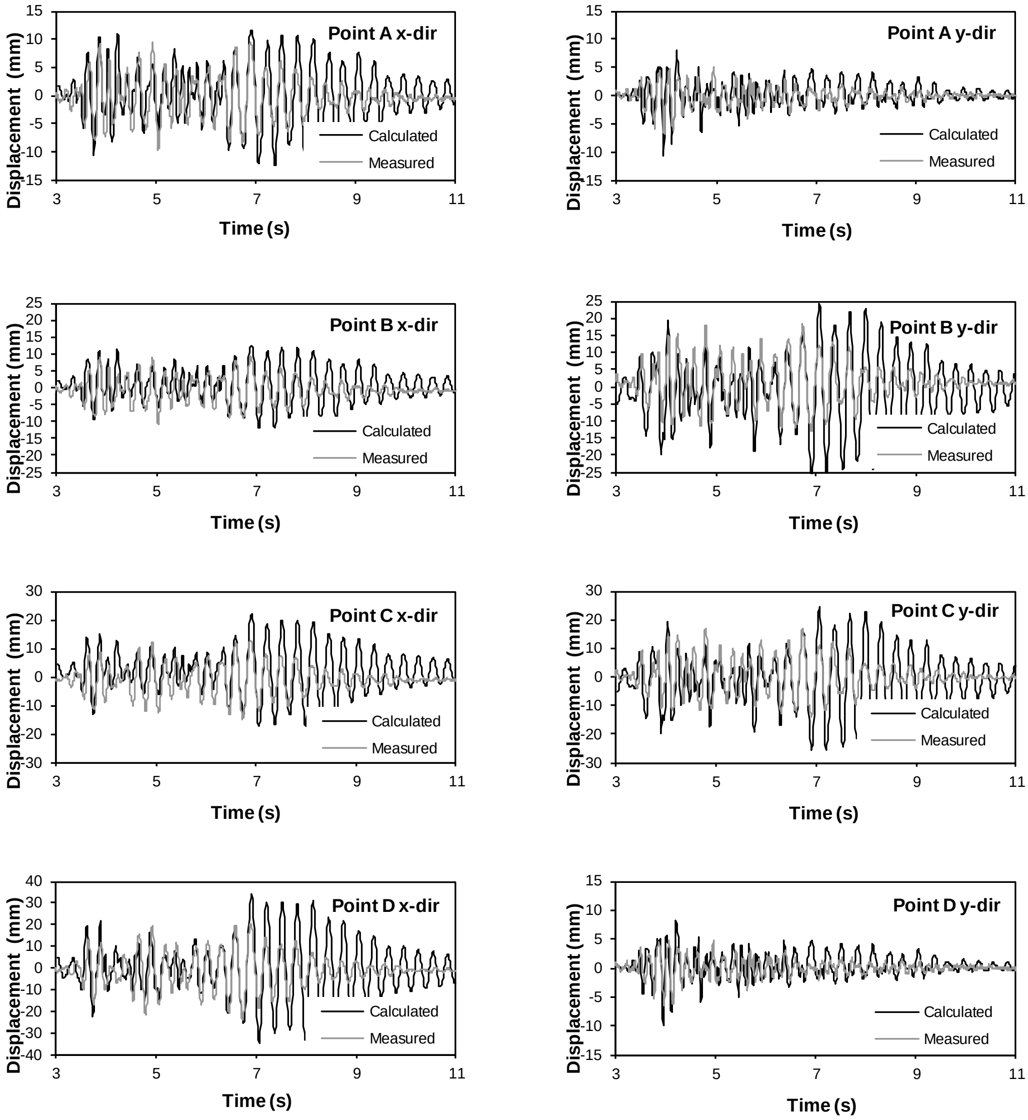

Figure 3.12 Displacement comparison of the experimental results and analytical results at the 3rd floor for Run 10 (Accsyn-1.0g) shaking table model

3.1.2.3. Comparison of accelerations

Influence of shaking table on acceleration response is displaced through comparisons of floor response spectra calculated at specified point on the third floor (Figures 3.13-3.15).

Although a significant improvement over the response is observed for Run 3, there is still clear disagreement for other excitations. Despite good match at points A and in certain cases at point D, this model does not provide adequate results at other points.

Similar to fixed-base model, except point D, the maximum value of accelerations of numerical model occurs in y-direction.

The maximum spectral acceleration is 4.34 g corresponding to frequency of 9.53 Hz and 9.25 Hz at points B and C, respectively, at y-direction for Run3.

For Run 7 we can observe that, this maximum value is 10.10 g corresponding to the frequency of 12.71 Hz at point D, x-direction.

At Run 10 the value of maximum spectral acceleration is 16.9 g at frequency of 11.36 Hz and occurs at point C, y-direction.

The Figures 3.13-3.15 depict that experimental spectra are overestimated at the low seismic tests and underestimated at the high seismic tests.

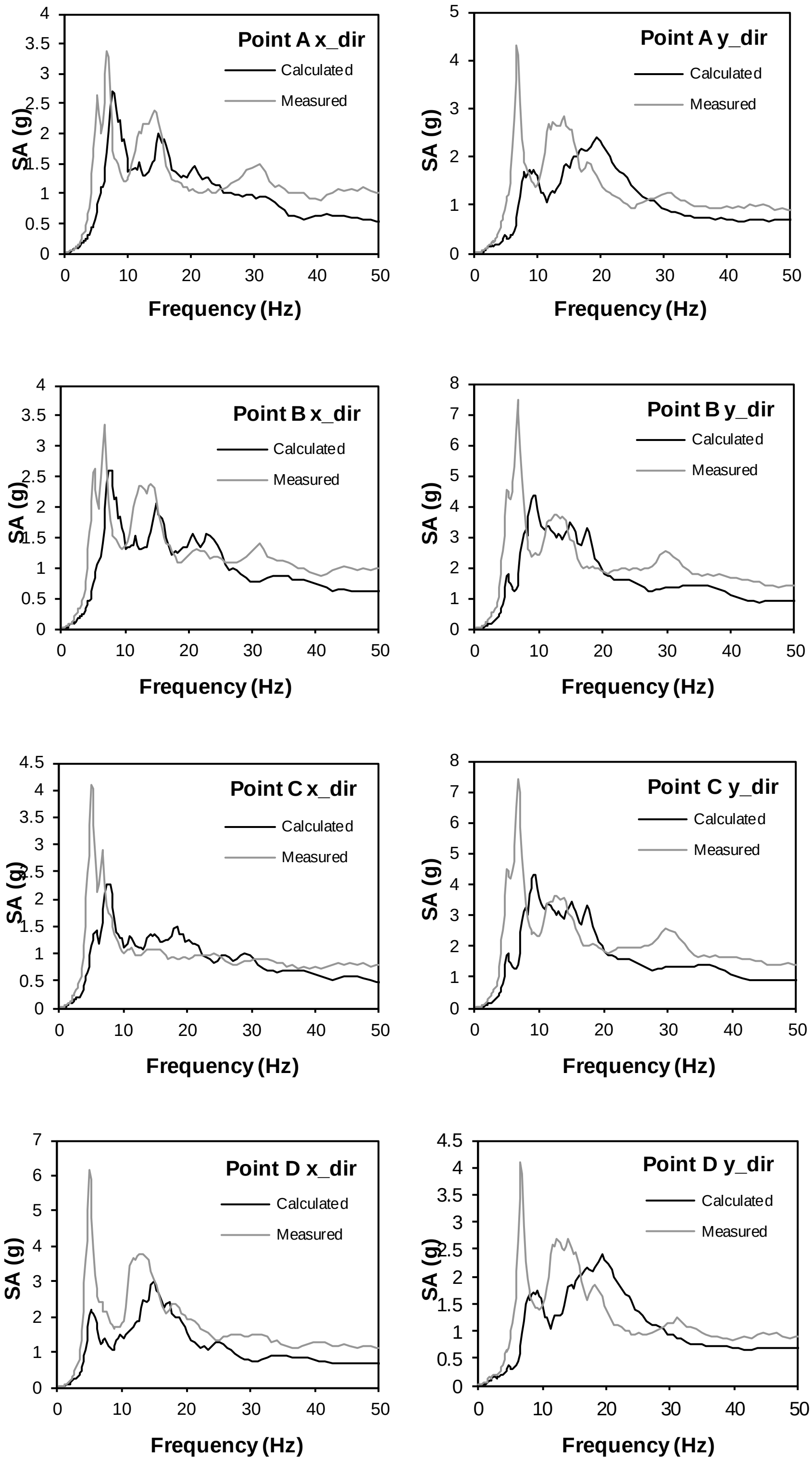

Figure 3.13 Acceleration Response Spectrum comparison of the experimental and analytical results at the 3rd floor for Run 3 (Accsyn-0.3 g) shaking table model, Damping ratio=5 percent

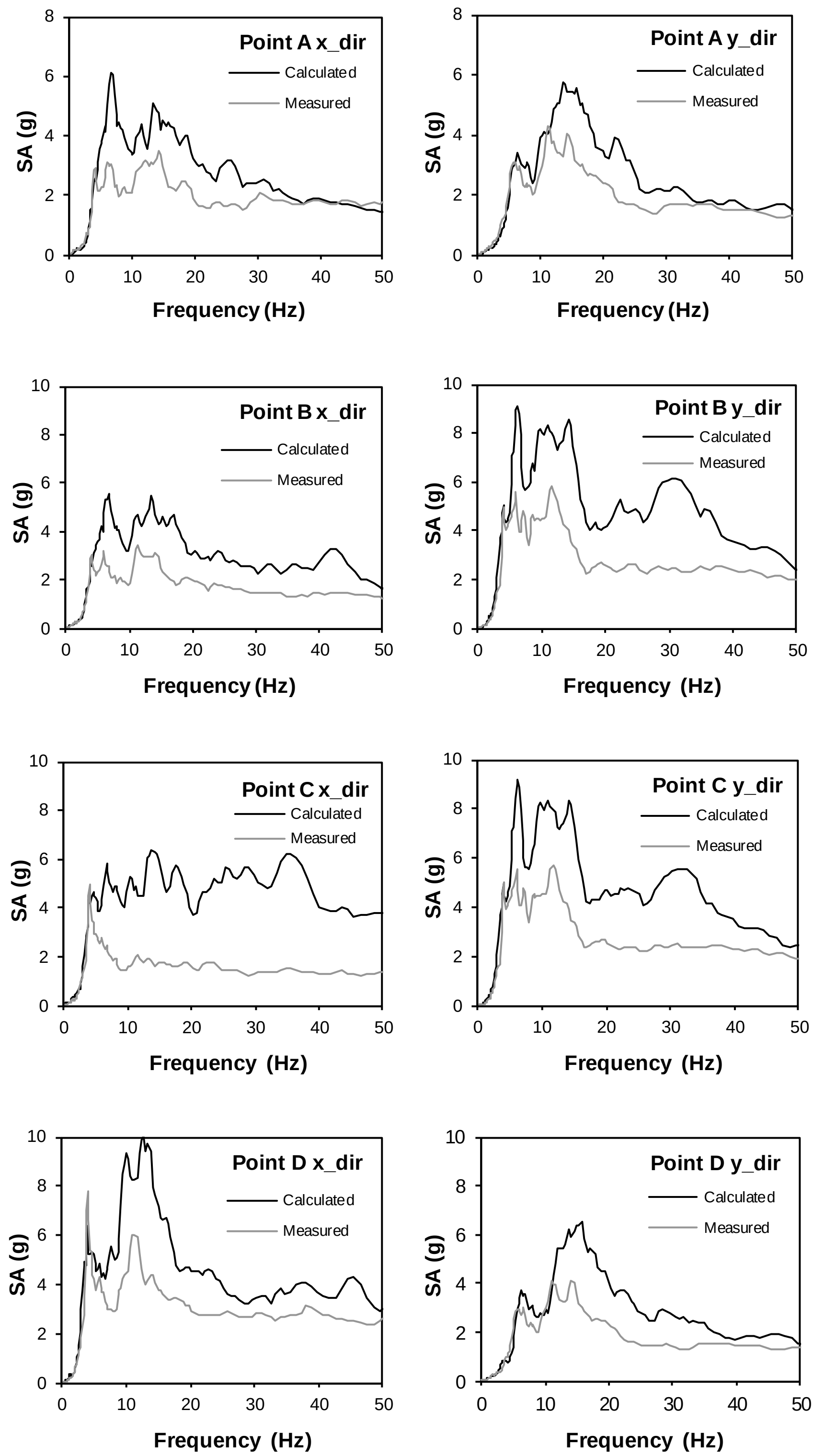

Figure 3.14 Acceleration Response Spectrum comparison of the experimental and analytical results at the 3rd floor for Run 7 (Accsyn-0.7 g) shaking table model, Damping ratio=5 percent

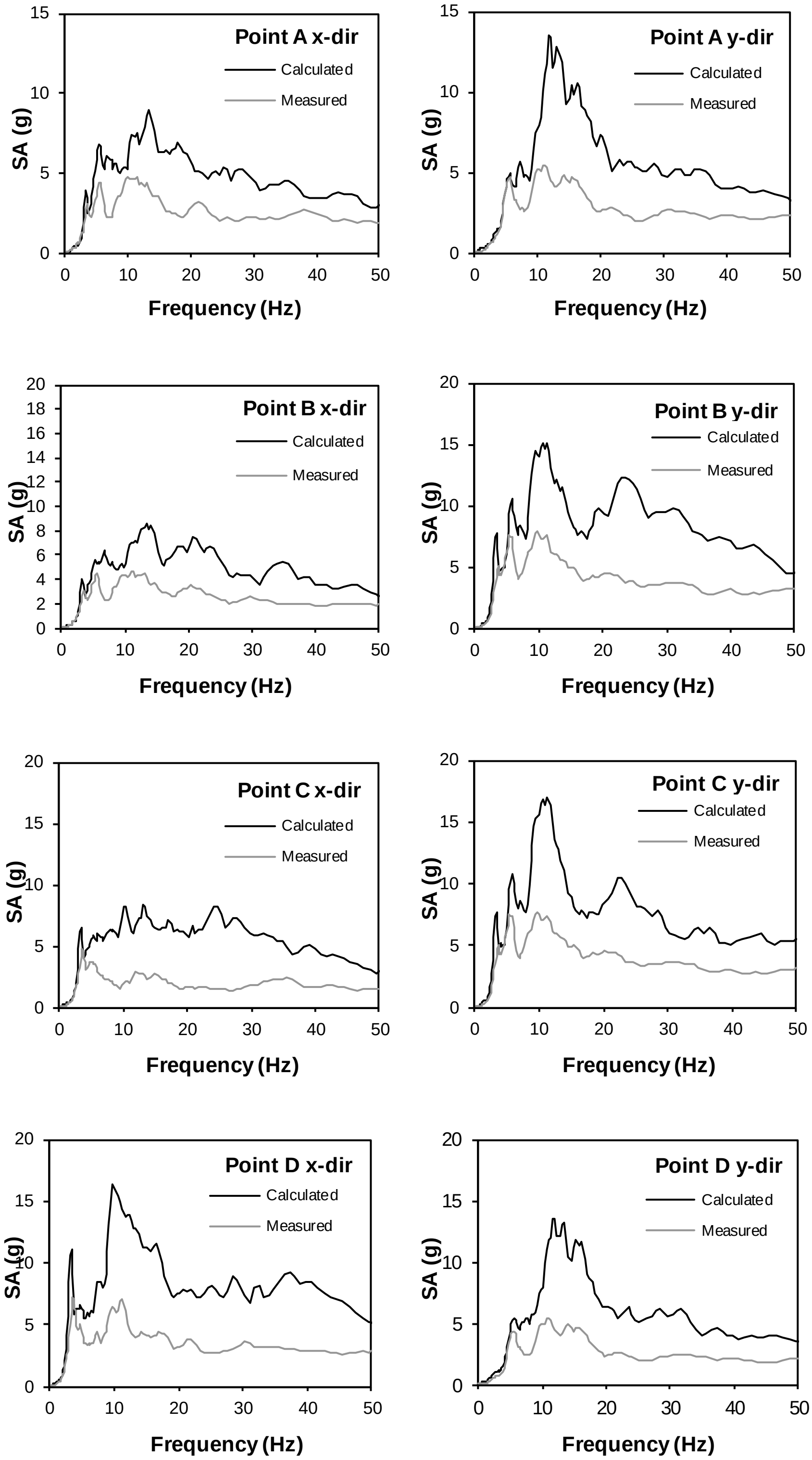

Figure 3.15 Acceleration Response Spectrum comparison of the experimental and analytical results at the 3rd floor for Run 10 (Accsyn-1.0 g) shaking table model, Damping ratio=5 percent

CHAPTER 4

INTERPRETATION AND DISCUSSION OF RESULTS

4.1. General

The objective was to investigate the adequacy of the analytical model in reflecting the behavior obtained experimentally. From the Phase 1 it was concluded that the finite element model cannot replicate the behavior under the low seismic excitations.

Many reasons can result in this situation such as the connection of mock-up to the shaking table, element inadequacy of finite model or assumptions considered for the basement nodes. In addition, there are many other unknown factors that can affect this behavior, and should be studied in another research. Acceptable results were obtained under the stronger seismic excitations.

This problem was also experienced by other researchers who participated in SMART 2008 Phase 1-Benchmark Study (SMART Workshop, 2010). All analytical and experimental results are discussed and re-evaluated here.

Tables 4.1 and 4.2 provide modal response obtained from each model and compared with the experimental measurements. Evaluations based on frequencies imply that even the model with shaking table is still stiffer than the mock-up. As can be seen in figure 3.9, the specimen oscillation induced vertical displacements on the shaking table, leading to significant reductions of the corresponding natural frequencies of the whole system (shaking table + specimen).

Table 4-1 Comparison of frequencies

	Experimental –f (Hz)	Model with shaking table-f (Hz)	Model with fixed base f (Hz)
Mode 1	6.24	7.87	9.23
Mode 2	7.86	10.62	15.93
Mode 3	15	16.61	32.76

Table 4-2 Comparison of periods

	Experimental –T(s)	Model with shaking table-T (s)	Model with fixed base-T (s)
Mode 1	0.16	0.13	0.11
Mode 2	0.13	0.09	0.06
Mode 3	0.07	0.06	0.031

Aside from comparisons of displacement traces, the maximum values calculated in x- and y- directions for each excitation are compared in Tables 4.3 and 4.5. The trend observed is not regular; both models generally underestimate the displacements at smaller excitations (PGA< 0.4g) but overestimate it at larger excitations. Although shaking table model yields better estimates, in certain cases fixed base model gives closer results to the experimental values. These comparisons are also plotted in Figures 4.1-4.2.

The behavior in the x-direction is correctly predicted by both models and peak values are quite similar to the experimental results. Considering the displacement ratios, the observed discrepancies are more important in y-direction.

Table 4-3 x-direction absolute maximum relative displacements (mm)

Models		0.1g	0.2g	0.3g	0.4g	0.5g	0.6g	0.7g	0.8g	0.9g	1g
F_base	A	0.40	1.63	1.90	6.42	7.73	8.50	9.21	10.28	11.08	11.39
Sh_table	A	0.58	2.66	2.17	6.58	7.00	8.16	10.24	11.77	11.95	12.58
Exp.	A	2.47	2.72	5.39	6.78	6.58	6.84	7.57	7.42	10.02	9.74
F_base	B	0.38	1.64	1.99	5.61	8.39	9.31	9.98	11.03	11.93	11.57
Sh_table	B	0.57	2.85	2.26	7.05	6.75	8.87	11.20	12.84	13.03	12.62
Exp.	B	3.11	3.00	5.10	7.30	6.19	7.39	7.81	7.75	10.40	10.70
F_base	C	0.51	2.41	2.40	8.95	9.92	12.86	12.53	14.26	15.61	16.43
Sh_table	C	0.73	4.01	2.67	8.45	9.23	10.68	13.97	17.02	18.91	21.92
Exp.	C	4.02	4.41	6.38	9.94	9.29	10.49	11.91	11.55	13.10	14.73
F_base	D	0.83	4.10	2.63	11.88	12.04	16.86	18.35	20.06	21.13	25.87
Sh_table	D	1.00	6.61	3.54	10.41	14.94	16.43	17.35	23.10	28.41	34.58
Exp.	D	5.65	5.55	7.99	14.83	14.10	17.61	18.99	17.62	20.68	24.25

Table 4-4 x-direction displacement ratios

Models		0.1g	0.2g	0.3g	0.4g	0.5g	0.6g	0.7g	0.8g	0.9g	1g
F_base	A	0.84	0.40	0.65	0.05	-0.18	-0.24	-0.22	-0.39	-0.11	-0.17
Sh_table	A	0.76	0.02	0.60	0.03	-0.06	-0.19	-0.35	-0.59	-0.19	-0.29
F_base	B	0.88	0.45	0.61	0.23	-0.36	-0.26	-0.28	-0.42	-0.15	-0.08
Sh_table	B	0.82	0.05	0.56	0.03	-0.09	-0.20	-0.43	-0.66	-0.25	-0.18
F_base	C	0.87	0.46	0.62	0.10	-0.07	-0.23	-0.05	-0.23	-0.19	-0.12
Sh_table	C	0.82	0.09	0.58	0.15	0.01	-0.02	-0.17	-0.47	-0.44	-0.49
F_base	D	0.85	0.26	0.67	0.20	0.15	0.04	0.03	-0.14	-0.02	-0.07
Sh_table	D	0.82	-0.19	0.56	0.30	-0.06	0.07	0.09	-0.31	-0.37	-0.43

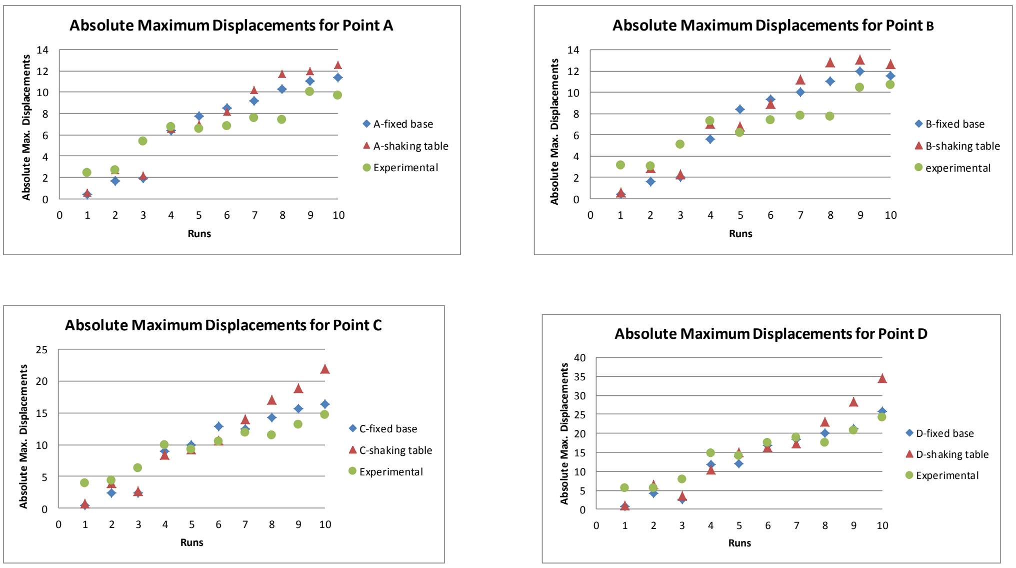

Figure 4.1 Absolute maximum displacements in 3rd floor at points A,B,C and D in the x direction

Table 4-5 y-direction absolute maximum relative displacements (mm)

Models		0.1g	0.2g	0.3g	0.4g	0.5g	0.6g	0.7g	0.8g	0.9g	1g
F_base	A	0.18	0.78	0.88	6.40	3.60	4.23	4.94	5.69	6.51	7.50
Sh_table	A	0.42	1.00	0.95	3.32	4.14	4.87	7.33	7.33	9.37	10.63
Exp.	A	1.38	1.28	3.46	2.14	2.86	3.21	4.12	4.12	4.88	6.70
F_base	B	0.55	4.63	3.16	13.04	14.97	17.90	22.73	22.73	23.45	24.58
Sh_table	B	1.03	6.02	3.30	14.12	15.57	15.86	17.72	17.79	21.86	25.82
Exp.	B	5.85	4.77	10.04	12.41	14.01	15.13	16.45	14.65	17.42	18.19
F_base	C	0.56	4.64	3.16	13.02	14.95	17.86	22.60	22.60	23.32	24.56
Sh_table	C	1.04	6.05	3.31	14.15	15.60	15.86	17.69	17.94	22.35	25.87
Exp.	C	5.03	4.06	9.56	11.86	13.13	13.51	15.77	13.38	16.47	17.17
F_base	D	0.18	0.77	0.86	11.88	3.61	4.24	4.98	5.78	6.65	7.84
Sh_table	D	0.42	0.99	0.94	3.27	4.11	4.88	6.99	6.99	8.93	9.99
Exp.	D	1.51	1.33	3.35	2.07	2.69	3.19	3.63	4.02	4.94	6.52

In Figure 4.1, higher displacement values occurred at points C and D in the x direction. At points B and C, motion in the y direction is dominant (Figure 4.2).

Table 4-6 y-direction displacement ratios

Models		0.1g	0.2g	0.3g	0.4g	0.5g	0.6g	0.7g	0.8g	0.9g	1g
F_base	A	0.87	0.39	0.75	-2.00	-0.26	-0.32	-0.20	-0.38	-0.33	-0.12
Sh_table	A	0.69	0.22	0.73	-0.56	-0.44	-0.52	-0.78	-0.78	-0.92	-0.59
F_base	B	0.91	0.03	0.69	-0.05	-0.07	-0.18	-0.38	-0.55	-0.35	-0.35
Sh_table	B	0.82	-0.26	0.67	-0.14	-0.11	-0.05	-0.08	-0.21	-0.25	-0.42
F_base	C	0.89	-0.14	0.67	-0.10	-0.14	-0.32	-0.43	-0.69	-0.42	-0.43
Sh_table	C	0.79	-0.49	0.65	-0.19	-0.19	-0.17	-0.12	-0.34	-0.36	-0.51
F_base	D	0.88	0.42	0.74	-4.73	-0.34	-0.33	-0.37	-0.44	-0.35	-0.20
Sh_table	D	0.72	0.26	0.72	-0.58	-0.52	-0.53	-0.93	-0.74	-0.81	-0.53

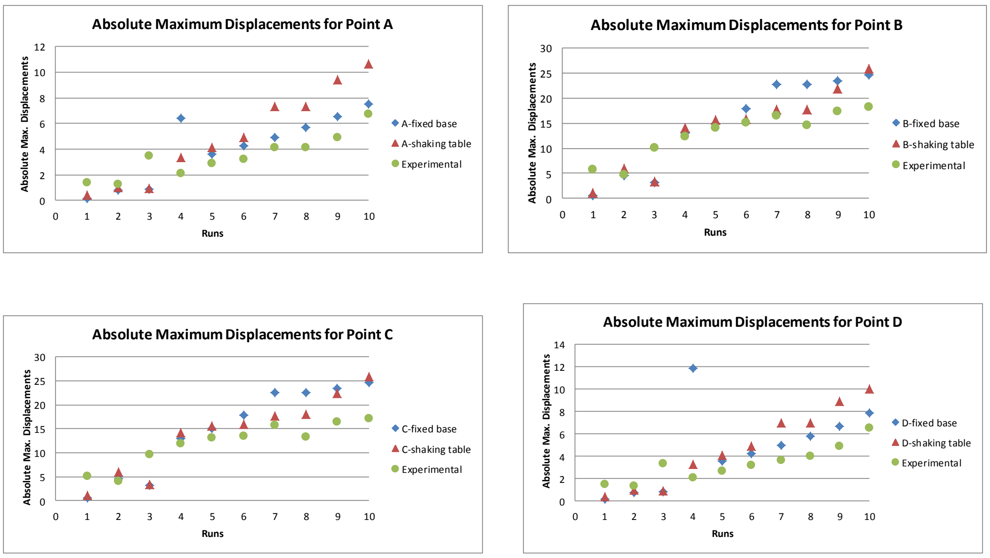

Fiqure 4.2 Absolute maximum displacements for point A,B,C and D in the y direction

Comparing the accelerations we can observe that, except point D, the maximum value of accelerations of numerical model occurs in y-direction.

4.2. Sensitivity to Spring Stiffness

The response of the shaking table model depends on many parameters such as spring stiffness. The stiffness of the springs included in the models have direct influence on the modal frequencies and response quantities calculated, so the influence of the spring stiffness is investigated.

In order to determine the importance and impact of this parameter on the behavior of the structure, the stiffness, K was changed in Run 7 and the results obtained were compared. In Figures 4.3-4.4 the results of time history analysis for K= 100 MN/m, K=215 MN/m and K=400 MN/m are given.

In Table 4.9 calculated maximum absolute displacements of points A,B,C and D for K= 100 MN/m, K=215 MN/m and K=400 MN/m in the 3rd floor are compared with the measured values.

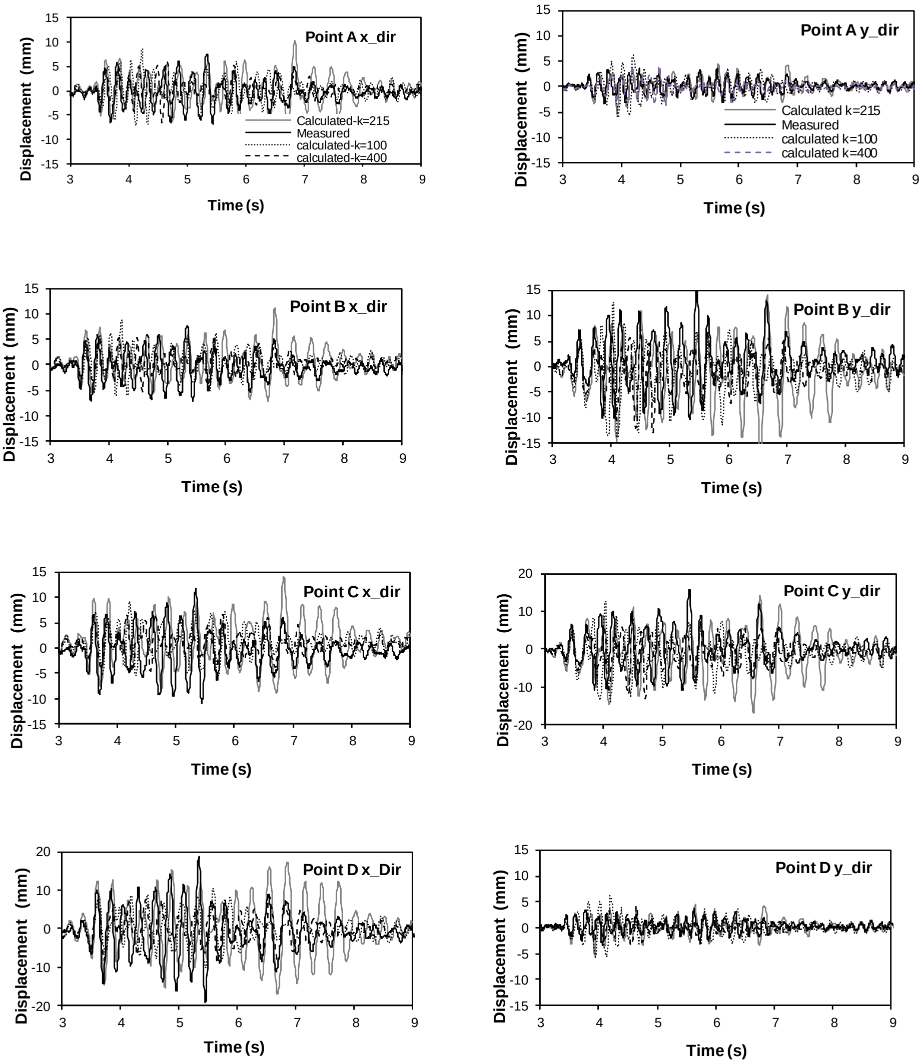

Figure 4.3 Comparison of Displacements of points A,B,C and D of 3rd floor for PGA=0.7g with K=100 MN/m, 215 MN/m and K=400 MN/m

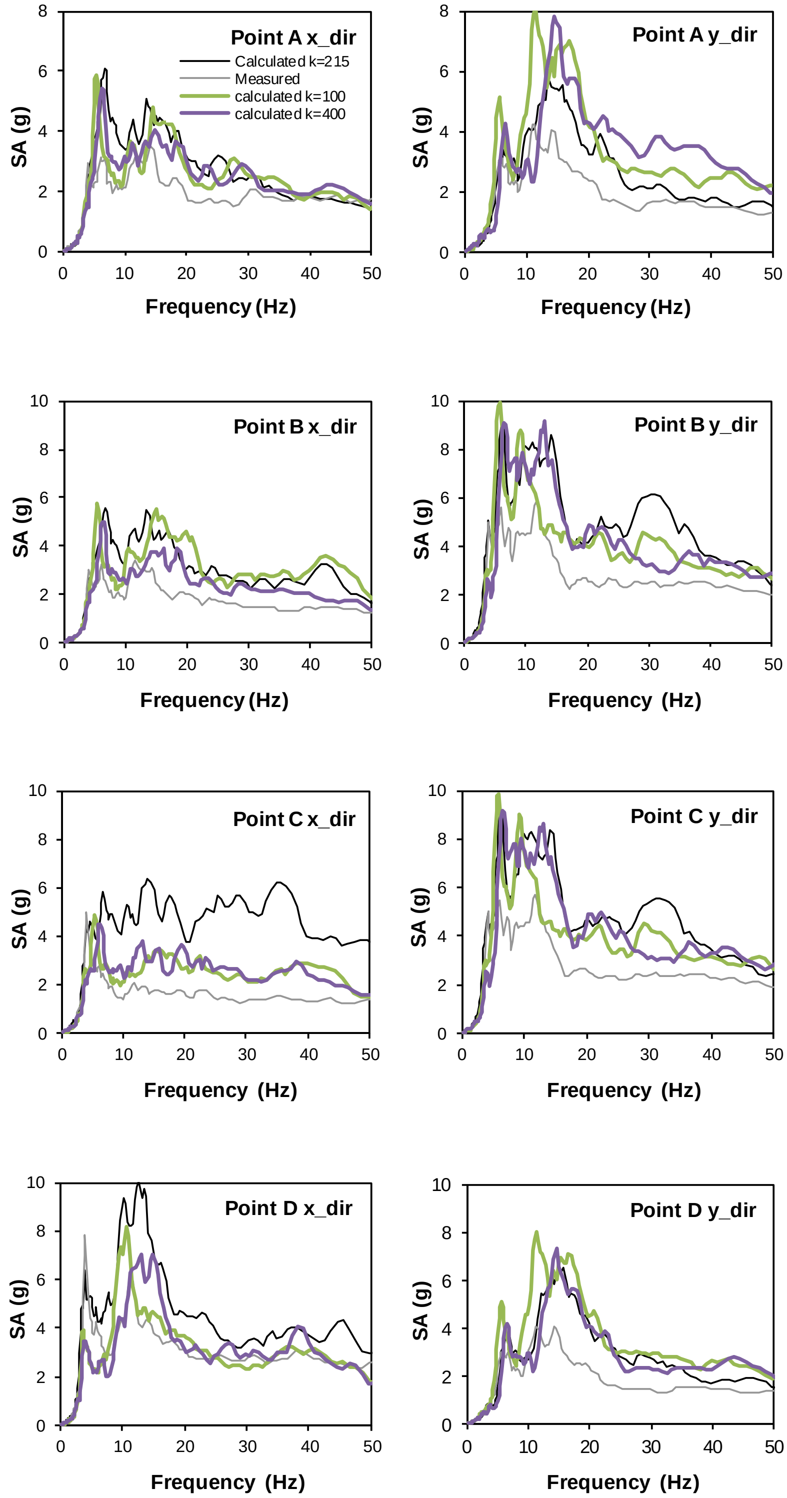

Figure 4.4 Comparison of Acceleration Response Spectra of points A,B,C and D of 3rd floor for PGA=0.7g with K=100 MN/m, 215 MN/m and K=400 MN/m

Table 4-7 Comparison of measured and calculated maximum absolute displacements of points A,B,C and D in the 3rd floor for different spring stiffnesses

	K=100 MN/m	K=215 MN/m	K=400 MN/m	Measured
Ax	8.48	10.24	6.55	7.57
Bx	8.84	11.2	6.03	7.81
Cx	9.16	13.97	6.66	11.91
Dx	10.59	17.34	9.05	18.99
Ay	6.24	5.42	4.22	3.61
By	13.9	17.08	12.95	16.54
Cy	13.91	17.06	12.97	15.77
Dy	6.34	5.23	4.23	3.63

The comparison of maximum measured and calculated absolute displacements for different spring stiffnesses shows that the trend observed is not regular but for K=215 MN/m the results are more close to the results of measured values.

CHAPTER 5

CONCLUSIONS

5.1. Summary and conclusions

Experimental behavior of a 3-story scaled model of a shear wall building with torsional irregularities that was tested on a shaking table was simulated through two analytical models: a fixed-base model and a shaking-table model.

The model structure is a ¼ scale of a three story reinforced concrete building that has torsion due to plan irregularity and layout of structural walls. In order to simulate response quantities measured for the specimen tested on a shaking table, a series of non-linear time history analyses were performed. This structure was subjected to AZALEE shaking table tests in Saclay, France under the project of "SMART 2008" which was led by CEA (Atomic Energy Agency).

The SMART-2008 project consisted of two phases. The first phase of the project also consisted of two parts, Phase 1A and Phase 1B (RAPPORT DM2S, 2007 and RAPPORT DM2S, 2009). In the present study, Phase 1B of the SMART-2008 project has been studied.

Phase 1B was related to the benchmark study. The main aim was to allow the participants to improve their best estimate predictions by updating their model with information available for some of the seismic runs, as to perform new analyses at higher loading levels.

The objectives of the Phase 1B are to investigate the efficiency of the model in the non-linear range through the comparison with the experimental results and to adjust the model in order to match the experimental response of the specimen under different seismic loadings.

The primary objective of this thesis was to obtain a valid and adequate model that can simulate the experimental response of the specimen. For this reason, two models were generated. In the first model, the effect of shaking table was ignored and the base of the specimen was considered as fixed. In the second model, the shaking table was also included in the model.

The model building was tested under a set of bi-directional synthetic and real ground motions that have varying intensities, peak ground accelerations ranging from 0.1g to 1g. Ground motions were applied sequentially to the specimen, starting with the one having the smallest intensity. Displacements and accelerations measured at different locations on the plan at third story were compared with the numerically computed values in order to check the validity of the Finite Element Model that has been obtained in ANSYS ver.12.1.

A fixed-based model that ignored the effect of shaking table was developed. Simulations based on the fixed-base model showed that experimentally measured displacements were captured with reasonable accuracy despite deviations from the modal frequencies and spectral accelerations.

A more flexible model including the shaking table yielded better estimates of accelerations and frequencies but overestimates of displacements were obtained.

Although both models captured the torsional behavior adequately, neither was adequate to simulate all experimental results. Modeling of the specimen-table interaction which is believed to be affected by the specimen properties, needs more investigations. In addition to this, experimental data needs to be further examined for consistency.

Comparing the modal analyses results indicated that, the results achieved from analyzing the shaking-table model is much more closer to the experimentally obtained results.

Comparing the displacements and accelerations depicted that, the maximum value of displacements ratio and accelerations of numerical model occurs in y-direction.

5.2. RECOMMENDATIONS FOR FURTHER STUDIES

This study can also be improved in the future in order to increase the accuracy of the simulation of the AZALEE shaking table and to increase the agreement of the numerical data with the experimental data.

- Also some practical softwares such as ARTEMIS can be used for more precise investigation of the dynamic behavior of the structure.

- The interaction between the shaking table and the specimen can be evaluated in order to do more precise comparisons.

- More detailed evaluation of the sensitivity to spring stiffness and other parameters can be also carry out.

REFERENCES

ANSYS R 12.1, Engineering Analysis System, 2011, User and Theoretical Manual.

Aziminejad A. and Moghadam A. S., 2009, "Performance of asymmetric multistory shear buildings with different strength distributions", Journal of Applien Science Vol.9, No.6, pp. 1080-1089

Akansel V.H., 2011, "Fragility of a Shear Wall Building with Torsional Irregularity", M.Sc. Thesis, Middle East Technical University, August.

Balkaya C. and Kalkan E., 2002, "Nonlinear seismic response evaluation of tunnel form building structures", Journal of Computers and Structures, 81 (2003):153-165.

Bisch P. and Coin A., 2007, "Seismic behavior of slightly reinforced concrete walls: experiments and theoretical conclusions" Bulletin of Earthquake Engineering, Vol. 5. No. 1, pp.45-65.

Chopra A., 2000, "Dynamics of structures: Theory and application to earthquake engineering", Prentice – Hall, 3rd edition.

Clough R. W. and Penzien J., 1993, "Dynamics of Structures", McGraw-Hill, New York.

Clough R. W., 1980, "The finite element method after twenty – five years: A personal view", Computers & Structures, Vol. 12, pp. 361-370.

Cook R.D., Malkus D.S., Plesha M.E. and Witt R.J., 2001, "Concepts and applications of finite element analysis", Fourth Edition, John Willey and Sons, New York.

Fischinger M. and Isakovic T., 2000, "Benchmark analysis of a structural wall", 12^{th} World Conference on Earthquake Engineering, 0416

Gülkan P. and Sözen M., 1974, "Inelastic responses of reinforced concrete structures to earthquake motions", Proceedings of the ACI, Vol. 54, No. 5, pp. 333-345.

Galal K., and El-Sokkary H., 2008, "Advancement in modeling of RC shear walls", 14th World Conference on Earthquake Engineering, Beijing, China.

Hosoya H., Abe I., Kitagawa Y. and Okada T., 1995, "Shaking table tests of three-dimensional scale models of reinforced concrete high-rise frame structures with wall columns", ACI Structural Journal, Vol. 92, No. 6, pp. 765-780.

Ile N. and Reynouard J.M., 2003, "Lightly reinforced walls subjected to multi – directional seismic excitations: Interpretation of CAMUS 2000-1 dynamic tests", Journal of Earthquake Technology, Vol. 40, No. 2-4, pp. 117-135.

Ile N. and Reynouard J.M., 2008, "Lightly reinforced walls subjected to seismic excitations: Interpretation of CAMUS 2000-1 and 2000-2 dynamic tests", Journal of Earthquake Engineering, Vol. 12, No. 1, pp. 91-114.

Ile N. and Reynouard J.M., 2005, "Behaviour of U-shaped walls subjected to uniaxial and biaxial cyclic lateral loading", Journal of Earthquake Engineering, Vol. 9, No. 1, pp. 67-94.

Ile N., Nguyen X. H., Kotronis P. and Mazars J. M., 2008, "Shaking table tests of lightly RC walls: Numerical Simulations", Journal of Earthquake Engineering, Vol. 12, No. 6, pp. 849-878.

Ile N., and Reynouard J.M., 2004, "Seismic behavior of R/C walls subjected to multi-directional seismic loading", 13th World Conference on Earthquake Engineering, No. 3243.

Jingjiang S., Tao W. and Hu Q., 2007, "Earthquake simulator tests and associated study of an 1/6-scale nine-story RC model", Journal of Earthquake Engineering and Engineering Vibration, Vol. 6, No. 3, pp. 281-288.

Kabeyasawa T., Shiohara H., Otani S. and Aoyama, H., 1983, "Analysis of the full – scale seven story reinforced concrete test structure", Vol.37, No. 2, pp. 432-478.

Kazaz İ., Yakut A. and Gülkan P., 2006, "Numerical simulation of dynamic shear wall tests: A benchmark study", Computers and Structures, Vol. 84, pp. 549-562.

Kazaz İ., 2010, "Dynamic characteristics and performance assessment of reinforced concrete structural walls", Phd Thesis, Middle East Technical University, February.

Khan, F.R. and Sbarounis, J.A., 1964, “Interaction of Shear Walls and Frames”, ASCE Journal of Structural Division, Vol.90, No.3, 285-335.

Kim YS. and Kabeyasawa T., 2002, “Shaking table test on eccentric pilotis wall-frames to collapse, Part 1 : Response behavior on reinforced concrete specimen” The 11th Japan Earthquake Engineering Symposium.

Kotronis P. Ragueneau F. and Mazars J., 2005, “A simplified modeling strategy for R/C walls satisfying PS92 and EC8 design” Engineering Structures, Vol. 27, No. 8, pp. 1197-1208.

Kwak H.–G. and Kim D.–Y., 2004, “FE analysis of RC shear walls subjected to monotonic loading”, Magazine of Concrete Research, 56, No. 7, pp. 387-403.

Lee HS. and Ko DW., 2007, “Seismic response characteristics of high-rise RC wall buildings having different irregularities in lower stories”, Engineering Structures 29 (2007) 3149-3167.

Le maoult A. and Queval J-C., 2010, “Seismic response characteristics of high-rise RC wall buildings having different irregularities in lower stories”, Engineering Structures 29 (2007) 3149-3167.

Le maoult A. and Queval J-C.,2010 , “Advances in Performance-Based Earthquake Engineering”, ISBN: 978-90-481-8745-4, Vol 13, Part.4, pp. 431-440.

Lermitte S. Chaudat T., Payen T., Vandeputte D. and Viallet E., 2008, “SMART 2008: Experimental tests of a reinforced concrete building subjected to torsion”, The 14th World Conference on Earthquake Engineering.

Lu Y., Tassios TP., Zhang G-F. and Vintzileou E., 1999, “Seismic response of reinforced concrete frame with strength and stiffness irregularities”, ACI Structural Journal, Vol. 96, No. 2, pp. 221-229.

Mazars J., Ragueneau F., Casaux G., Colombo A., and Kotronis P., 2004, “Numerical modeling for earthquake engineering: The case of lightly RC structural walls”, International Journal for Numerical and Analytical Methods in Geomechanics, Vol. 28, No. 7-8, pp. 857-874.

Mazars J., Kotronis P., Ragueneau F. and Casaux G., 2006, “Using multifiber beams to account for shear and torsion applications to concrete structural elements”, Journal of computer methods in applied mechanics and engineering, Vol. 195, pp. 7264-7281.

Miranda E. and Taghavi, S., 2005, “Approximate floor acceleration demands in multistory buildings. I: Formulation”, Journal of Structural Engineering, Vol. 131, No. 2, pp. 203-211.

Miranda E. and Taghavi, S., 2005, “Approximate floor acceleration demands in multistory buildings. II: Applications”, Journal of Structural Engineering, Vol. 131, No. 2, pp. 212-220.

Miranda E., 1999, “Approximate seismic lateral deformation demands in multistory buildings”, Journal of Structural Engineering, Vol. 125, No. 4, pp. 417-425.

Moehle J. P., 1996. “Displacement – based seismic design criteria”. 11th World Conference on Earthquake Engineering, 2125, ISBN: 0 08 042822 3.

Moehle J. P., 1984. “Seismic response of vertically irregular structures”. Journal of Structural Engineering, ASCE 1984;110(9):2002-14

Newmark N. M. and Hall, W. J., 1982, “Earthquake spectra and design”, Engineering monographs on earthquake criteria, structural design, and strong motion records, Earthquake Engineering Research Institute, Oakland, California.

Palermo D. and Veccihio F.J., 2007, “Simulation of cyclically loaded concrete structures based on the finite element method”, Journal of Structural Engineering, Vol. 33, No. 5, pp. 728-738.

Palermo D., and Vecchio F.J.., 2002. “Behavior of Three-Dimensional Reinforced Concrete Shear Walls”. ACI Structural Journal/Title no. 99-S9.

Park R. and Paulay T.,1975, “Reinforced concrete structures”, New York: Wiley.

Priestley M. J. N., 2000, “Performance Based Seismic Design”, 12th World Conference on Earthquake Engineering, 2831.

Quintana Gallo P., Akguzel U., Pampanin S. and Carr A.J., 2011, “Shake table tests of non-ductile as-built and repaired RC frames”, Proceedings of the Ninth Pacific Conference on Earthquake Engineering, Building an Earthquake-Resilient Society, Auckland, New Zealand.

RAPPORT DM2S, 2007, “Presentation of blind prediction contest”, COMMISSARIAT A L’ ÉNERGIE ATOMIQUE, SEMT/EMSI/PT/07-003/C.

RAPPORT DM2S, 2009, “Presentation of the Benchmark Contest –Phase 2 Project SMART 2008”, COMMISSARIAT A L’ÉNERGIE ATOMIQUE, SEMT/EMSI/PT/09-011/A

Shimazaki, K. and Sözen, M. A., 1984, “Seismic drift of reinforced concrete structures”, Res. Reports, Hazama – Gumi, Tokyo, Japan

SMART – 2008 Workshop, Saclay, Paris,France.

Sözen M.A., 1989, “Earthquake response of buildings with robust walls”, Fifth Chilian Conference on Earthquake Engineering, Santiago, Chile.

Shahrooz BM. and Mohele JP., 1990, “Seismic response and design of setback buildings”, Journal of Structural Engineering, ASCE 1990, Vol.116, No. 5, pp.1423-1439.

Vulcano A., Bertero V. V. and Colloti V., 1988, “Analytical modeling of R/C structural walls”, Proceedings of Ninth World Conference on Earthquake Engineering, 9-1-7

Wallace J. W. and Moehle J. P., 1992, “Ductility and detailing requirements of bearing wall buildings”, Journal of Structural Engineering, Vol. 118, No.6, ASCE, ISSN 0733-9445/92/0006-1625.

Willam, K. J. and Warnke, E. D., "Constitutive Model for the Triaxial Behavior of Concrete", Proceedings, International Association for Bridge and Structural Engineering, Vol. 19, ISMES, Bergamo, Italy, p. 174. 1975.

Wood SL., "Seismic response of R/C frames with irregular profile", Journal of Structural Engineering, Vol. 118, No. 2, pp. 545-566.

APPENDIX A

Results of time history analyses (displacements and acceleration response spectra) for fixed-base model

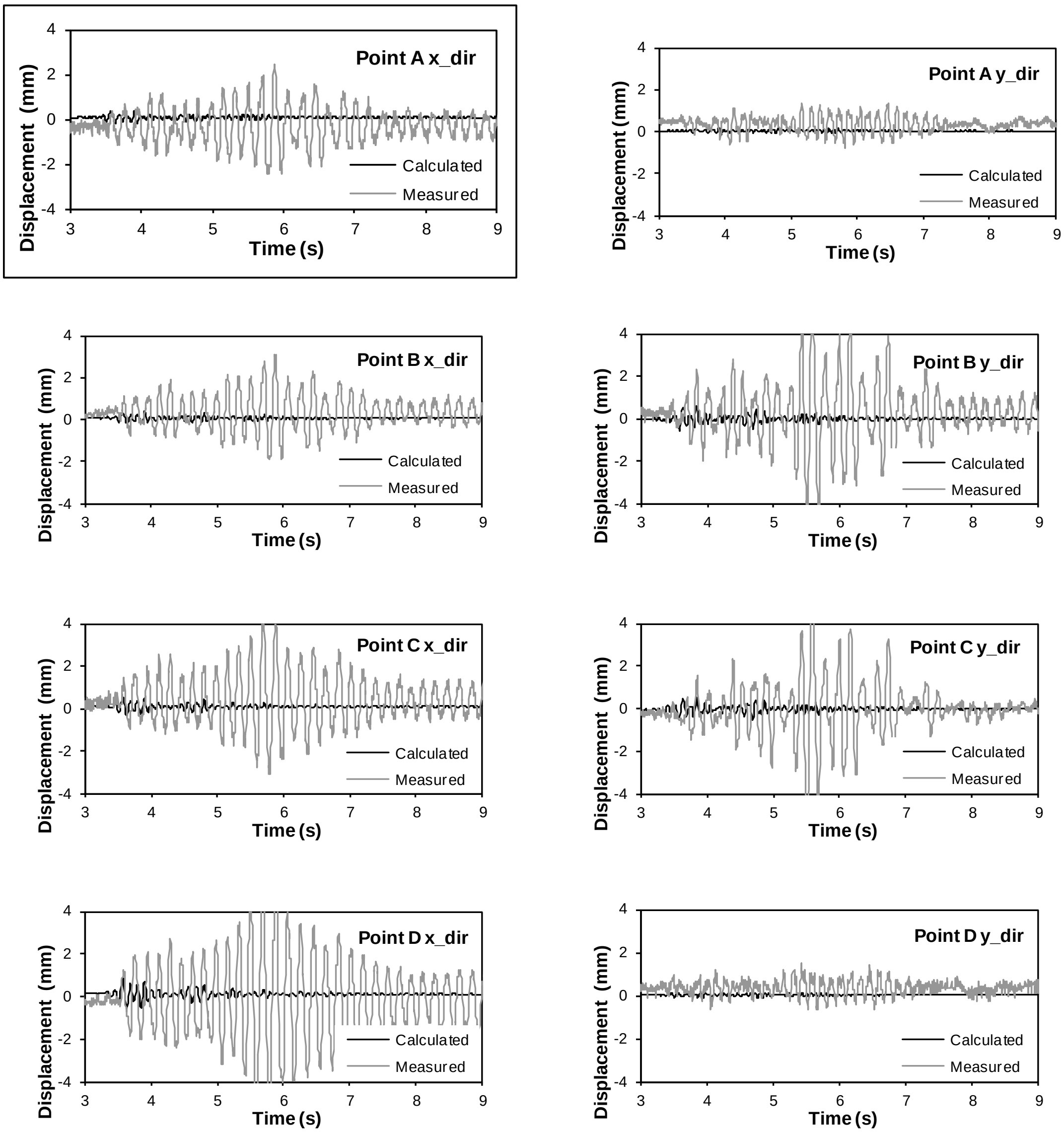

Figure A.1 Displacement comparison of the experimental results and analytical results at the 3rd floor for Run 1 (Accsyn-0.1g) fixed-base model

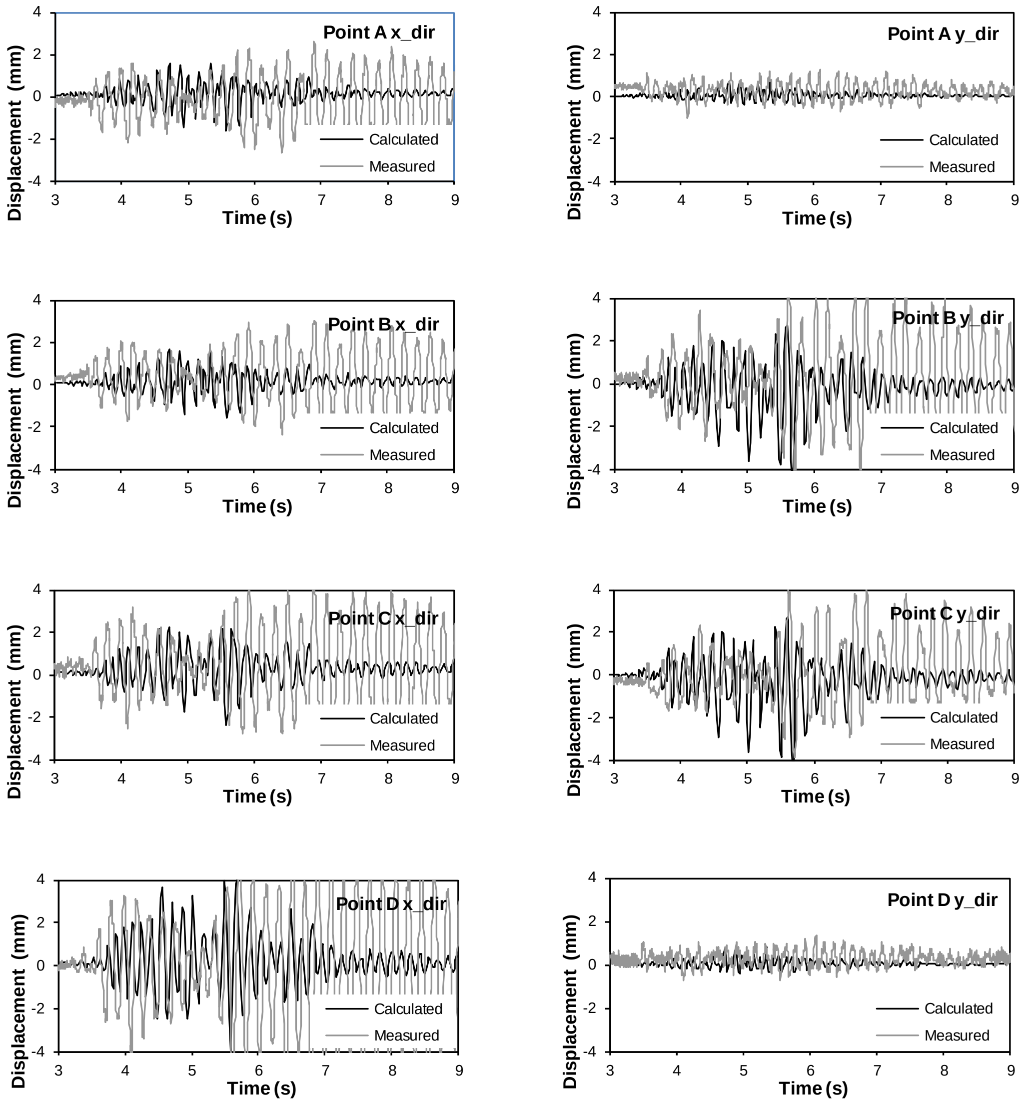

Figure A.2 Displacement comparison of the experimental results and analytical results at the 3rd floor for Run 2 (Accsyn-0.2g) fixed-base model

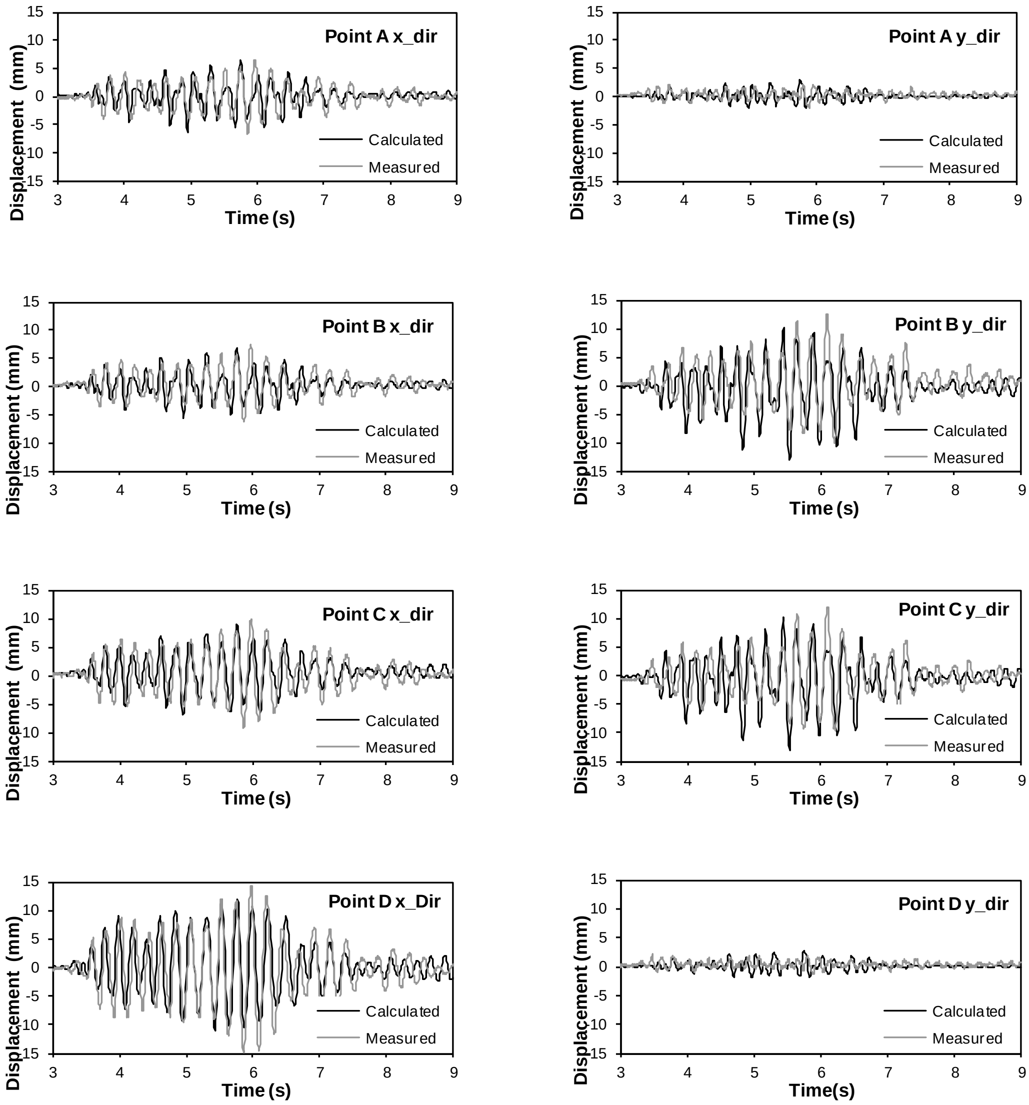

Figure A.3 Displacement comparison of the experimental results and analytical results at the 3rd floor for Run 4 (Accsyn-0.4g) fixed-base model

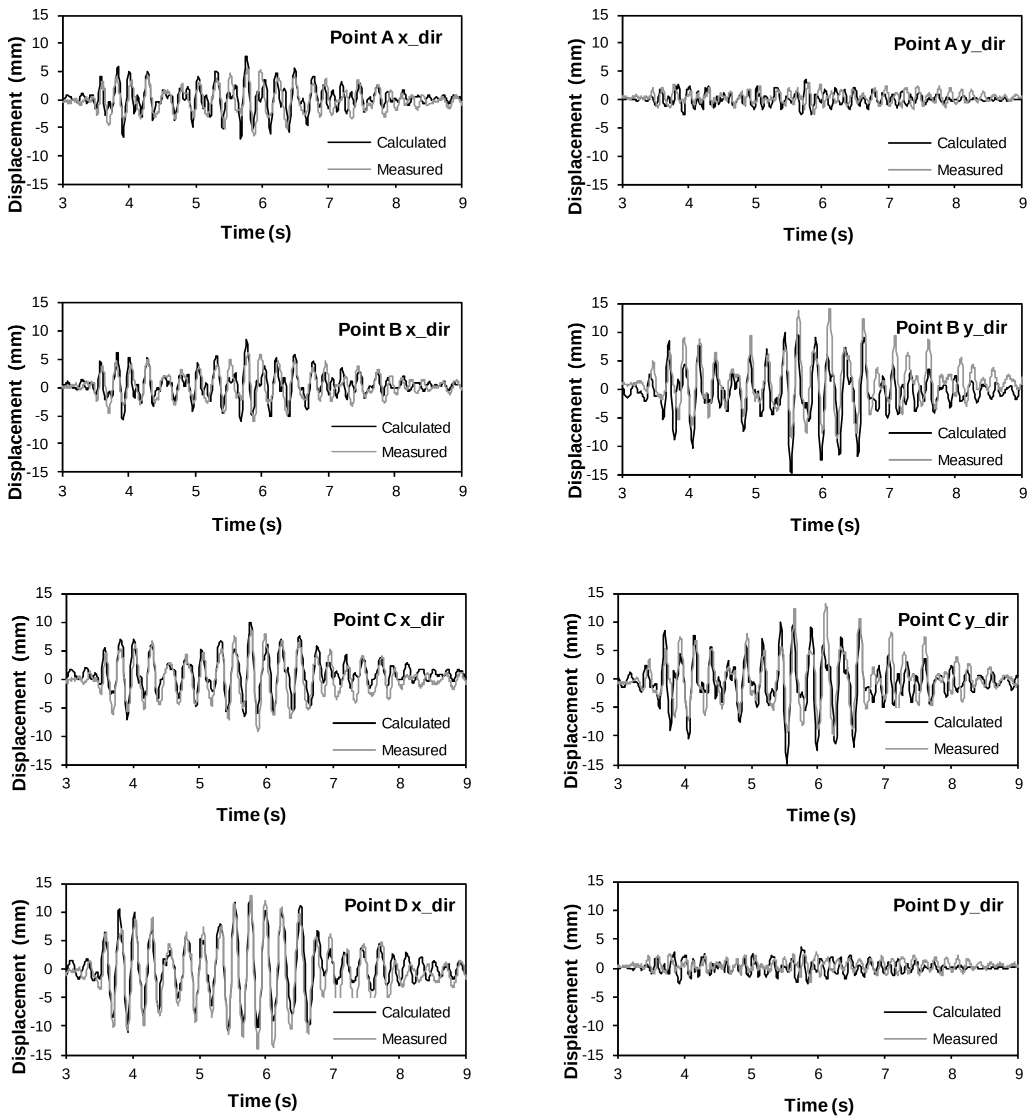

Figure A.4 Displacement comparison of the experimental results and analytical results at the 3rd floor for Run 5 (Accsyn-0.5g) fixed-base model

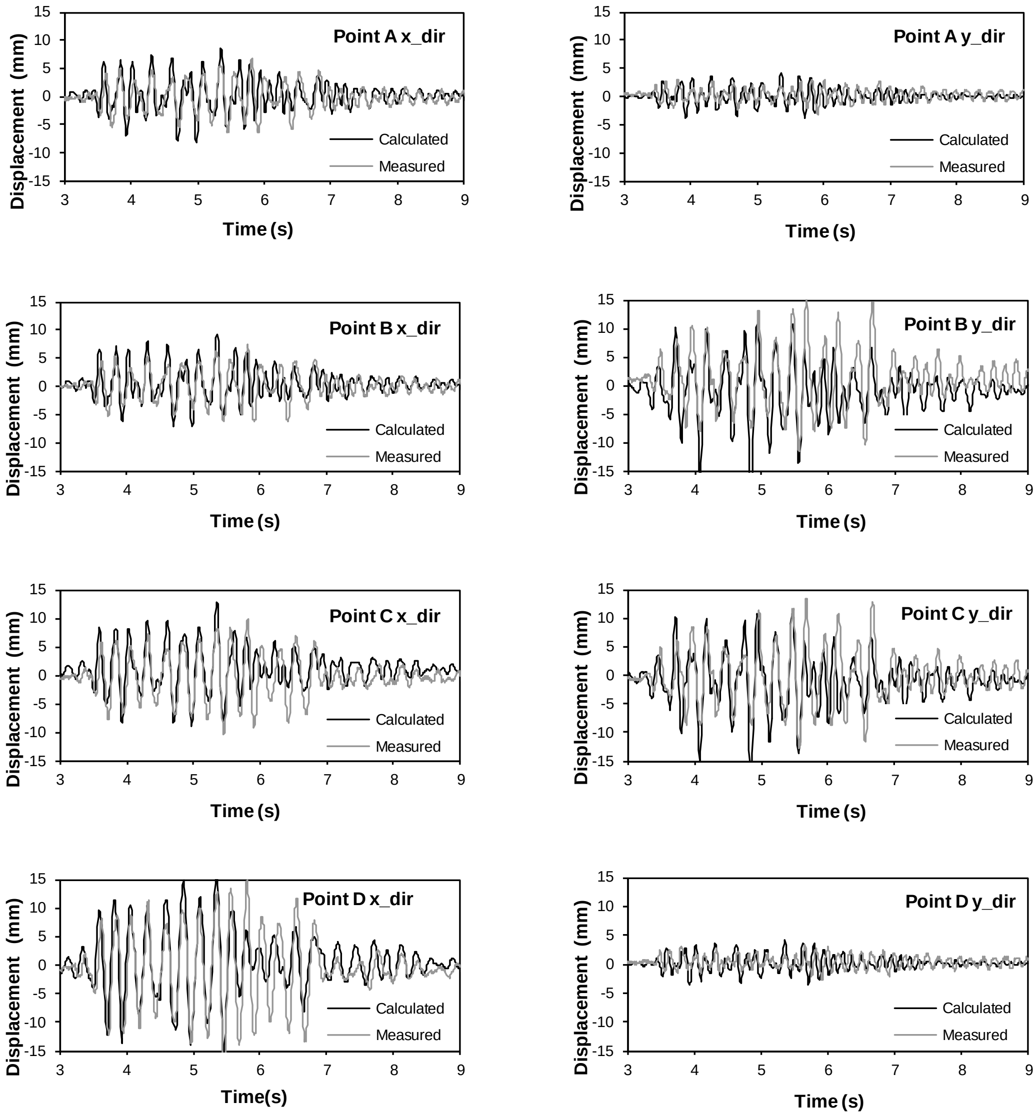

Figure A.5 Displacement comparison of the experimental results and analytical results at the 3rd floor for Run 6 (Accsyn-0.6g) fixed-base model

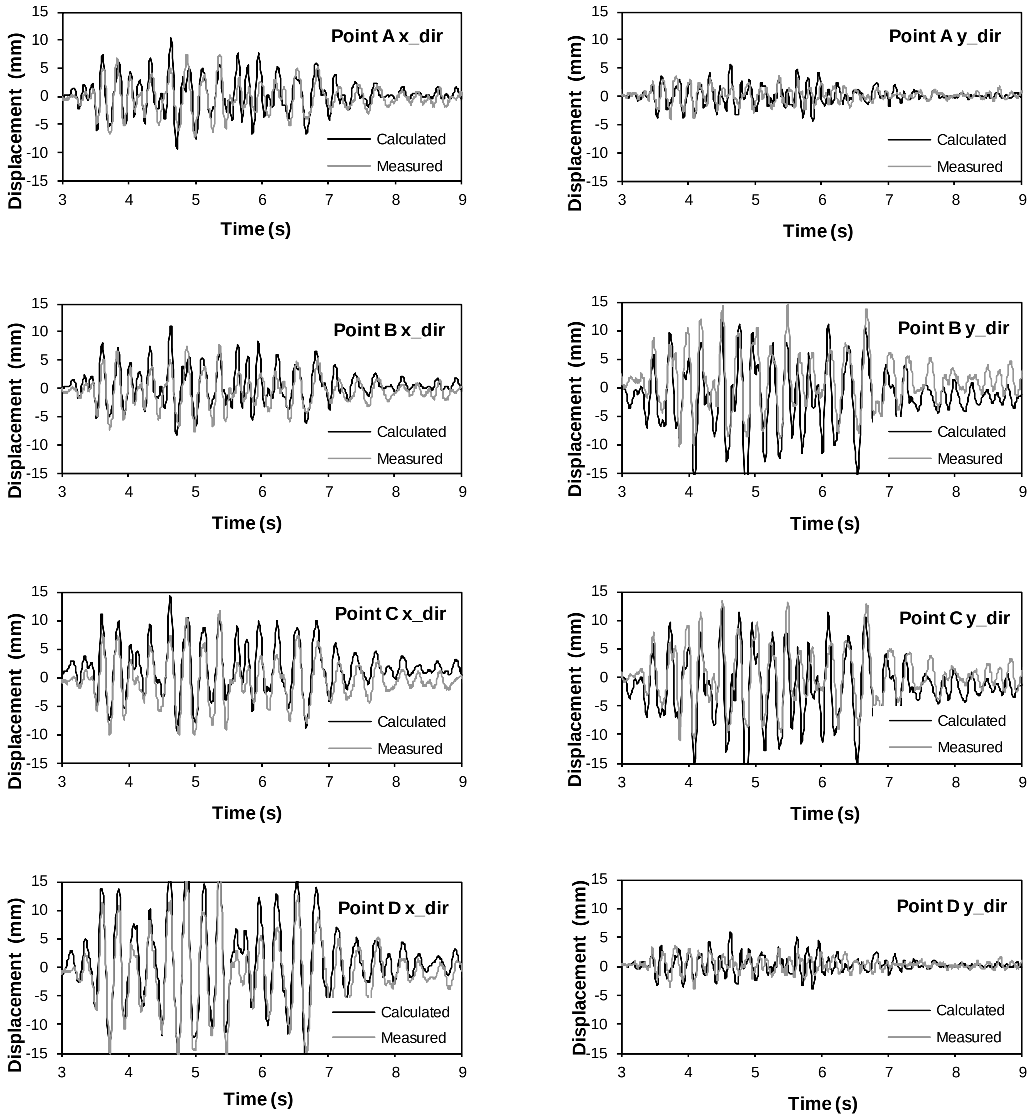

Figure A.6 Displacement comparison of the experimental results and analytical results at the 3rd floor for Run 8 (Accsyn-0.8g) fixed-base model

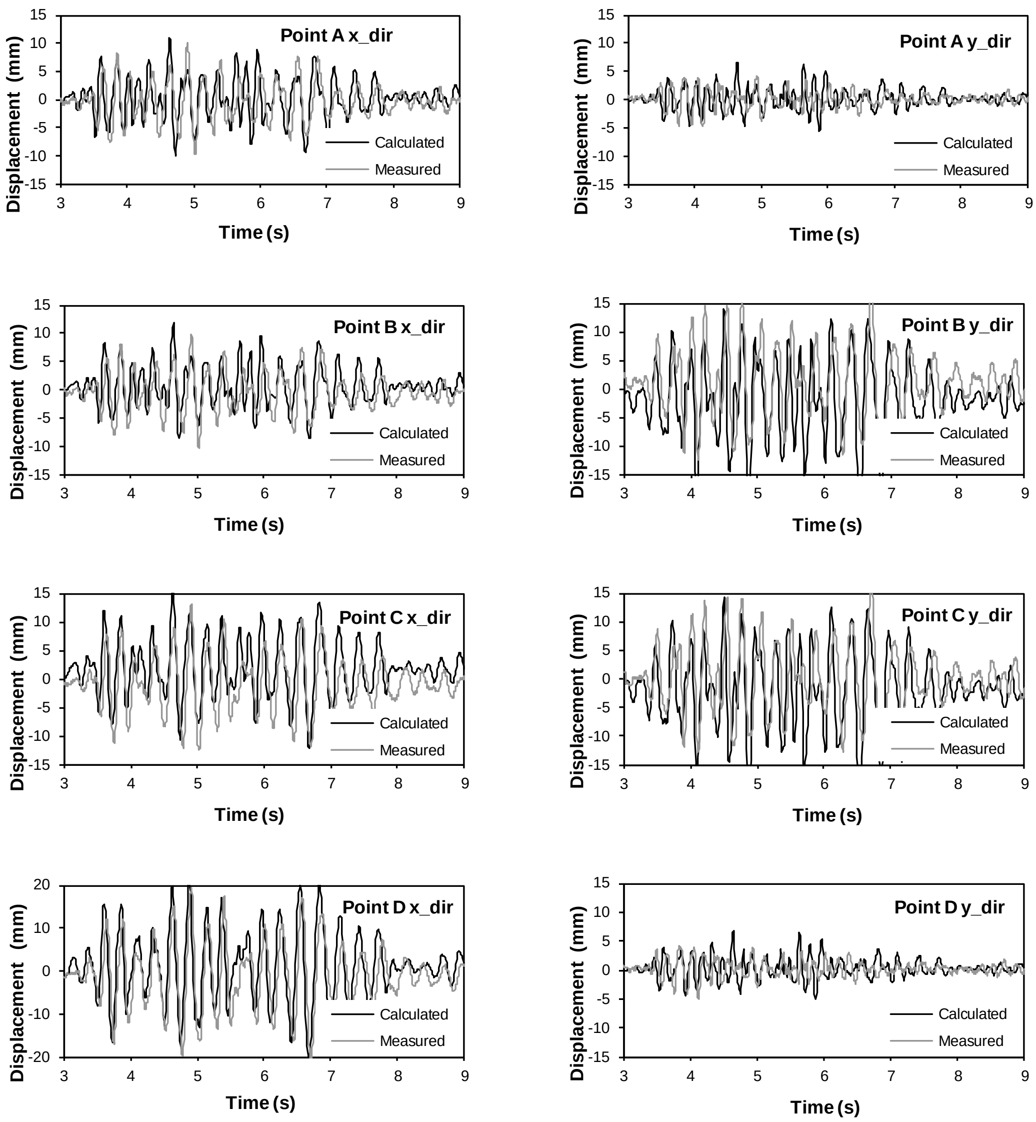

Figure A.7 Displacement comparison of the experimental results and analytical results at the 3rd floor for Run 9 (Accsyn-0.9g) fixed-base model

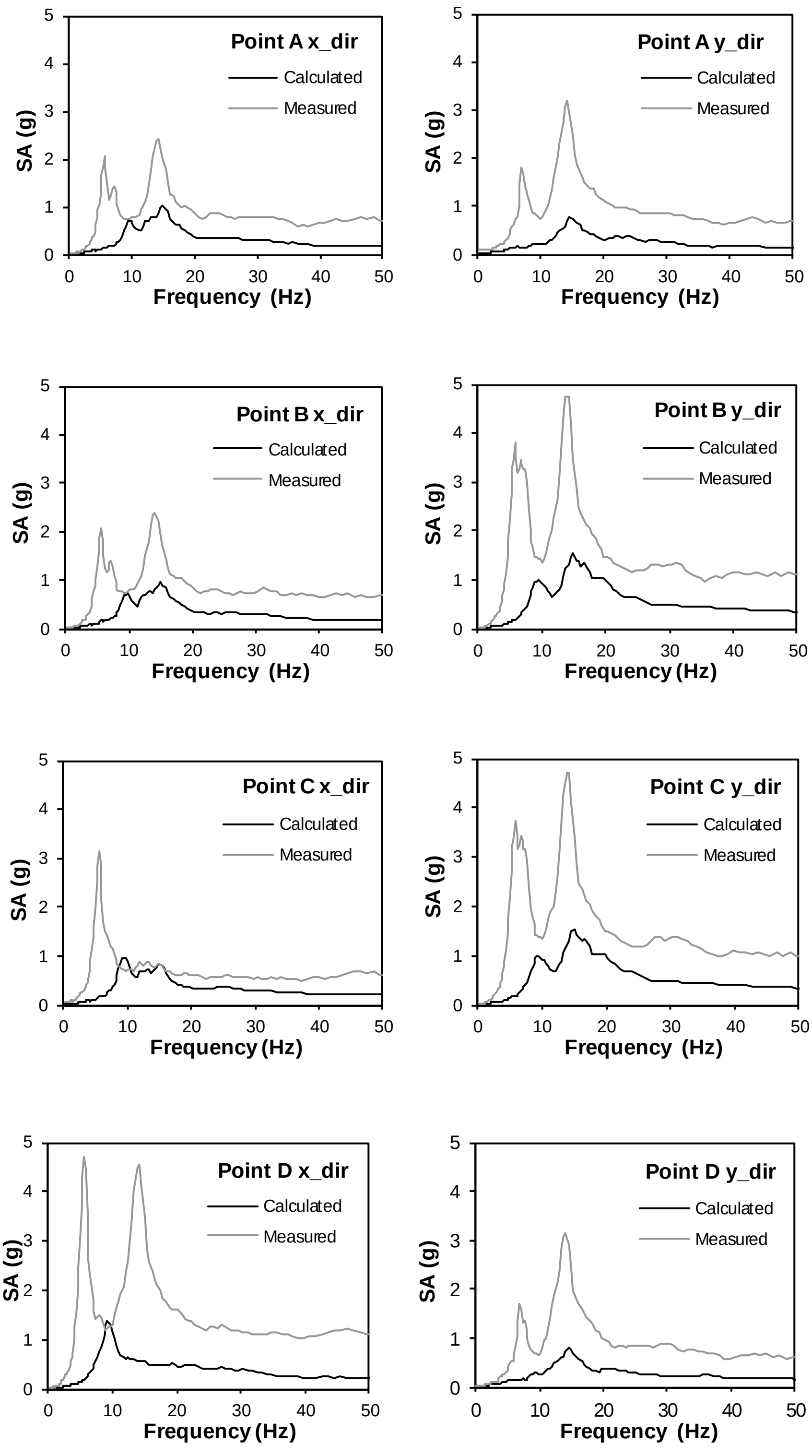

Figure A.8 Acceleration Response Spectrum comparison of the experimental and analytical results at the 3rd floor for Run 1 (Accsyn-0.1 g) fixed-base model, Damping ratio=5%

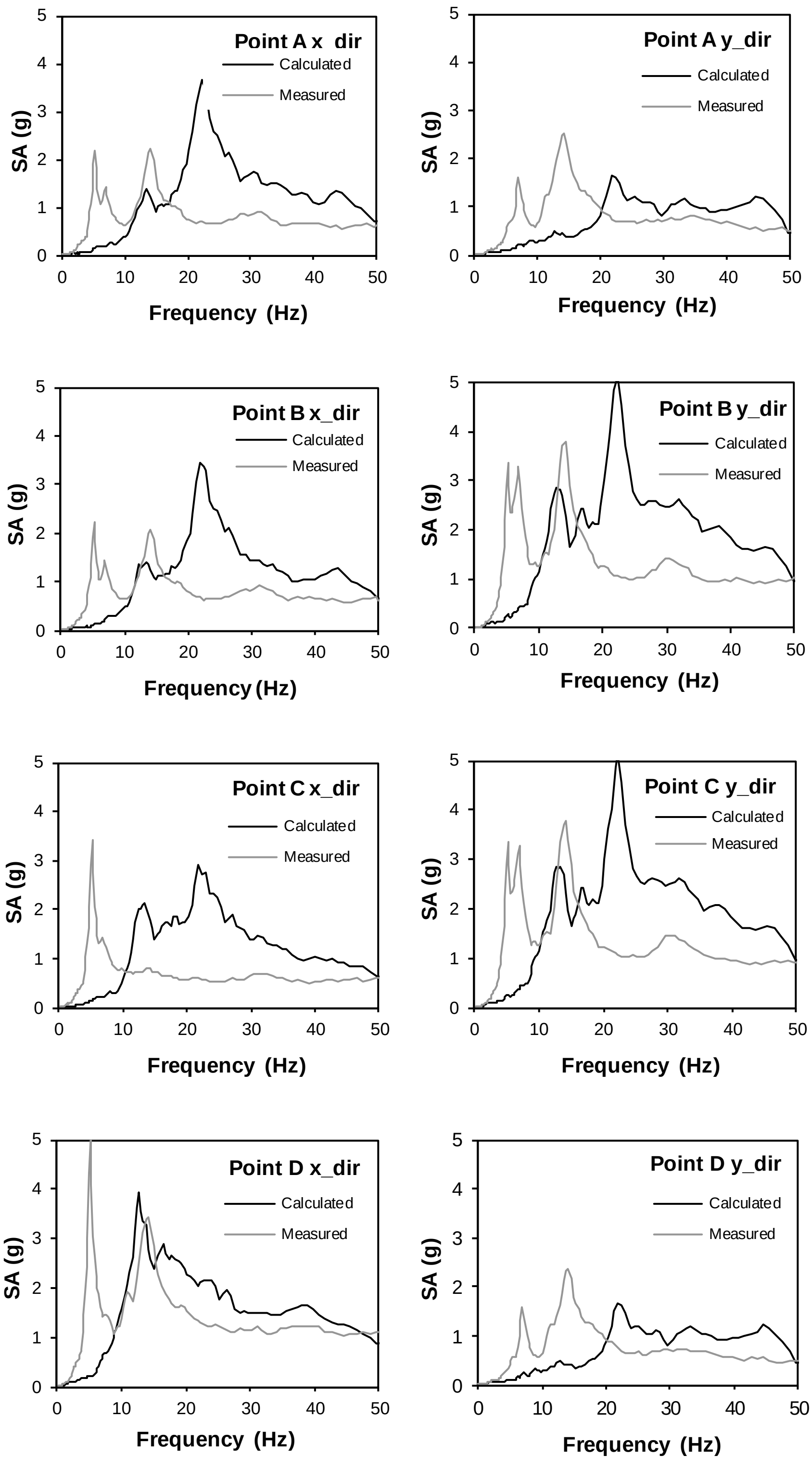

Figure A.9 Acceleration Response Spectrum comparison of the experimental and analytical results at the 3rd floor for Run 2 (Accsyn-0.2 g) fixed-base model, Damping ratio=5%

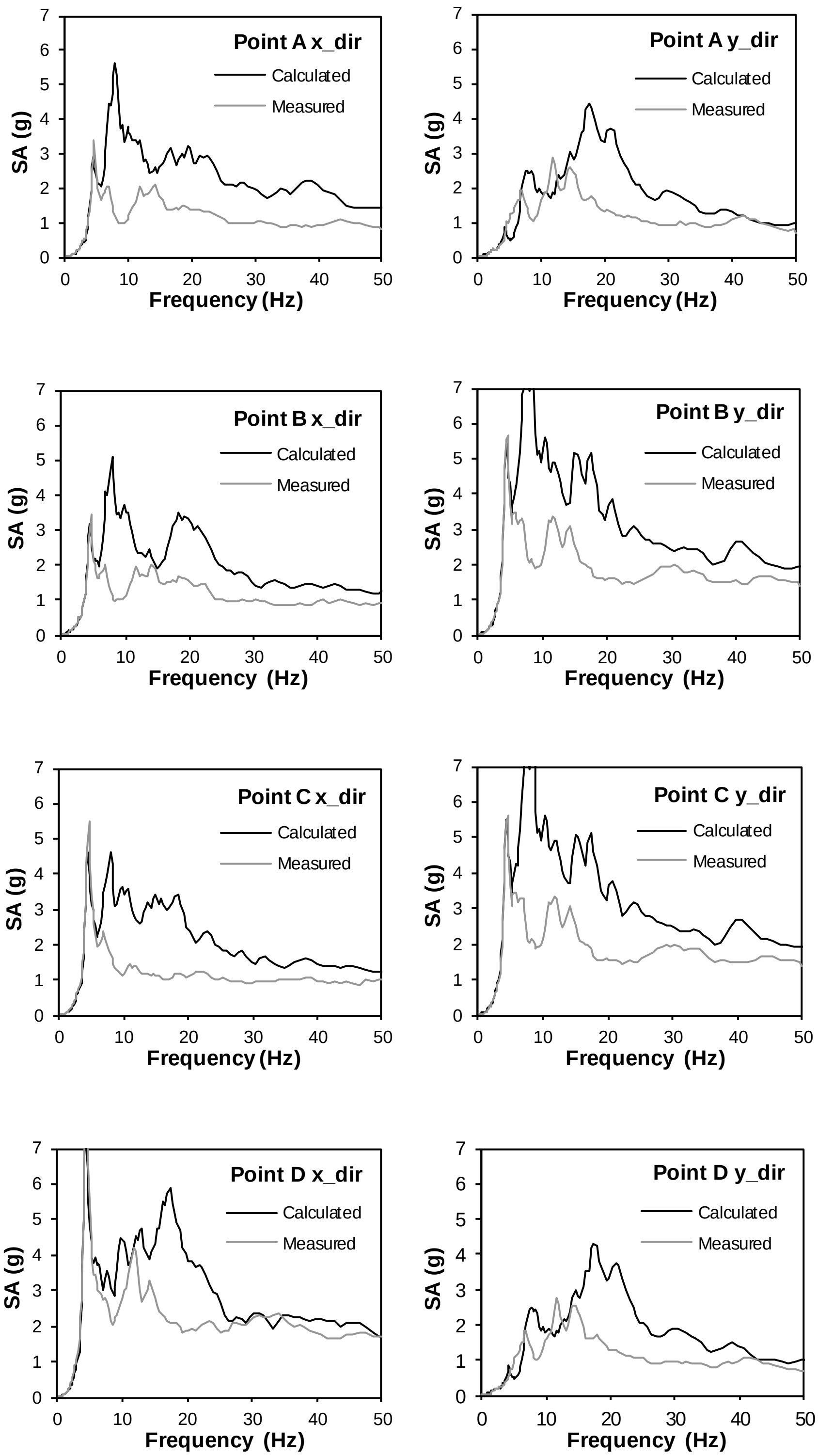

Figure A.10 Acceleration Response Spectrum comparison of the experimental and analytical results at the 3rd floor for Run 4 (Accsyn-0.4 g) fixed-base model, Damping ratio=5%

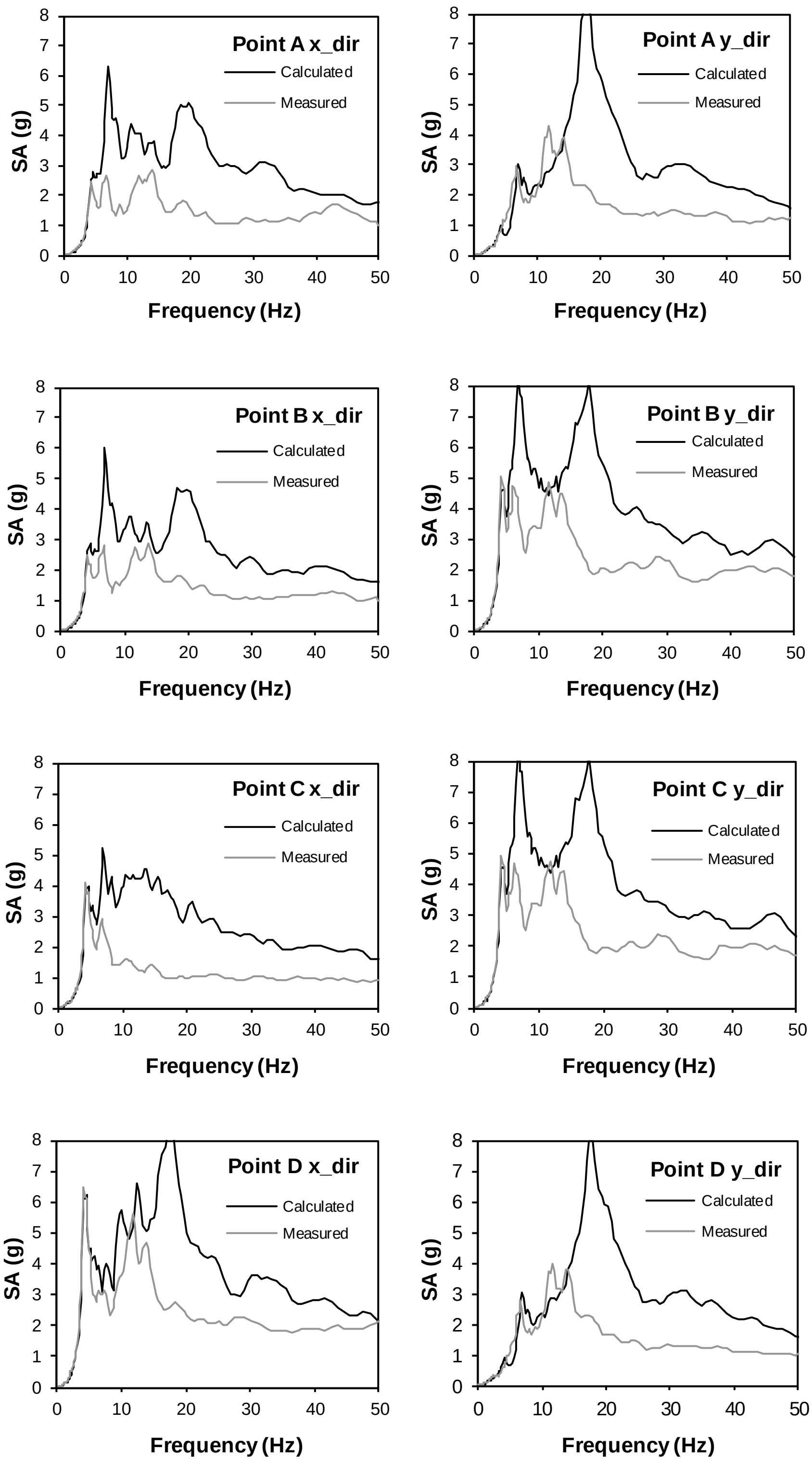

Figure A.11 Acceleration Response Spectrum comparison of the experimental and analytical results at the 3rd floor for Run 5 (Accsyn-0.5 g) fixed-base model, Damping ratio=5%

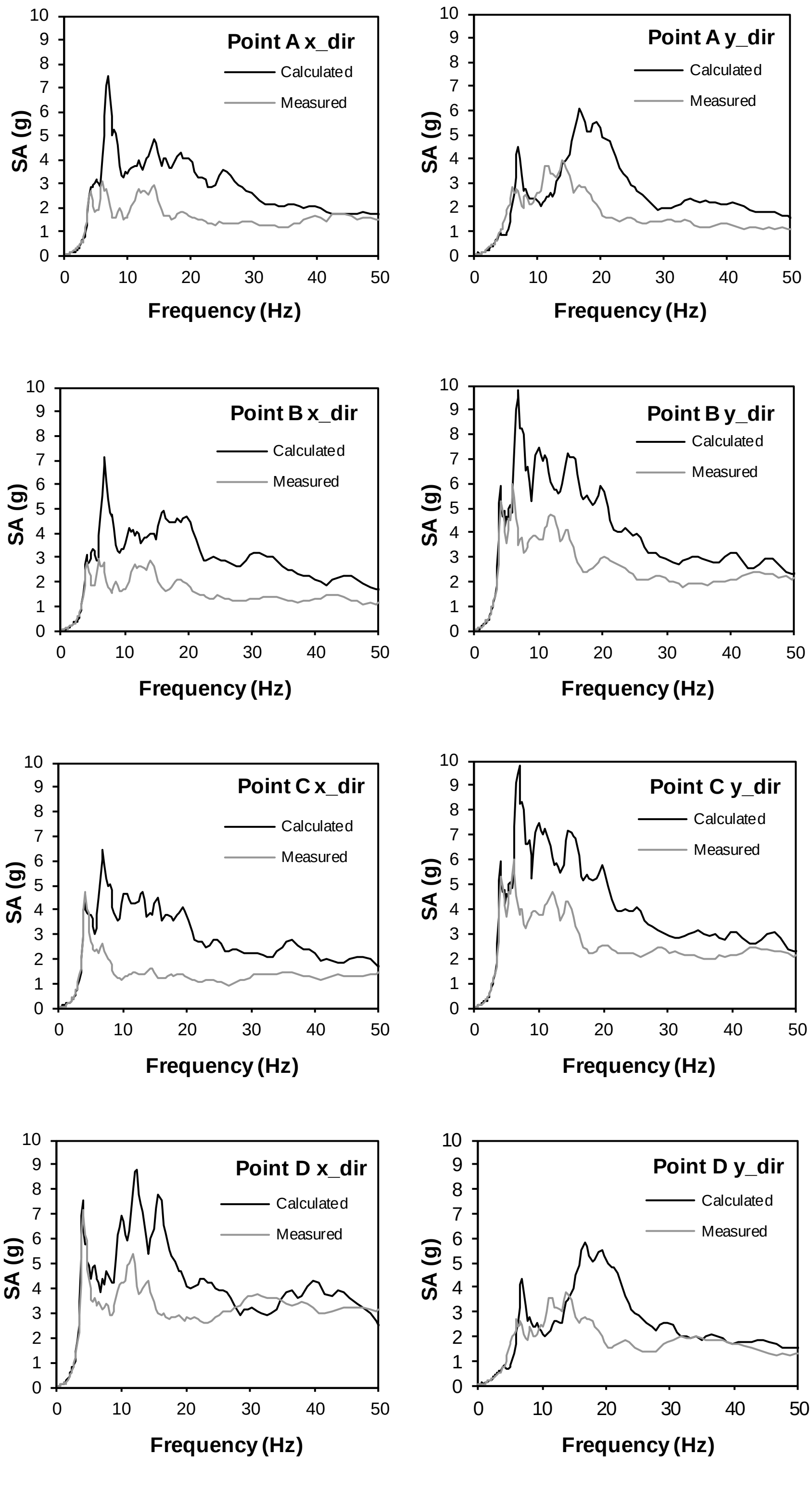

Figure A.12 Acceleration Response Spectrum comparison of the experimental and analytical results at the 3rd floor for Run 6 (Accsyn-0.6 g) fixed-base model, Damping ratio=5%

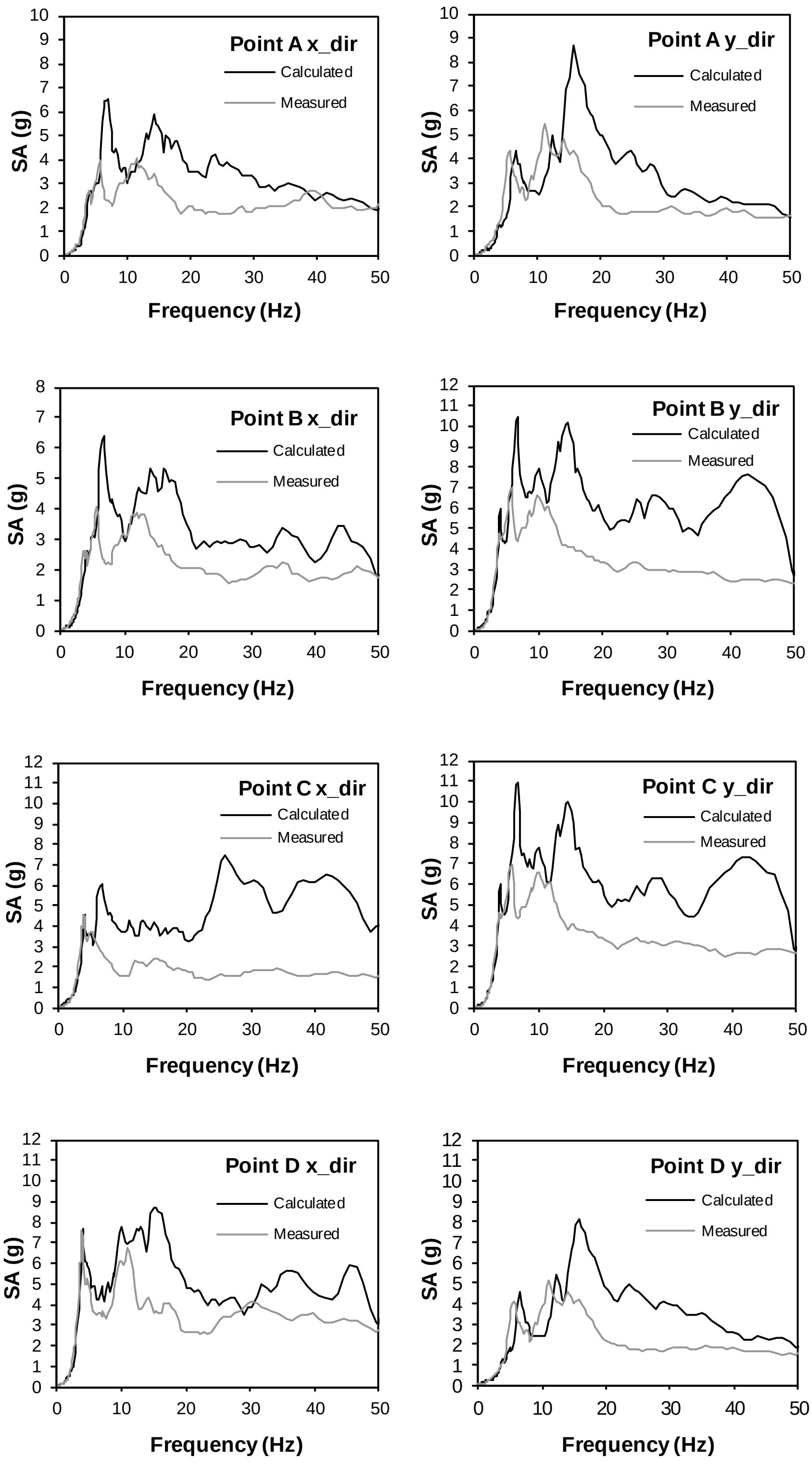

Figure A.13 Acceleration Response Spectrum comparison of the experimental and analytical results at the 3rd floor for Run 8 (Accsyn-0.8 g) fixed-base model, Damping ratio=5%

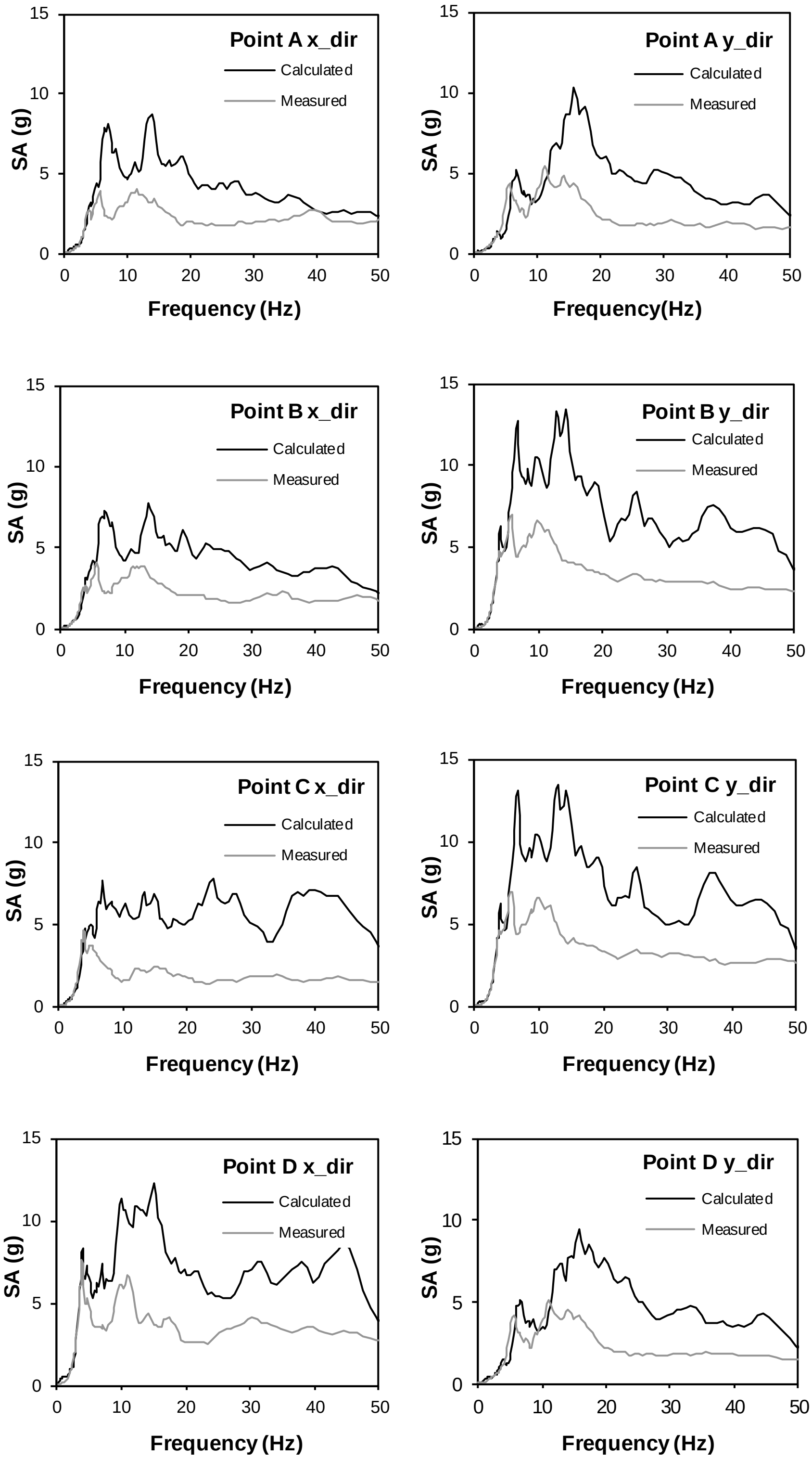

Figure A.14 Acceleration Response Spectrum comparison of the experimental and analytical results at the 3rd floor for Run 9 (Accsyn-0.9 g) fixed-base model, Damping ratio=5

APPENDIX B

Results of time history analyses (displacements and acceleration response spectra) for shaking table model

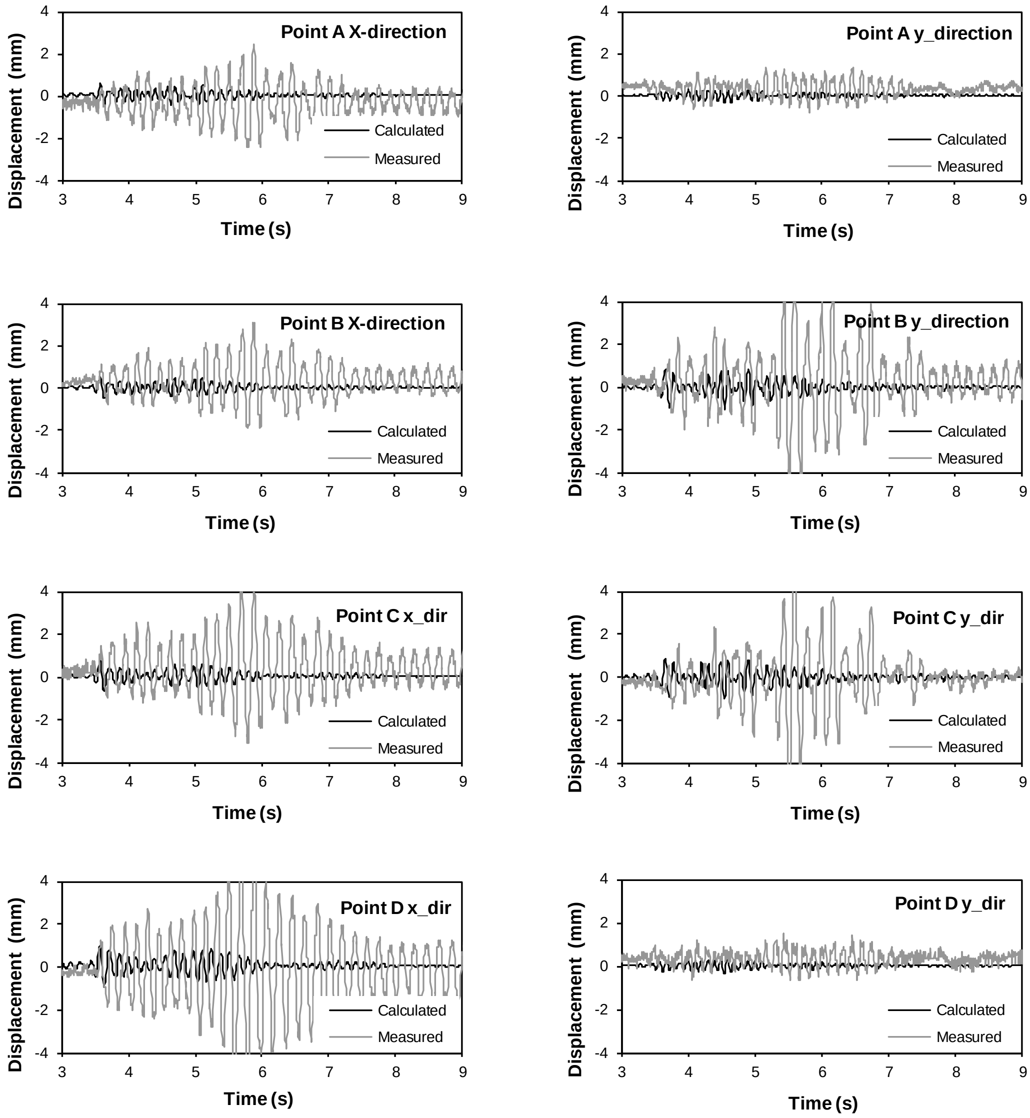

Figure B.1 Displacement comparison of the experimental results and analytical results at the 3rd floor for Run 1 (Accsyn-0.1g) shaking table model

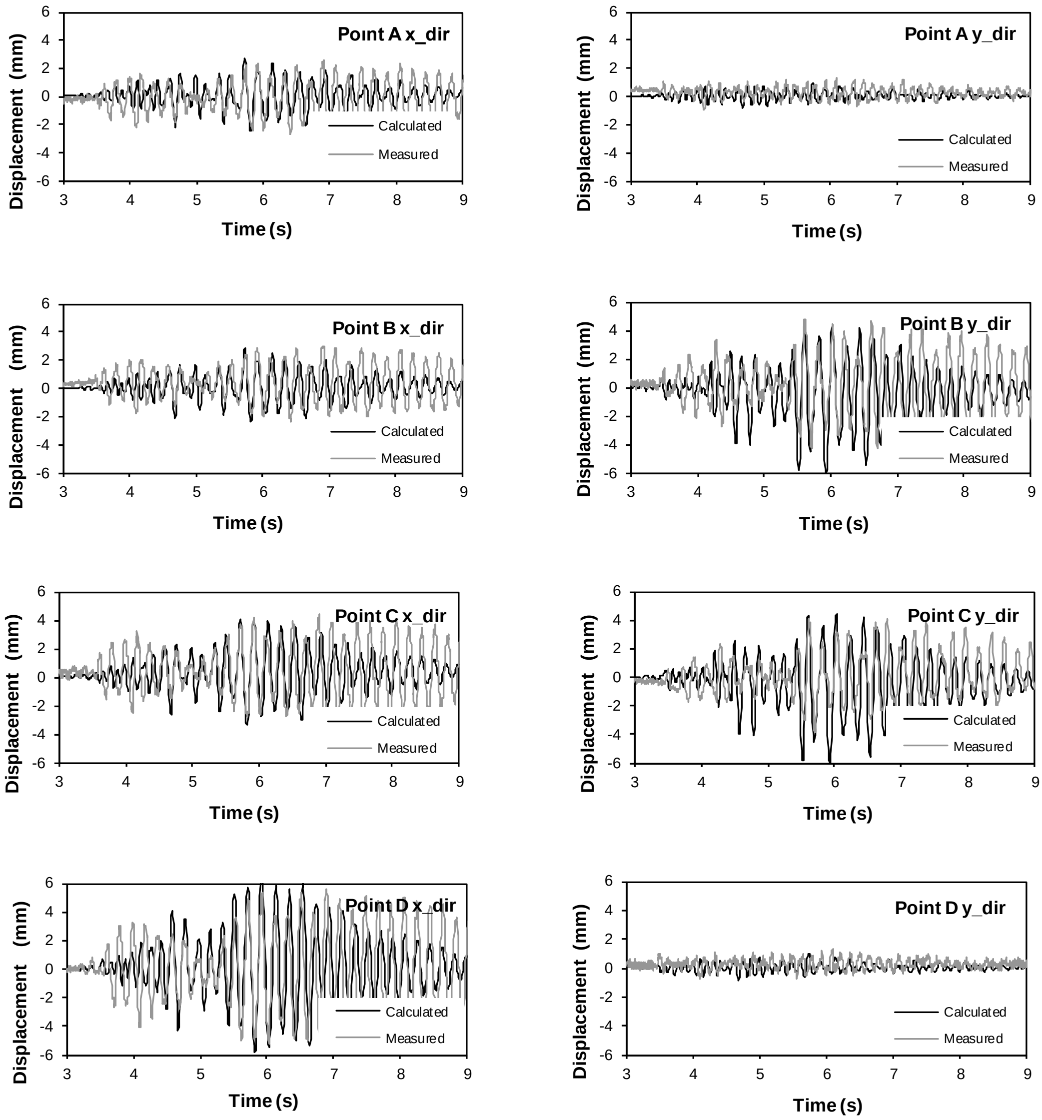

Figure B.2 Displacement comparison of the experimental results and analytical results at the 3rd floor for Run 2 (Accsyn-0.2g) shaking table model

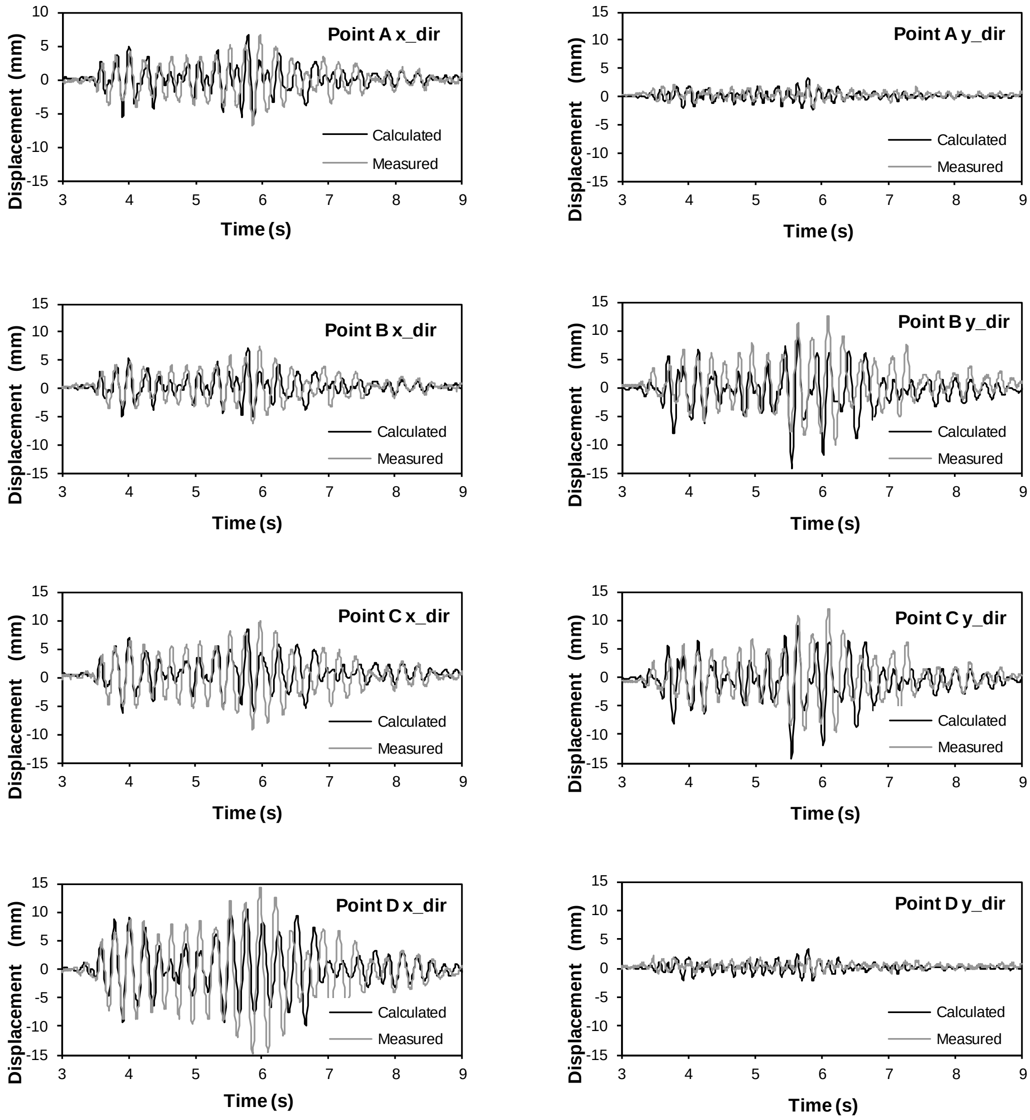

Figure B.3 Displacement comparison of the experimental results and analytical results at the 3rd floor for Run 4 (Accsyn-0.4g) shaking table model

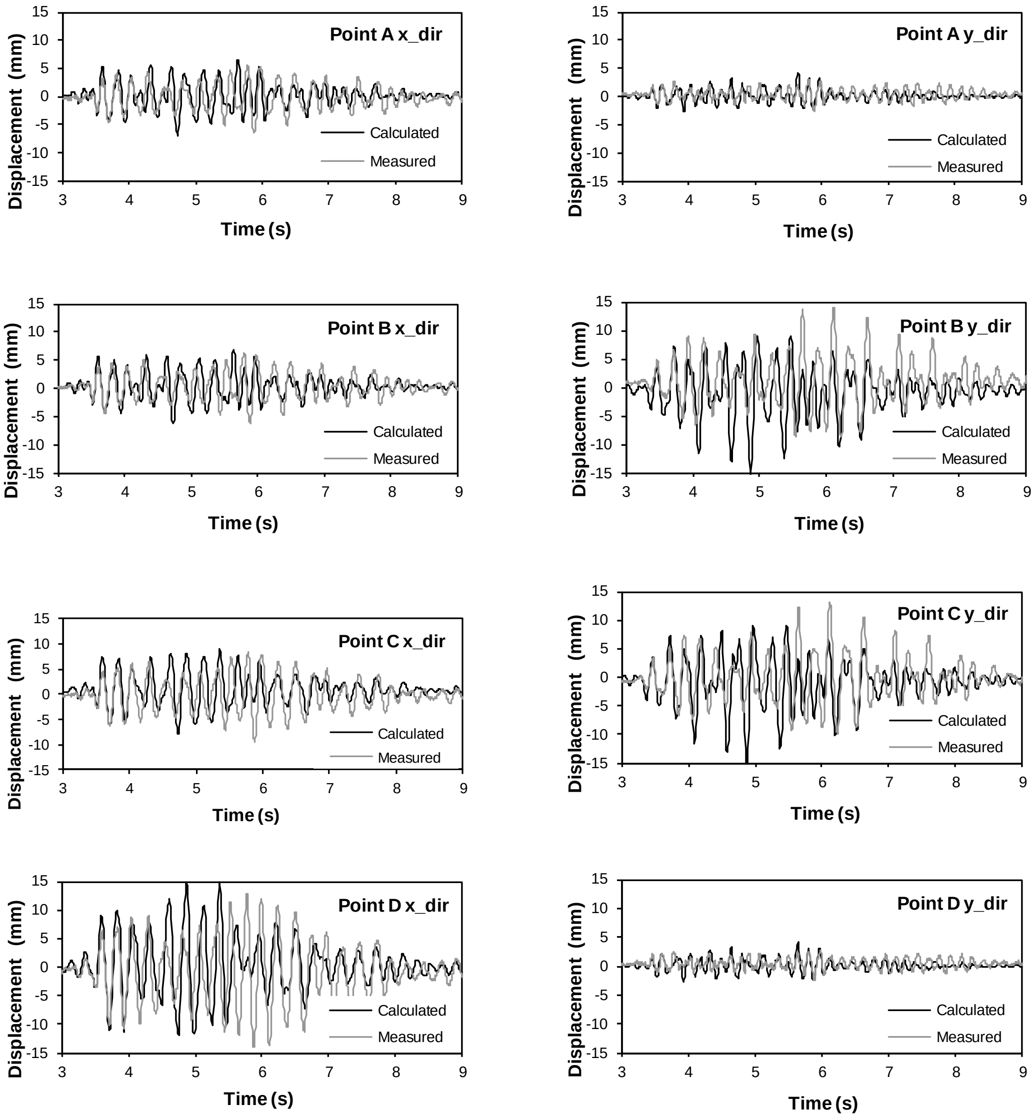

Figure B.4 Displacement comparison of the experimental results and analytical results at the 3rd floor for Run 5 (Accsyn-0.5g) shaking table model

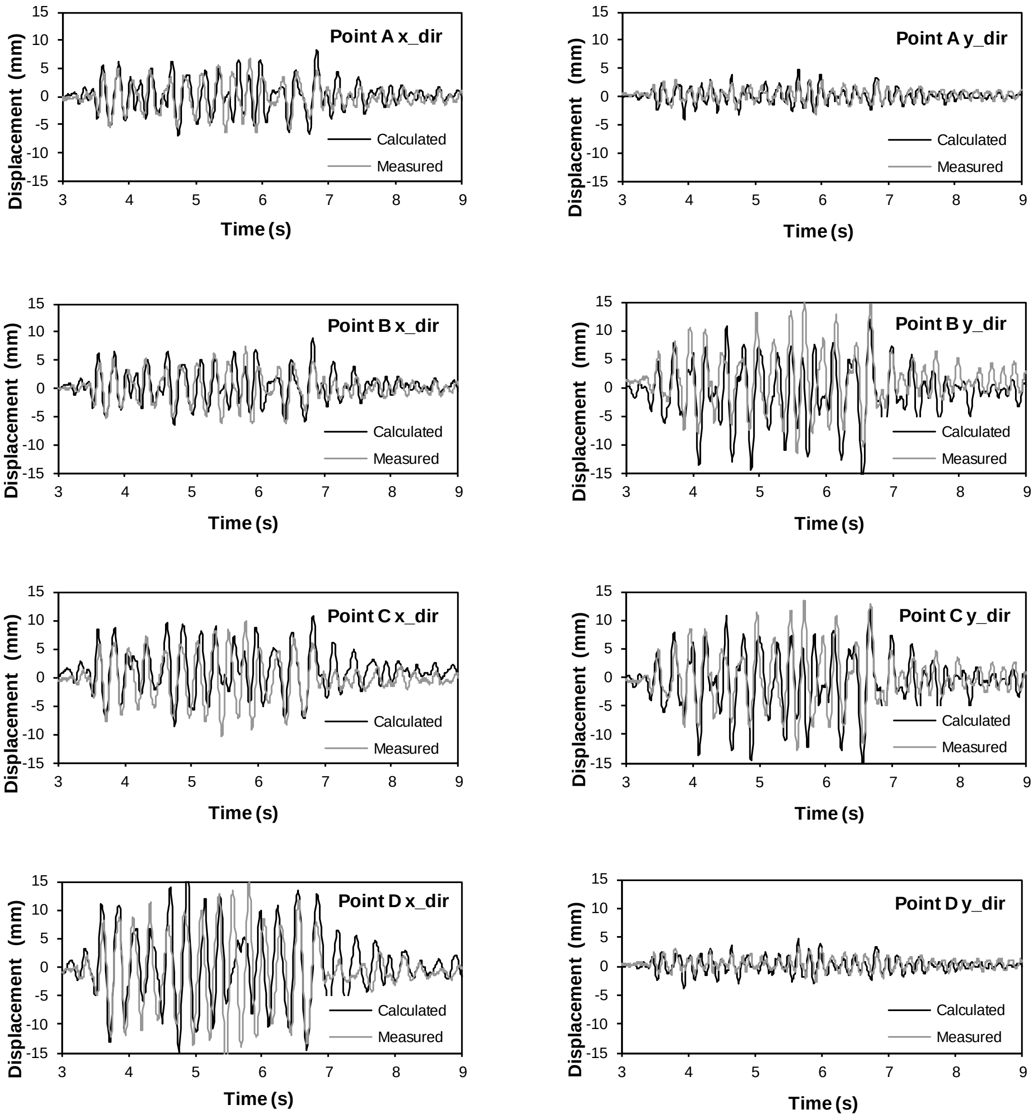

Figure B.5 Displacement comparison of the experimental results and analytical results at the 3rd floor for Run 6 (Accsyn-0.6g) shaking table model

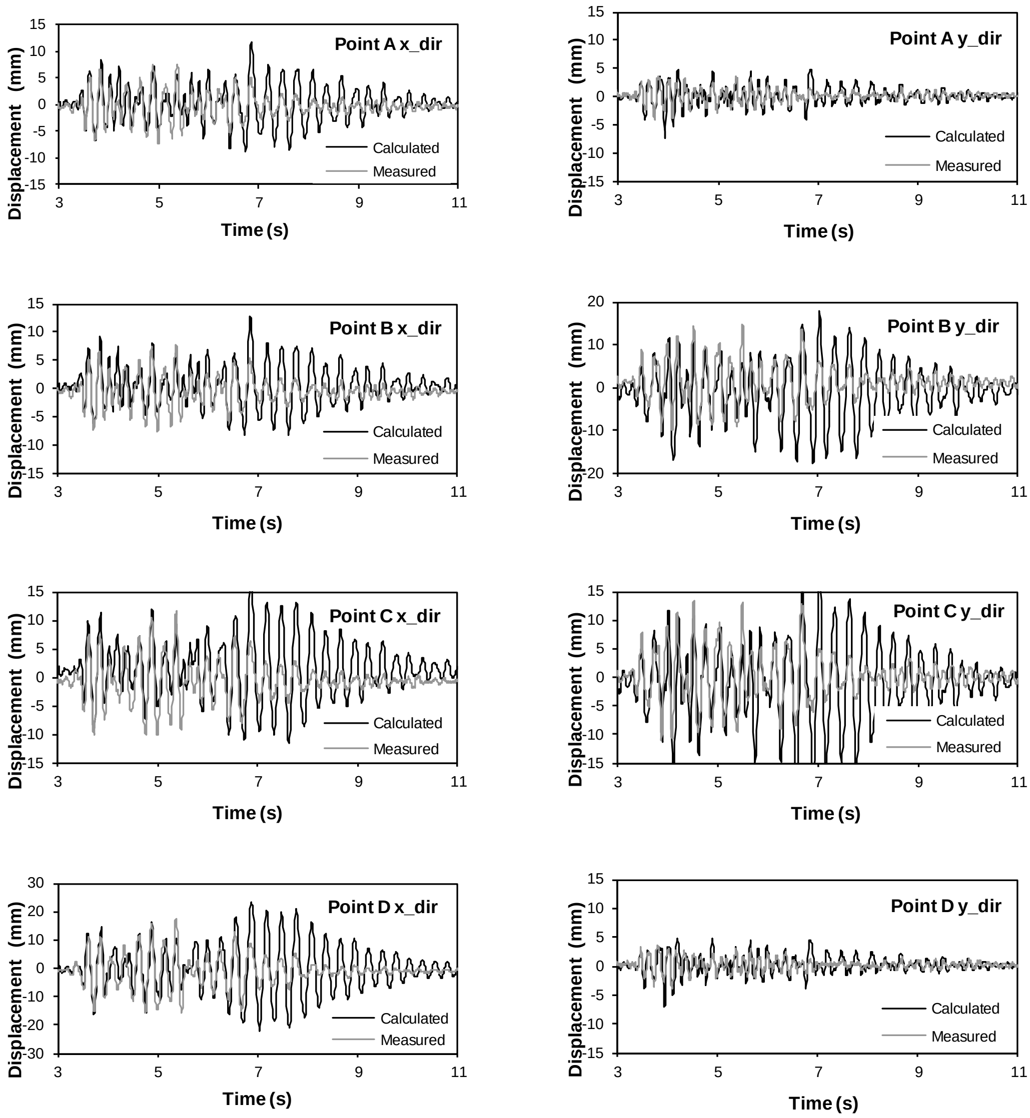

Figure B.6 Displacement comparison of the experimental results and analytical results at the 3rd floor for Run 8 (Accsyn-0.8g) shaking table model

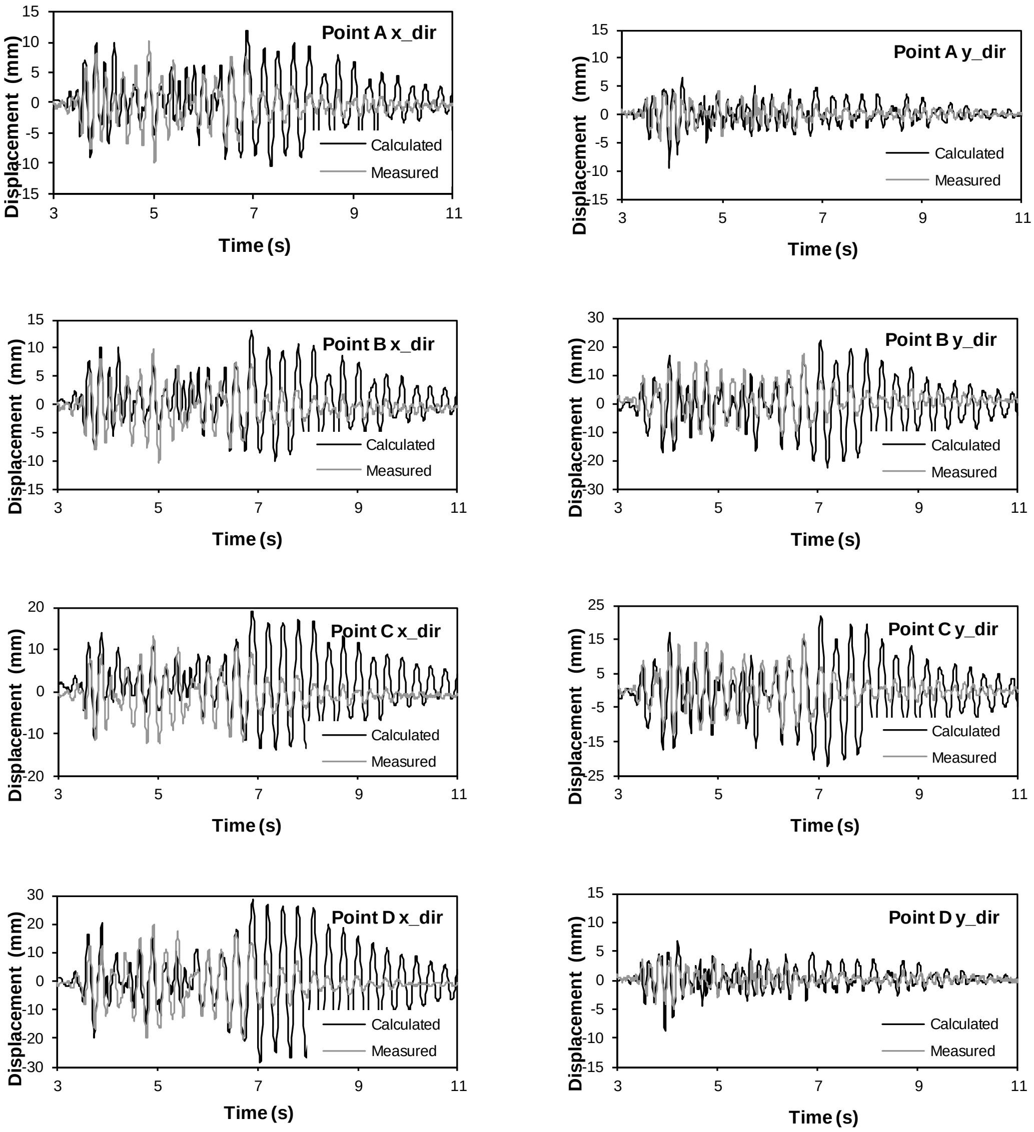

Figure B.7 Displacement comparison of the experimental results and analytical results at the 3rd floor for Run 9 (Accsyn-0.9g) shaking table model

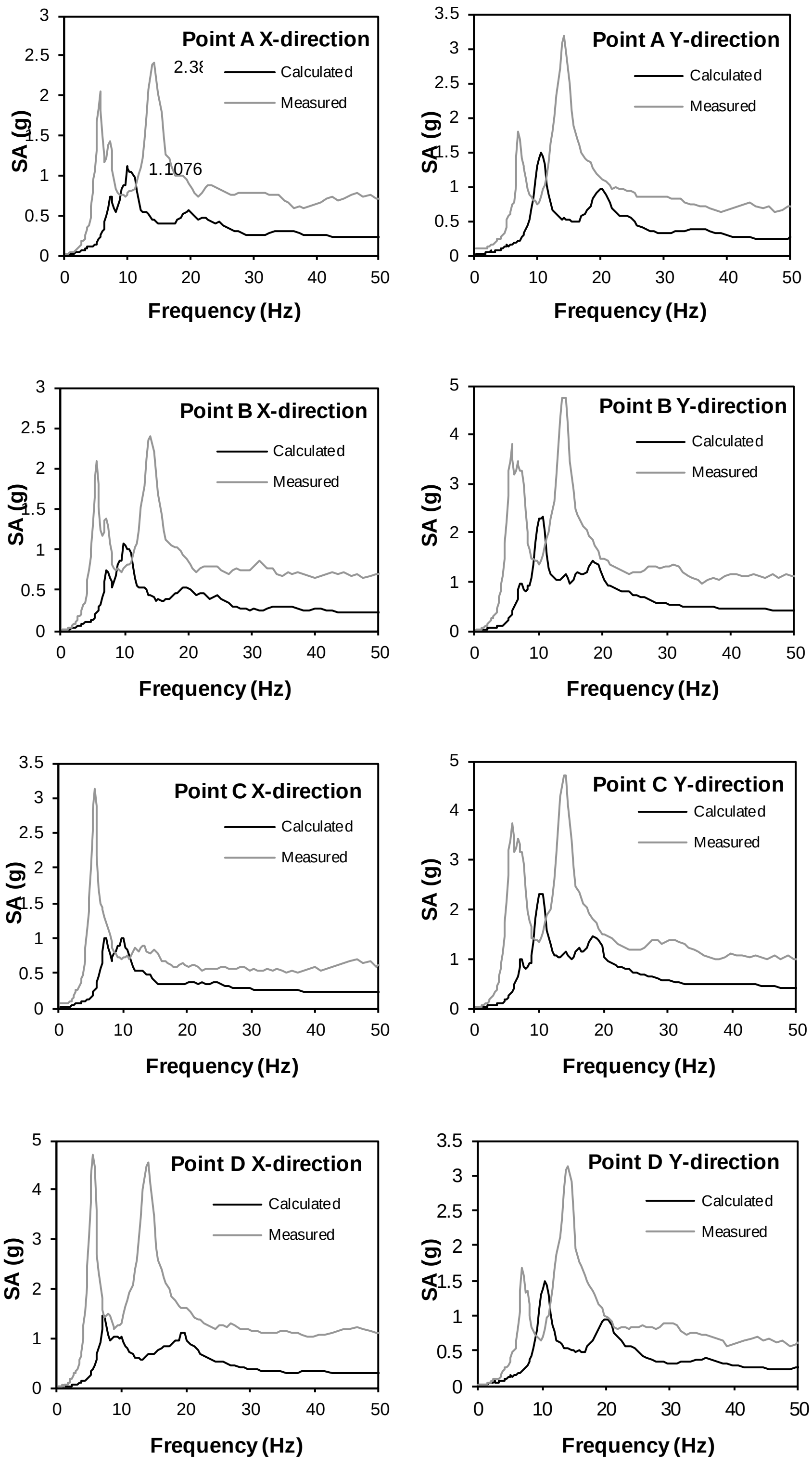

Figure B.8 Acceleration Response Spectrum comparison of the experimental and analytical results at the 3rd floor for Run 1 (Accsyn-0.1 g) shaking table model, Damping ratio=5%

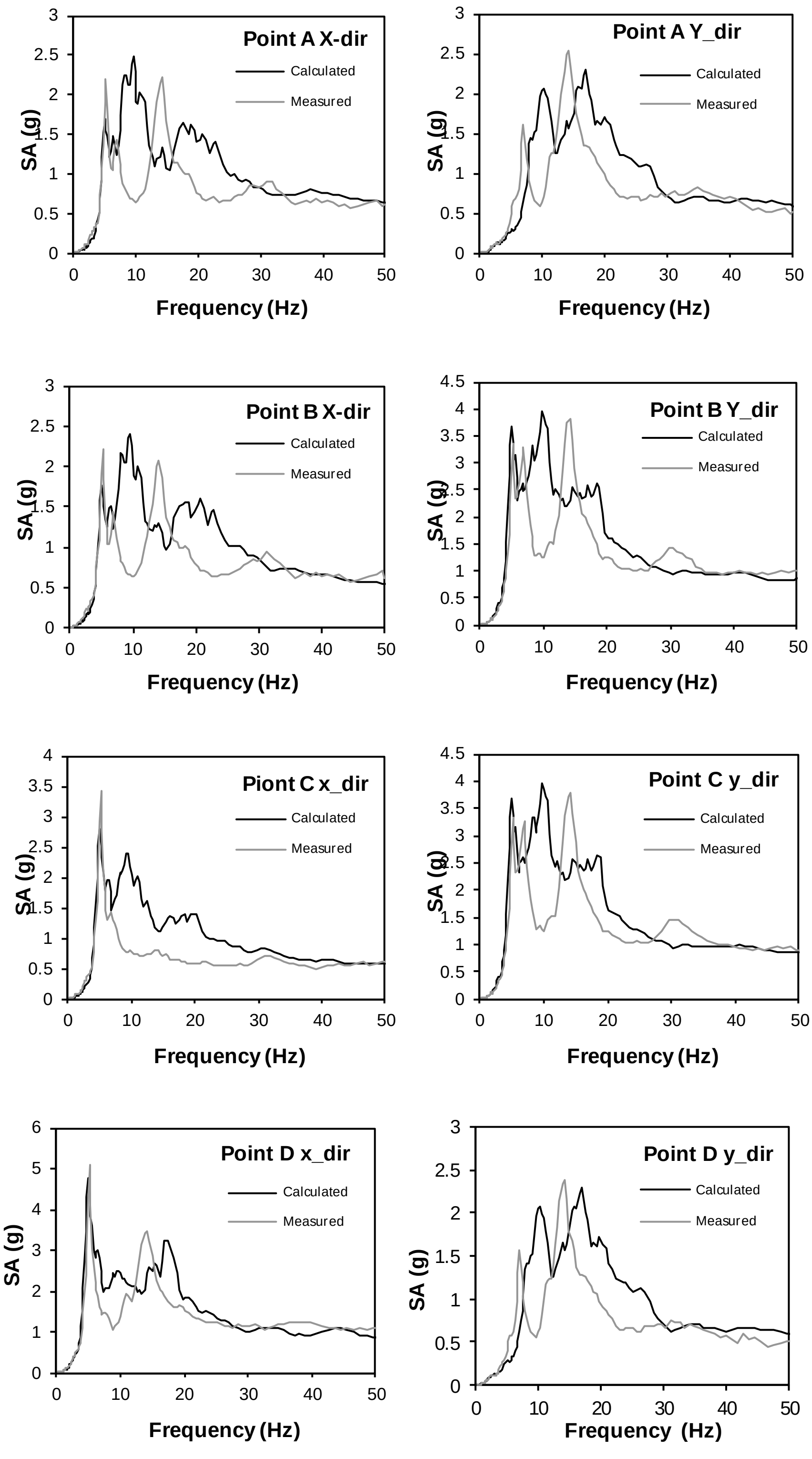

Figure B.9 Acceleration Response Spectrum comparison of the experimental and analytical results at the 3rd floor for Run 2 (Accsyn-0.2 g) shaking table model, Damping ratio=5%

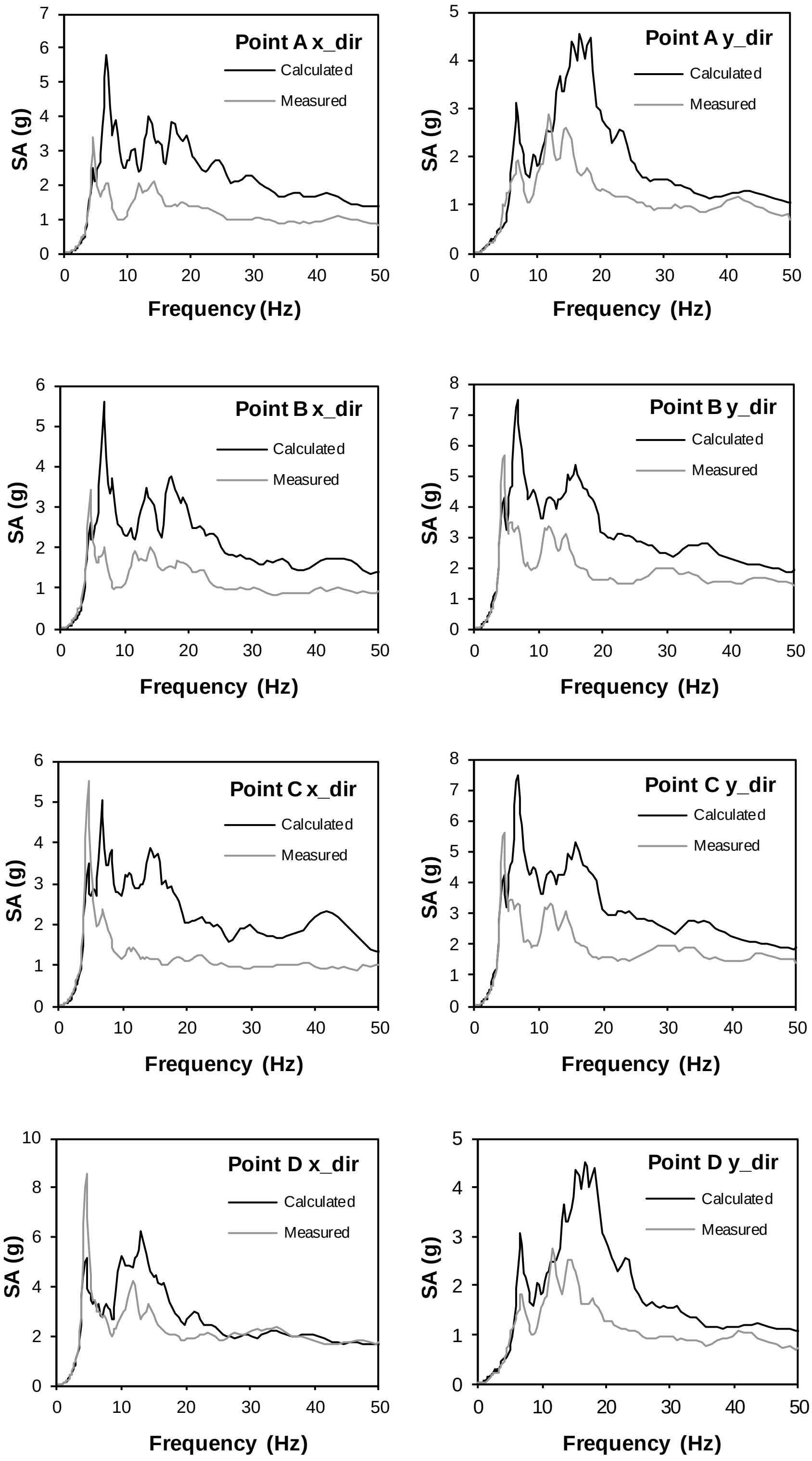

Figure B.10 Acceleration Response Spectrum comparison of the experimental and analytical results at the 3rd floor for Run 4 (Accsyn-0.4 g) shaking table model, Damping ratio=5%

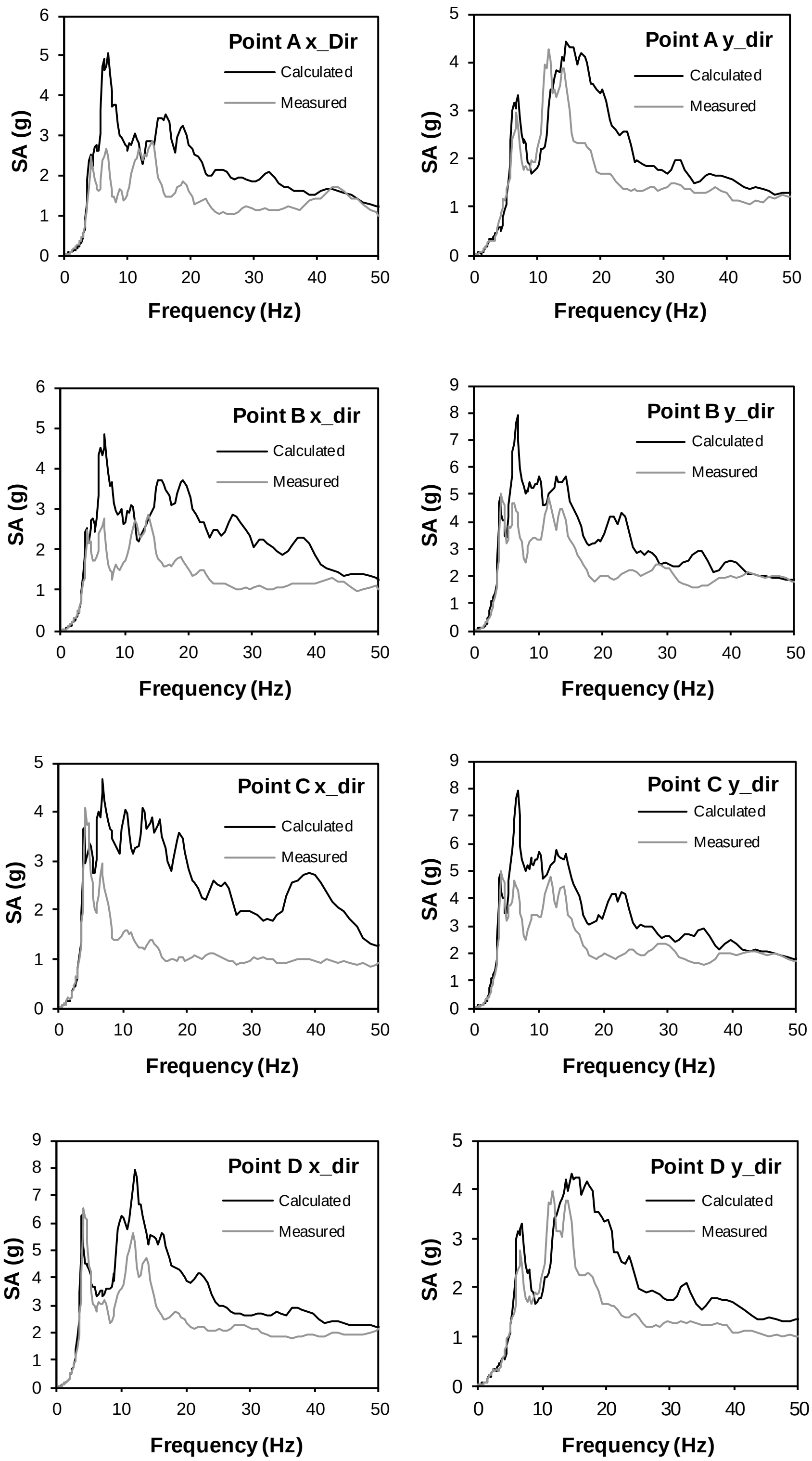

Figure B.11 Acceleration Response Spectrum comparison of the experimental and analytical results at the 3rd floor for Run 5 (Accsyn-0.5 g) shaking table model, Damping ratio=5%

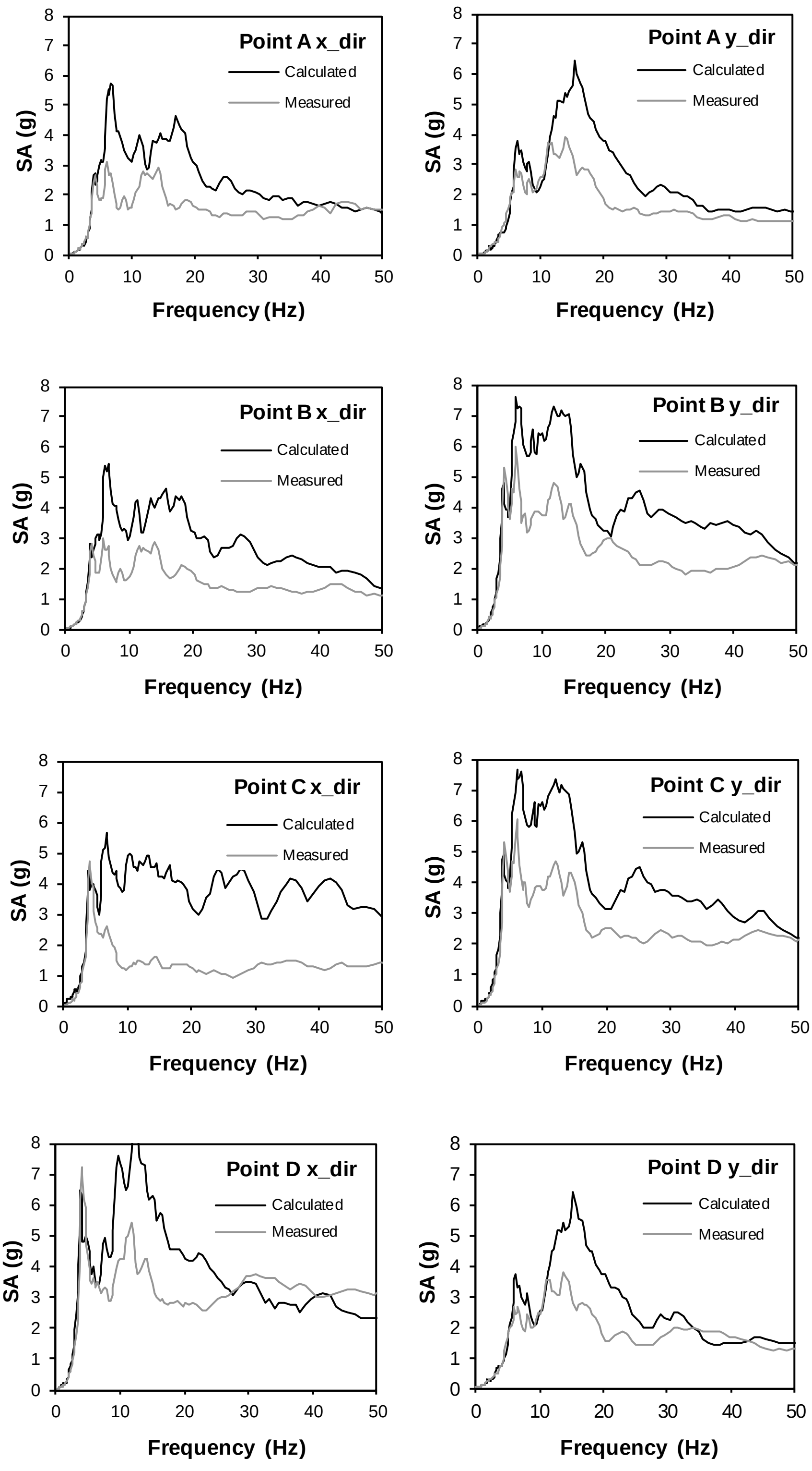

Figure B.12 Acceleration Response Spectrum comparison of the experimental and analytical results at the 3rd floor for Run 6 (Accsyn-0.6 g) shaking table model, Damping ratio=5%

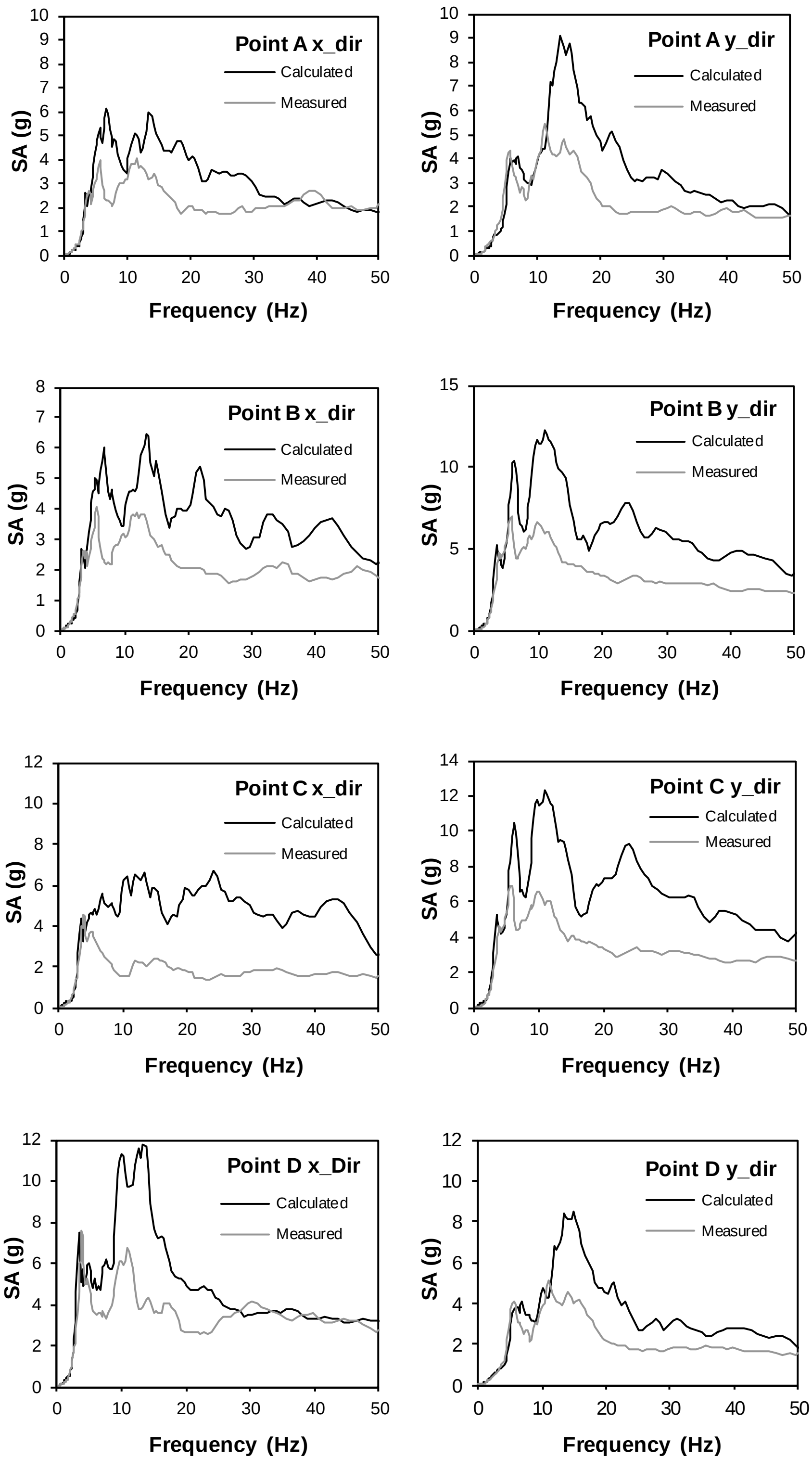

Figure B.13 Acceleration Response Spectrum comparison of the experimental and analytical results at the 3rd floor for Run 8 (Accsyn-0.8 g) shaking table model, Damping ratio=5%

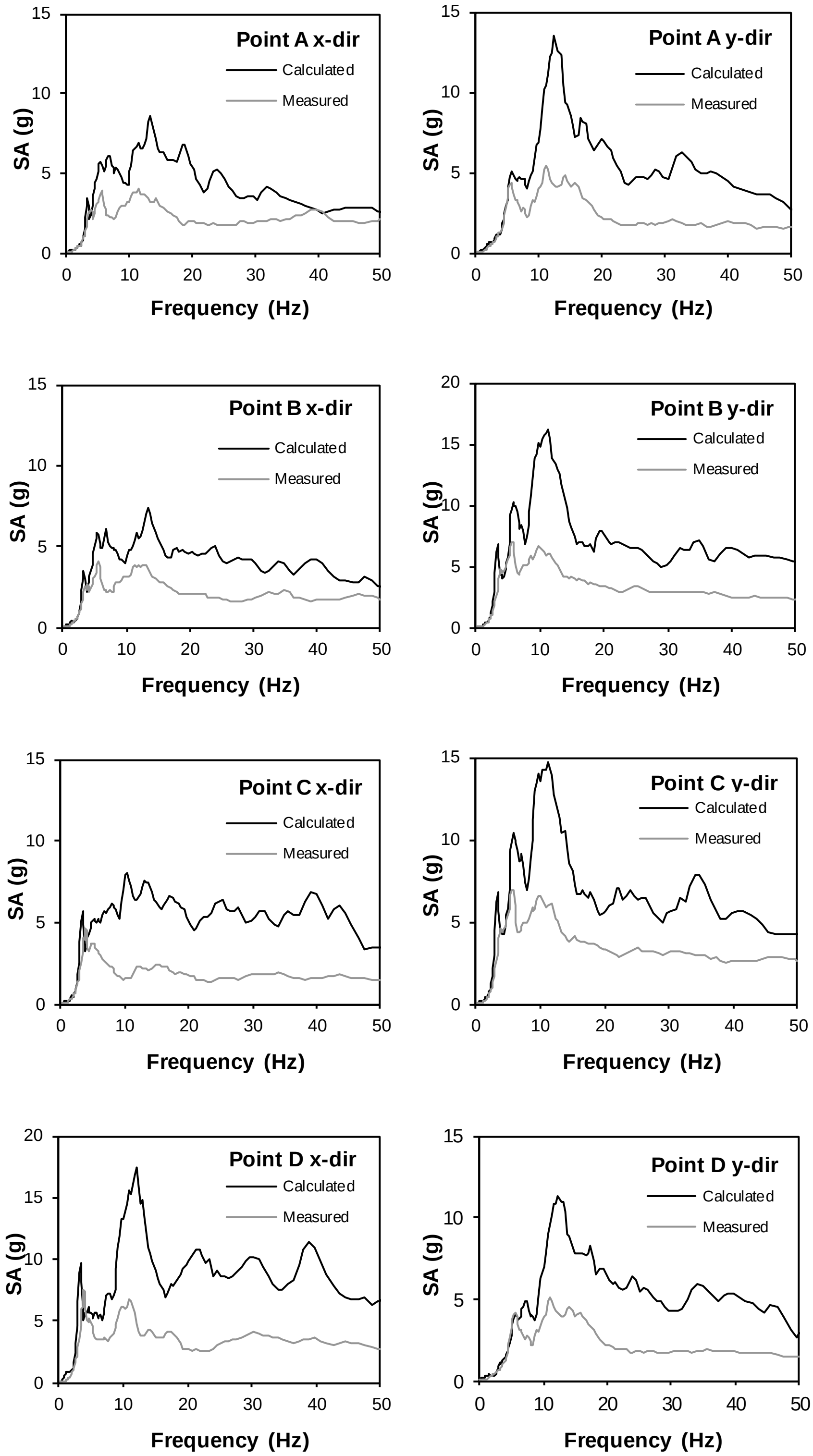

Figure B.14 Acceleration Response Spectrum comparison of the experimental and analytical results at the 3rd floor for Run 9 (Accsyn-0.9 g) shaking table model, Damping ratio=5%